AN INTEGRATIVE GENE-EXPRESSION ANALYSIS OF AXOLOTL LIMB WOUND HEALING AND REGENERATION

A THESIS SUBMITTED TO

THE GRADUATE SCHOOL OF

ENGINEERING AND NATURAL SCIENCES

OF ISTANBUL MEDIPOL UNIVERSITY

IN PARTIAL FULFILLMENT OF THE REQUIREMENTS FOR

THE DEGREE OF

MASTER OF SCIENCE

IN

BIOMEDICAL ENGINEERING AND BIOINFORMATICS

By

Mustafa SİBAİ

June, 2019

AN INTEGRATIVE GENE-EXPRESSION ANALYSIS OF AXOLOTL LIMB
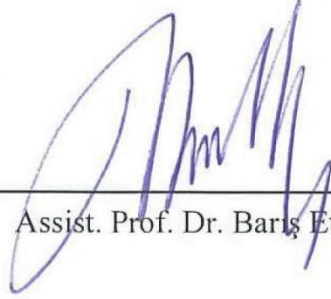WOUND HEALING AND REGENERATION

By Mustafa SİBAİ
June, 2019

We certify that we have read this thesis and that in our opinion it is fully adequate,
in scope and in quality, as a thesis for the degree of Master of Science.

_____
Assist. Prof. Dr. Cüneyd Parlayan (Advisor)

_____
Assist. Prof. Dr. Guvanchmyrat Ovezmyradov

_____
Assist. Prof. Dr. Barış Ethem Süzek

Approved by the Graduate School of Engineering and Natural Sciences:

_____
Assoc. Prof. Dr. Yasemin Yüksel Durmaz
Director of the Graduate School of Engineering and Natural Sciences

I hereby declare that all information in this document has been obtained and presented in accordance with academic rules and ethical conduct. I also declare that, as required by these rules and conduct, I have fully cited and referenced all material and results that are not original to this work.

Name, Last Name: Mustafa SİBAİ

Signature:

ABSTRACT

AN INTEGRATIVE GENE-EXPRESSION ANALYSIS OF AXOLOTL LIMB WOUND HEALING AND REGENERATION

Mustafa SİBAİ

M.S. in Biomedical Engineering and Bioinformatics

Advisor: Assist. Prof. Dr. Cüneyd PARLAYAN

June, 2019

Axolotl is a member of the urodele amphibians that exhibits extraordinary regenerative and scarless wound healing capabilities, fully restoring a lost limb as well as efficiently healing a damaged one. Axolotl has recently been used as a powerful experimental model for the fields of regenerative biology and medicine. Several studies have employed high-throughput, omics-based approaches to uncover the regenerative cues of the axolotl limb *en masse*. Microarrays and RNA-Sequencing technologies have been the most commonly used transcriptomic tools for detecting differentially expressed (DE) genes in different phases of the regenerating limb. Although those studies have found many important genes and pathways that are implicated in the regenerative process, the obtained results may lack sufficient consistency due to study designs originating from different labs, which undermines the statistical power of their experiments. Therefore, to bridge this statistical gap, the aim of this thesis was to perform an integrative analysis of publicly available microarray and RNA-Seq data from Axolotl limb samples having comparable study designs. Three biological groups were conceived for the analysis; control group (intact tissue), wound healing group (up to around 50 hours post amputation), and regenerative group (from 50 hours to 28 days post amputation). Cross-platform normalization (merging) method was selected for separately performing the integrative analysis of microarray and RNA-Seq data from Axolotl limb samples. Differential expression analysis was separately carried out using the R/Bioconductor "limma" package after processing data from both technologies. We found 91 genes, 351 genes, and 280 genes as the top DE genes which showed adjusted $p < 0.01$ from data of both technologies in wound healing vs. control, regenerative vs. control, and regenerative vs. wound healing, respectively. Detailed analyses showed consistent correlation of the logarithmic fold changes of the differentially expressed genes distributed among the biological comparisons, within and between both technologies. Gene ontology annotations demonstrated concordance with the literature on the biological processes involved in the axolotl limb wound healing and regeneration. Future studies on axolotl limb regeneration may benefit from the utilized methodology for enhanced statistical power and more consistent results.

Keywords: axolotl, wound healing, regeneration, merging, differential expression.

ÖZET

AKSOLOTL YARA İYİLEŞMESİ VE REJENERASYONUNUN İNTEGRATİF GEN EKSPRESYON ANALİZİ

Mustafa SİBAİ

Biyomedikal Mühendisliği ve Biyoenformatik, Yüksek Lisans

Tez Danışmanı: Dr. Öğr.Üye. Cüneyd PARLAYAN

Haziran, 2019

Aksolotl, üstün rejeneratif ve hasarsız yara iyileşme kabiliyeti sergileyen, kaybedilen ve zarar görmüş olan bir uzvu tamamen ve etkin bir şekilde iyileştiren ürodele amfibilerinin bir üyesidir. Aksolotl yakın zamanda rejeneratif biyoloji ve tıp alanlarında güçlü bir deneysel model olarak kullanılmaya başlanmıştır. Bazı çalışmalarda, aksolot uzvunun rejeneratif ipuçlarını topluca açığa çıkarmak için yüksek verimli, omik tabanlı yaklaşımlar kullanılmıştır. Mikrodizi analizi ve RNA sekanslama teknolojileri, rejenere olan uzuvun farklı fazlarında diferansiyel olarak eksprese edilen (DE) genleri tespit etmek için en yaygın kullanılan transkriptomik araçlardır. Her ne kadar bu çalışmalar ile rejeneratif süreçte yer alan birçok önemli gen ve yolak bulunmuş olsa da, elde edilen sonuçlar, farklı laboratuarların çalışma tasarımları nedeniyle deneylerinin istatistiksel gücünü zayıflatıp sonuçların tutarlılığını etkileyebilmektedir. Bu tezin amacı bu istatistiksel açığı kapatmak için, halka açık mikroarray ve RNA-Seq aksolotl verilerinin bütünleştirici bir analizini yapmaktır. Analiz için üç biyolojik grup tasarlanmıştır; kontrol grubu (sağlam doku), yara iyileşme grubu (amputasyondan sonra yaklaşık 50 saate kadar) ve rejeneratif grup (amputasyon sonrası 50 saat ile 28 gün arası). Mikroarray ve RNA-Seq verilerinin bütünleştirici analizini ayrı ayrı yapmak için çapraz platform normalleştirme (birleştirme) yöntemi seçilmiştir. DE analizi, her iki teknolojiden veri işlendikten sonra R / Bioconductor "limma" paketi kullanılarak ayrı ayrı gerçekleştirildi. Yapılan karşılaştırmalarda sırasıyla, yara iyileşmesi grubu vs. kontrol de 91 gen, rejeneratif grup vs. kontrol grubunda 351 gen, ve rejeneratif grup vs. yara iyileşmesi grubunda 280 gen istastiksel olarak kuvvetli anlamlı bulunmuştur (düzeltilmiş p değeri; p<0.01). Detaylı analizler, biyolojik gruplar arasında, her iki teknolojinin içinde ve arasında bulunan DE gösteren genler logaritmik kat değişiklikleriyle tutarlı bir korelasyon sergilemiştir. Gen ontolojisi analizleri, sonuçlarımızın aksolotl uzuv yara iyileşmesinde ve yenilenmesinde literatürle uyumlu olduğunu göstermiştir. Geliştirdiğimiz metadoloji aksolotl ekstremite rejenerasyonu üzerine yapılacak gelecek çalışmalara gelişmiş istatistiksel güç ve daha tutarlı sonuçlar için faydalı olabilecektir.

Anahtar Sözcükler: aksolotl, yara iyileşmesi, rejenerasyon, birleşme, diferansiyel ifade.
.

Acknowledgment

Contents

List of Figures

List of Tables

Chapter 1

Introduction

The axolotl, *Ambystoma mexicanum*, is a tetrapod vertebrate which has been an imperative model system for the fields of developmental, evolutionary, and regenerative biology, due to its unique ability of reliably and fully regenerating various body parts, while most adult vertebrates lack such supremacy [1,2]. The Ambystomatidae*, Ambystoma tigrinum* complex, is a clade of 17 closely related, rapidly evolving species, living in an area spanning southern Canada to central Mexico, and having the axolotl as one of its recently derived members [2]. More specifically, the axolotl is a member of the Urodele amphibians, a group consisting of newts and salamanders that have similar vigorous regeneration capacities [1,3]. Axolotls are unique in their regenerative potential due to the fact that their juvenile features are preserved despite reaching sexual maturity [4]. Since they do not undergo metamorphosis naturally, they exhibit some embryonic-like cell traits [5] during adulthood, and thus, can regenerate their body parts efficiently throughout their whole life [1]. The organs which axolotls can faithfully regenerate are many, including their hearts [6–8], spinal cords [9], and even brain [10]. After induction of metamorphosis by thyroid hormone administration, decrease in regenerative power of this species is observed for some body parts such as limb [11,12], however based on recent studies

for other parts of the body regeneration capacity doesn't seem to be hindered [1,13]. Besides, unlike other vertebrates such as the amniotes, which have limited regenerative capacity, axolotls have a simpler adaptive immune system, suggesting that successive regeneration may require a weak inflammatory response [1,14].

Axolotl's regenerative capacity has been tested for many tissues. In response to partial ventricular amputation (PVA) in the heart of axolotl, proliferation of cardiomyocytes is initiated, and this is followed by restoration of the heart's functional capacity as well as the myocardium's structural recovery [6]. Factors such as Baf60 (BRG1/BRM-associated factor 60c), a component of ATP-dependent chromatic-remodeling complexes, has a central role in driving cardiomyocyte proliferation post-cardiac injury [7]. This process is also stimulated by an evolutionarily conserved response mediated by the activation of complement 5a receptor 1, suggesting a pivotal role of the complement pathway in promoting successful heart regeneration [8]. This animal is also capable of completely regenerating its injured or amputated spinal cord with cellular and functional accuracy [9]. When its tail is amputated, a unipolar injury is sensed and regeneration would proceed towards the tip. On the other hand, bipolar injuries resulting from transecting the spinal cord would initiate a diverse regenerative action; the caudal and rostral severed ends ultimately reconnect by bridging the gap. Acting as progenitor cells, ependymal cells expand themselves to form a neuroepithelial tube, thereby facilitating spinal cord regeneration [9]. The axolotl brain also has some regenerative potential, particularly when it comes to regenerating specific neural subtypes, however limited on the functional repair level [10]. It is able to regenerate molecularly-defined neuronal subtypes, while it fails to recover the axonal tracts circuitry that existed prior to injury, having settled in an altered tissue architecture, despite the electrophysiological functionality they seem to attain [10].

Another exceptional feature of axolotl is ability to regenerate its limbs. The phases and process that ensues from axolotl limb amputation can be described as follows: within around 24 hours post-amputation, a stump of epidermal cells migrates to the site of amputation forming a thin wound epidermis across the severed stump, which differs from intact, fully differentiated epidermis at the molecular and structural level [15,16].

This process is followed by infiltration of macrophages to the wound area to remove the pathogens from the wound zone and phagocyte the dead cells' debris within 48 hours post-amputation. Previous studies have demonstrated that macrophage activity is indispensable for successful regeneration [17]. Secretion of mitogens and growth factors from the epidermal cells is accompanied by innervation and, as a result, dedifferentiation of terminally differentiated cells and activation of progenitor cells by re-entering into the cell cycle are the key processes to form what's known as the blastema [16]. Blastema cells are characterized as highly proliferative, heterogeneous in origin and potential [18], morphologically resemble fibroblasts, exhibit unidirectional signaling that is influenced by wound epidermis factors, and behave as autonomous units [16]. Blastemas of a foot amputation and of a full leg amputation are fated to produce only a foot and a full leg, respectively, even when transplanted elsewhere [16]. Hence, blastemas are encoded with precise positional information. The blastema cells continue enriching their pool until reaching a definitive size, that's when they flatten out, allowing cartilage cells to merge and condense, and ultimately paving the way for the varied tissue types to be differentiated, ending up with a perfectly regenerated limb that is identical to the amputated one and finely sized regardless of the age or size of the animal [16].

Some important genes were shown to be directly implicated in axolotl wound healing and regenerative processes. For instance, fibroblast growth factors 8 (fgf8) and MARCKS-like protein were found enriched in early wound epidermis, and their function is proposed to be promoting cellular proliferation [19–22]. Further, heme oxygenase 1 (hmox1), matrix metalloproteinases 11, 1, 3, 9, 10 (mmp11, mmp1, mmp3, mmp9, mmp10), and tsp1 were proposed to function in the overall wound healing process [23–25]. Besides, fibroblast growth factor 10 (fgf10), msh homeobox 1 (msx1), msh homeobox 2 (msx2), and wingless-type MMTV integration site family members 5a and 5b (wnt5a, wnt5b) were found enriched in amputation wounds vs. lateral wounds [19,26–29]. As for genes involved in the regeneration, among the blastema-enriched genes are cold-inducible RNA-binding protein (cirbp) that was found to be cytoprotective for blastema cells, FUS RNA-binding protein (fus), heterogenous nuclear ribonucleoprotein A1 (hnRNP a1), growth-promoting kazal type

serine peptidase inhibitor domain 1 (kazald1), prothymosin alpha (ptma), retinol-binding protein 2a (rbp2a), and serine and arginine rich splicing factor (sfrs1) [25,30]. The tumor protein p53 was found to be downregulated during blastema formation and upregulated within 24 hpa over 2-3 days as well as during redifferentiation [25,31,32]. SMAD family member 2 (smad2) was found upregulated during late regeneration and is thought to be functioning in TGF-β1 signal transduction pathway [33].

Using Axolotl as a model organism is advantageous from several viewpoints. Their generation time is around 1 year or less and year-round breeding in the laboratory is not that difficult [16,34]. Several techniques such as transgenesis and genome editing have been implemented on these animals with relative success [35–39]. It is currently feasible to study mutant cells *in vivo* due to the development of localized genome editing [16]. Although the axolotl's genome is a simple diploid with 14 pairs of chromosomes, it's very large and highly repetitive, containing long introns [40]. Technical hurdles such as the inability of obtaining sufficient read-length and an improved assembly methodology have been some of the major obstacles towards having a full genome assembly [16], and only very recently sequencing and assembly of axolotl genome was reported [41]. Therefore, majority of studies aiming at unraveling the pathways and gene networks in the regenerative mechanisms in axolotl have utilized proteomic and transcriptomic tools [16,30,42–45]. By using the mRNA in the axolotl regenerative tissue as an experimental guide, techniques such as microarrays and transcriptomics (RNA-seq), along with the utilization of *de novo* assembled transcriptomes, have been the primary tools for studying the mechanisms of limb regeneration and discovering the identities of the involved transcripts [16].

Due to their standardization advantage, microarrays were an indispensable tool, capable of unlocking the identities of some of the genes driving the axolotl limb regeneration. Although downstream analyses cannot consider expressed genes that are not represented on the microarray, the technology can still be used to design probes for any condition of interest [16]. Similarly, gene discovery in axolotl limb regeneration was further fostered by the advancements in transcriptomics. RNA-seq is superior to microarrays in mainly two aspects; firstly, there is more dynamic range for expression

values that could be detected by RNA-seq at a single-nucleotide resolution, and secondly, highly expressed genes can be accurately detected by their relative expression values with RNA-seq, eliminating the saturation effect that comes with using microarrays [16]. In addition, novel mRNA discovery for non-model systems as well as the ability to quantify isoforms of genes are other important features of RNA-Seq. Recent advances have made it possible to even use individual cells as the source of a very low RNA input, thereby drastically improving our knowledge on the specific cells and tissues involved in the limb regeneration [16,46].

Despite all of the aforementioned advancements in unraveling the mechanisms of axolotl limb regeneration by the use of microarrays and RNA-seq technologies, the axolotl literature is still missing a key methodology that has the potential in advancing the current knowledge on the limb regeneration even further. The various genes that have been identified to be implicated in the different stages of axolotl limb regeneration have been discovered by separate experiments from separate labs and with limited replicates. "Meta-analysis" is a key methodology widely used in many fields of science that mainly aims to provide scientific consensus on any particular research question [47]. The axolotl regeneration field could greatly benefit from this methodology due to the increasing amount of publicly available microarray and RNA-Seq data, along with freely available bioinformatic tools. One approach of doing so would be to improve candidate gene selection and establishing "biomarkers" for the axolotl wound healing process as well as the limb regenerative process, which is the core scope of this thesis. Meta-analysis is a commonly approach in biomedical sciences to detect differentially-expressed (DE) genes which may be further considered for selecting gene signatures or may be used as features for improving an existing classifier and coming up with a better gene signature for clinical applications [48–50].

The application of meta-analysis in many of the fundamental biological research as well as preclinical medical sciences has not been embraced very quickly due to the fact that experimental techniques may be a lot different for direct comparisons [47]. Besides, some data would be deposited with no relevant publication, making the analysis a lot more challenging. However, microarray and RNA-Seq data are being

deposited to public repositories along with their related publications and detailed experimental designs [47]. In addition, the advantages of implementing the meta-analysis methodology can be realized from the limitations of individual studies. First of all, the cost of utilizing new technologies is almost always considered a limiting factor when it comes to determining the scale of an experiment conducted by some lab. Moreover, after an individual experiment has been conducted, researchers are faced with challenging statistical issues [47]. Lastly but not least, in some cases experimental design of individual studies overlap with each other due to lack of an established pipeline to perform meta-analysis and as a consequence, researchers may generate similar data. These issues are manifested in both high false-positive observations due to the analysis of limited number of samples and huge number of transcripts, and false-negative observations when false positives are accounted for by introducing stringent cut-offs [47,51]. Therefore, gene signature selection could be enhanced when multiple data sets are integrated by means of meta-analysis [47,50,52]. In other words, the more sample size increases, the more statistical power, the less individual study-specific biases, and the more precise differential gene expression integration and heterogeneity assessment can be achieved [50,53–56].

When the term "Meta-analysis" is used, it's often understood as the concept of integrative data analysis (IDA). However, conceptually, integrative data analysis has recently been expanded to refer to experiments which aim to integrate information from several layers of "omics" information (aka multi-omics), such as integration of epigenomics, genomics, transcriptomics, proteomics, and metabolomics [57]. In this thesis, we refer to IDA as the process of combining information of independent studies originating from different platforms or slight variations of the same platform [50,53]. Technically, there are two fundamental approaches to perform the latter concept of integrative data analysis; meta-analysis and cross-platform normalization (aka "merging") [50]. Meta-analysis is classified as "late stage" data integration when final statistics are combined from different studies, whereas merging is classified as "early stage" data integration when it integrates data before running the statistical test [50]. Relatively-homogenous datasets which have been selected to answer unambiguous, particularized questions can be used more suitably by the merging method for

biomarker discovery [50,58]. Besides, both data integration methods are applicable under comparable conditions and for biological questions, whether it's differential expression analysis or class prediction [50].

In this thesis, integrative data analysis was independently performed on publicly available Microarray and RNA-Seq data from Axolotl samples, using the cross-platform normalization (merging) method to identify the genes which might be considered as biomarkers of different phases of regeneration. The samples were collected from different Microarray and RNA-Seq data sets, referring to three main groups of axolotl biological conditions; control (homeostasis), wound healing, and limb regeneration conditions. By separately using the merging methodology on the samples of Microarray and RNA-Seq technologies, followed by comparing their results, the aim was to identify a set of transcriptomic patterns that drive the wound healing and regenerative processes in the axolotl limb. The statistical test yielded 170, 1254, and 1047 differentially expressed (DE) genes (adjusted p-value < 0.01), commonly identified by Microarray and RNA-Seq integrative data analyses in wound healing vs. control, regenerative vs. control, and regenerative vs. wound healing comparisons, respectively. Moreover, the top 91 DE genes (commonly identified by the analyses of both technologies) in wound healing vs. control comparison enriched several biological processes (adjusted p-value < 0.05) such as collagen metabolic processes, regulation of cell adhesion, proliferation, and death, as well as extracellular matrix disassembly. On the other hand, the top 351 DE genes (commonly identified by the analyses of both technologies) in regenerative vs. control comparison enriched several biological processes (adjusted p-value < 0.05) such as regulation of cell cycle processes, mitotic nuclear division, regulation of mRNA metabolic processes, muscle filament sliding and contraction, muscle structure development, and cardiac muscle tissue morphogenesis.

Chapter 2

Methods

2.1   Gene-expression Data Collection

Gene-expression microarray data sets and RNA-seq data sets were collected from the public Gene Expression Omnibus (GEO) database [59,60] (http://www.ncbi.nlm.nih.gov/geo/) and the European Nucleotide Archive (ENA) database [61] (https://www.ebi.ac.uk/ena), respectively. The following criteria, prepared according to *Preferred Reporting Items for Systematic Reviews and Meta-Analyses (PRISMA)* [62], were used to select GEO series from which data were collected (Figure 1 and Figure 2):

1) GEO series data deposited until September 2018.
2) Non-redundant series.
3) Series pertinent to Axolotl tissues.
4) Series having unduplicated datasets.

The accession number of the GEO series (GSE number), title, publication, number of the selected samples, number of the total samples, platform type, link to the gene-expression data, and the year of each study can be found in Table A.1 for Microarray

technology and in Table A.2 for RNA-seq technology. The number of GSM files representing our meta-data design (group types), how many of each group belong to which sub-platforms and to which study (series), is provided in Table 1 for Microarray technology and in Table 2 for RNA-seq technology. For more detailed information on the GSM accession, timepoint, amputation/injury site, and replicate number of each sample, under each group type, for every selected GSE study, Table A.3 and Table A.4 were generated for Microarray and RNA-seq technologies, respectively.
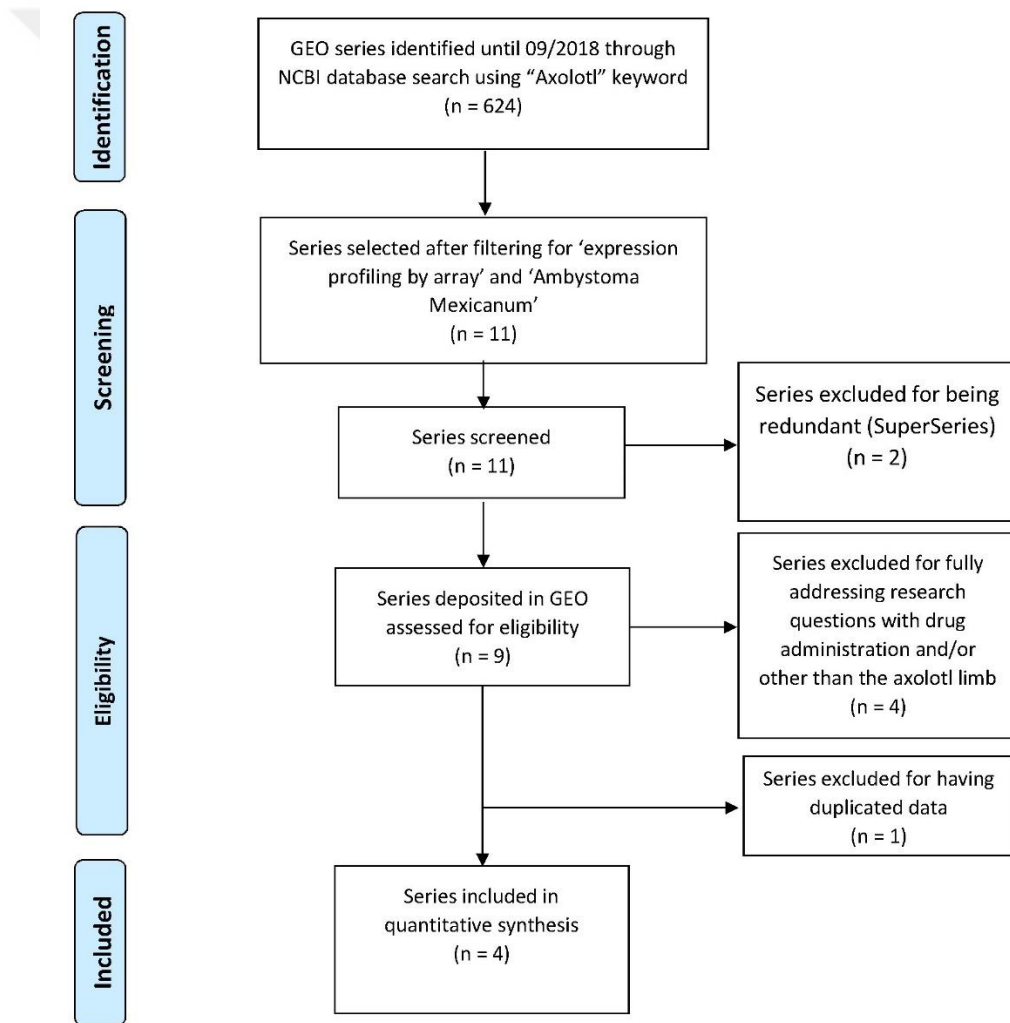
Figure 1: Flow diagram illustrating the selection criteria used for performing integrative analysis on microarray data. The diagram is prepared according to *Preferred Reporting Items for Systematic Reviews and Meta-Analyses (PRISMA)*
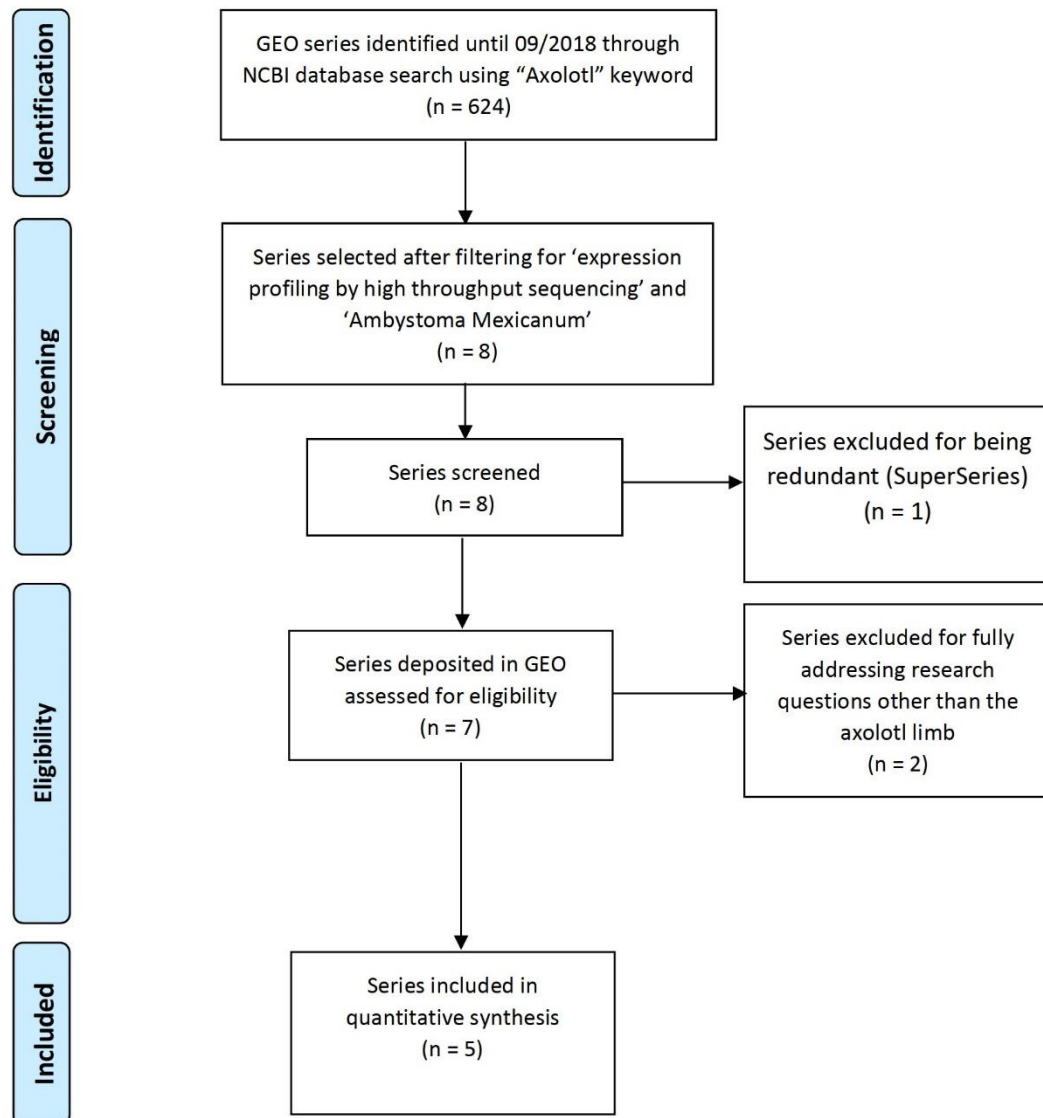
Figure 2: Flow diagram illustrating the selection criteria used for performing integrative analysis on RNA-seq data. The diagram is prepared according to *Preferred Reporting Items for Systematic Reviews and Meta-Analyses (PRISMA)*

Dataset GSE Accession	Platform	Group type			Total	Ref
		Control (0 dpa/dpi)	Wound Healing (up to ~ 50 hpa/hpi)	Regenerative (> ~ 50 hpa/hpi to 28 dpa/dpi)		
GSE116615	GPL25286 [AMBY_002a520748F] Affymetrix Ambystoma mexicanum	3	3	N/A	6	[63]
GSE67118	GPL15153 Affymetrix Ambystoma mexicanum AMBY_002 20k array [CDF: AMBY_002a520748F]	10	40	148	198	[25]
GSE37198	GPL15153 Affymetrix Ambystoma mexicanum AMBY_002 20k array [CDF: AMBY_002a520748F]	8	8	16	32	[64]
GSE36451	GPL15342 Agilent-019788 Ambystoma mexicanum 44k_v3_20080327	5	42	30	77	[19]
Total		26	93	194	313	

Table 1: Summary of microarray gene expression data used for integrative analysis

Dataset GSE Accession	Platform	Group type			Total	Ref
		Control (0 dpa/dpi)	Wound Healing (up to ~ 50 hpa/hpi)	Regenerative (> ~ 50 hpa/hpai to 28 dpa/dpi)		
GSE116777	GPL21473 Illumina HiSeq 2000 (Ambystoma mexicanum)	2	3	N/A	5	[63]
GSE103087	GPL22800 Illumina HiSeq 2500 (Ambystoma mexicanum)	N/A	N/A	4	4	[65]
GSE92429	GPL22800 Illumina HiSeq 2500 (Ambystoma mexicanum)	3	N/A	4	7	[30]
GSE74372	GPL14997 Illumina Genome Analyzer IIx (Ambystoma mexicanum)	1	N/A	3	4	[45]
GSE34394	GPL14997 Illumina Genome Analyzer IIx (Ambystoma mexicanum)	1	4	7	12	[66]
Total		7	7	18	32	

Table 2: Summary of RNA-Seq gene expression data used for integrative analysis

2.2 Gene-expression Data Processing

Gene-expression Microarray and RNA-seq integrative data analyses were performed using R software [67], software packages from the open development software Bioconductor Project [68,69], and parts of a published gene-expression analysis workflow [70].

The whole Microarray data processing workflow is provided in Figure B.1. The selected samples (CEL files) from the 3 Affymetrix datasets (GSE116615, GSE67118, GSE37198) were read and merged as a single dataset, due to their similarity at the probeset-level, using the R/Bioconductor "affy" package [71]. The resulting single dataset consists of 236 (21 control, 51 wound healing, 164 regenerative) samples (columns) and 20080 probesets (rows). This dataset was then summarized, quantile-normalized, and log2-transformed by applying the Robust Multichip Average (RMA) algorithm using the R/Bioconductor "affy" package [71]. Thereafter, the expression data underwent a filtering process based on row-wise transcript intensities. The medians of rows were calculated using the R/Bioconductor "Biobase" package [68], followed by keeping only the probesets with intensities higher than a threshold of "4" in at least as many samples of the smallest group (Figure 3A). The resulting filtered data consists of 17658 probesets. These probesets were then subjected to annotation using the AMBY_002a520748F probeset annotation file (~ 20k probesets) provided by Sal-Site (http://www.ambystoma.org/genome-resources/20-gene-expression). There were 13316 probesets mapping to the annotation file with some of them mapping to the same gene. In order to obtain unique genes for those multiple mappings, using the "WGCNA" R package [72], the duplicated probesets were collapsed from probeset-level to gene-level by taking the maximum row mean value of the probeset to represent the corresponding gene, resulting in a total of 10442 unique genes.

As for the Agilent dataset (GSE36451), the 77 selected samples (5 control, 42 wound healing, 30 regenerative) were obtained directly from GEO as summarized, quantile-normalized, and log2-transformed. The samples were combined together as a single

dataset having 77 samples (columns) and 43796 probesets (rows). The dataset underwent the same median intensity-based filtering as the Affymetrix datasets with the same threshold (Figure 3B), using the R/Bioconductor "Biobase" package [68]. This filtering resulted in 41579 probesets, which were further subjected to annotation using the annotation file obtained from GEO (https://www.ncbi.nlm.nih.gov/geo/query/acc.cgi?acc=GPL15342). Only 21419 probesets were mapped to the annotation file, some of which corresponding to the same gene. Unique genes were obtained by the same approach used for the Affymetrix data, by collapsing the duplicated probesets to the corresponding genes, using the "maximum row mean values" method, implemented by the "WGCNA" R package [72], resulting in a total of 5083 unique genes.
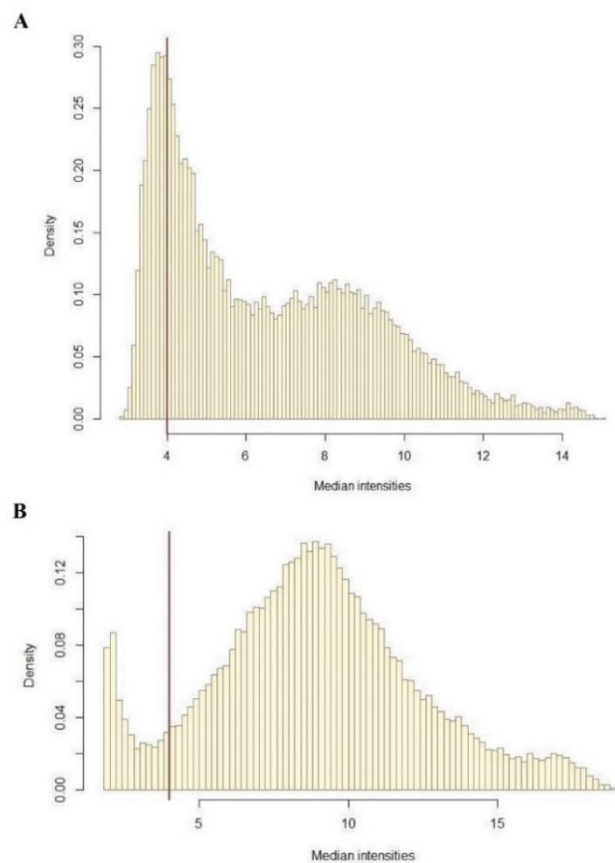
Figure 3: Histograms of Median intensities. A) Histogram of the median intensities of the merged 3 Affymetrix datasets. B) Histogram of the median intensities of the Agilent dataset. The vertical red line represents the threshold such that all of the probeset median intensities below the threshold are discarded

In order to obtain a set of common genes between the Affymetrix and Agilent datasets, the 10442 Affymetrix unique genes were merged with the 5083 unique genes, resulting in 4322 unique common genes. The Affymetrix log2-transformed data was prepared based on the 4322 unique common genes, and so was the Agilent log2-transformed data. In order to minimize the batch effect between the Affymetrix and Agilent platforms, the resulting Affymetrix and Agilent log2-transformed data were each independently transformed to standard score (a.k.a "z-score") [73], which is performed by the process of centering (subtracting the column means of the transposed matrix from their corresponding columns) followed by scaling (dividing the centered columns of the transposed matrix by their standard deviations), and then transposing the matrix back so that genes are rows and samples are columns. The Affymetrix and Agilent z-scored data were merged together to obtain a single dataset consisting of 313 (26 control, 93 wound healing, 194 regenerative) samples (columns) and 4322 genes (rows). Principle component analysis (PCA) was implemented to explore overall relationship occurring among samples of the z-scored, merged data.

The whole RNA-seq data processing workflow is provided in Figure B.2. The selected raw data for each of the 5 datasets were obtained from the European Nucleotide Archive (ENA) in fastq format. GSE116777 (2 control, 3 wound healing), GSE92429 (3 control, 4 regenerative), and GSE103087 (4 regenerative) are all paired-end libraries, whereas both GSE74372 (1 control, 3 regenerative) and GSE34394 (1 control, 4 wound healing, 7 regenerative) are single-end libraries. Dwaraka *et al.*, [63], recently produced the axolotl transcriptome "V5 contig assembly (contig length of 19,732 bp)" (data accessible at NCBI GEO database, accession GSE116777), and was downloaded to be used as our transcriptome reference. This particular transcriptome was chosen because, according to the authors, a total of 31,886 pairwise alignments with > 98% sequence similarity were identified between the V5 RNA-seq contigs and the 20,036 V3 contigs that were used to design the Affymetrix microarray probesets. Since the Affymetrix probesets already had an annotation file, and both were used in our microarray analysis pipeline, the same annotation file was used for generating a new annotation file for the 31,886 aligned contigs of the V5 assembly in our RNA-seq analysis pipeline. The RNA-seq annotation file was prepared by merging the 31,886

V5 assembly-V3 Affymetrix probesets alignment with the V3 Affymetrix probesets annotation file, yielding around 25k genes. The expression of transcripts of each of the 5 datasets were independently quantified using the transcriptome-wide quantifier "Salmon" tool [74], by building an index for the V5 transcriptome and directly quantifying the reads on it. Salmon operates on a dual-phase inference procedure, utilizes the concept of *quasi-mapping,* and accounts for technical biases by extensive bias modeling. These unique features enable salmon to carry out fast and accurate quantification of transcript abundance from RNA-Seq reads [74]. The resulting scaled counts generated from transcript abundances were imported along with the RNA-seq annotation file, using the R/Bioconductor "tximport" package [75]. This yielded a count matrix of the samples of all datasets combined (32 columns) with 10k unique genes (rows). Lowly expressed genes were filtered out using the R/Bioconductor "edgeR" package [76,77]. The filtering strategy is to keep genes that have minimum counts for at least some samples. The final format of the data post-filtering is a matrix with 32 (7 control, 7 wound healing, 18 regenerative) samples as columns and 7562 genes as rows. Normalization factors were calculated for this matrix using the R/Bioconductor "edgeR" package [76,77]. The normalization factors were used while converting the count data to log2-counts per million (logCPM), using the "voom" function of the R/Bioconductor "limma" package [78–80], which makes the data ready for linear modelling for differential expression analysis. When applying the "voom" function, a design matrix was implemented such that each sample's group type and study origin are accounted for. In order to explore overall relationship occurring among samples, principle component analysis (PCA) was performed on the "voom" counts data.

2.3   Differential Expression Analysis (DEA)

Microarray DEA was performed on the z-scored, combined data (313 samples, 4322 genes). RNA-seq DEA was performed on the logCPM (voom) counts (32 samples,

7562 genes). The following analyses were performed using the R/Bioconductor "limma" package [78–80].

For both Microarray and RNA-seq data, contrast matrices were constructed to represent 3 group comparisons; wound healing vs. control, regenerative vs. control, and regenerative vs. wound healing. The first comparison aims to observe gene expression changes occurring in wound healing tissues compared to control (homeostatic) tissues. The second comparison aims to observe gene expression changes occurring in regenerative tissues compared to control (homeostatic) tissues. The final comparison aims to observe gene expression changes occurring in regenerative tissues compared to wound healing tissues. For each contrast matrix, a design matrix was incorporated to account for the group type and study origin of every sample, and a linear model is fitted to the expression data for each gene. Empirical Bayes method was applied on those fitted linear models, so that genes can be ranked based on an order of evident differential expression. The raw p-value and adjusted p-value distribution for each contrast from both Microarray and RNA-seq data were plotted in a histogram format as a diagnostic check. The adjusted p-value method used here is the Benjamini-Hochberg (BH) that controls the expected false discovery rate (FDR) below a specified value. The cutoff for adjusted p-value was set to be 0.01, so genes with lower adjusted p-values were extracted as lists of differentially expressed genes, each list corresponding to each contrast of either the Microarray or RNA-seq data. In order to explore how differentially expressed genes drive the clustering of the samples, principal component analysis was performed for each of the 3 comparisons, for both the Microarray z-scored data as well as the RNA-seq logCPM counts data, with the batch effect minimized using the R/Bioconductor "limma" package. The comparison of DE Genes among the three comparisons within each technology, and the subsequent comparison of the DE genes between the two technologies (Microarray and RNA-seq), were performed using Venn diagram online tool (http://bioinformatics.psb.ugent.be/webtools/Venn/) and scatter plots using the R/Bioconductor "ggplot2" package [81]. Pair-wise correlation testing of logFC of the DE genes for the three comparisons within and between the two technologies was performed using the "Spearman" correlation test in base R.

2.4   Gene Ontology Enrichment Analysis

The top DE genes commonly identified by both technologies analyses were used to identify Gene Ontology (GO) annotations using the R/Bioconductor "clusterProfiler" package [82] . The genes were first converted to Entrez IDs prior to performing the statistical overrepresentation test, which was used to separately query the top up-regulated and down-regulated Entrez ID-mapped genes of each condition comparison against all GO lists (Biological Processes "BP", Cellular Components "CC", Molecular Functions "MF"), while also eliminating redundant GO terms. The background gene list consisted of all Entrez IDs from the axolotl Affymetrix "AMBY_002a520748F" annotation file. Bar plots were used to visualize the top 20 GO terms enriched by the up-regulated and down-regulated genes for the conditions of interest. The parameters of the overrepresentation test included using the homo sapiens "org.Hs.eg.db" as the organism database, Benjamini & Hochberg (BH) as the adjusted-P value method, and setting p and q value cut-offs to 0.05.

Chapter 3

Results

3.1 Gene-expression Data Selection and Search Criteria

According to our criteria, illustrated in Figure 1 for Microarray technology, 4 GSE datasets (series) were selected, 3 of which were performed using slightly different versions of the Affymetrix Ambystoma Mexicanum platform; the version used by GSE116615 is GPL25286 [AMBY_002a520748F], while the version used by both GSE67118 and GSE37198 is GPL15153 [AMBY_002a520748F]. The fourth study, GSE36451, was carried out using the Agilent-019788 Ambystoma Mexicanum platform with version GPL15342 [44k_v3_20080327]. Tables A.1 and A.3 provide detailed information on the selected studies' overall design, number of total and selected samples, and the group types we designed. The groups were categorized into three types; "control" group (intact/amputated/injured limbs and/or flank wounds at 0-hour time points), "wound healing" group (intact/amputated/injured limbs and/or flank wounds up until around 50-hour time points), and "regenerative" group (intact/amputated/injured limbs and/or flank wounds of time points later than around 50 hours to 28dpa). From these datasets, samples that are denervated limbs (in GSE37198) which don't aid in regeneration, or limb buds (in GSE36451) which are distinct from a fully mature amputated limb, were excluded. Totally, 6 samples from

GSE116615 dataset, 198 samples from GSE67118 dataset, 32 samples from GSE37198 dataset, and 77 samples from GSE36451 dataset were selected, forming a total of 313 samples to be analyzed. From these, 26 samples belong to the control group, 93 samples belong to the wound healing group, and 194 belong to the regenerative group (Table 1).

As for the criteria for RNA-seq technology, illustrated in Figure 2, 5 GSE datasets (series) were selected, all of which were performed using slightly different versions of the Illumina Ambystoma Mexicanum platform. The version used by GSE116777 is GPL21473 HiSeq 2000, while the version used by both GSE103087 and GSE92429 is GPL22800 HiSeq 2500, and the version used by both GSE74372 and GSE34394 is GPL14997 Genome Analyzer IIx. Tables A.2 and A.4 provide detailed information on the selected studies' overall design, number of total and selected samples, and the group types we designed. Three group types (control, wound healing, regenerative) were assigned similarly to that of the aforementioned Microarray groups categorization. From GSE116777 dataset, one sample was excluded due to it being an outlier, as identified by the authors [63]. From GSE103087, 4 samples were excluded because they underwent many rounds of amputation-regeneration. From GSE74372, 4 samples were small RNA (sRNA) profiling expression experiments, and so they were excluded. From GSE34394, 8 samples were excluded for being mouse samples. In the last dataset, GSE92429, there are many samples coming from various positions along the axolotl limb, among others, and so the upper-arm samples were selected as part of the control group in order to be as consistent as possible with the other samples from other datasets regarding the investigated site. Two other sample types from the latter dataset, distal and proximal, being the blastemal stage of the regenerating limb, were selected and all other samples were excluded. Totally, 5 samples from GSE116777 dataset, 4 samples from GSE103087 dataset, 7 samples from GSE92429 dataset, 4 samples from GSE74372 dataset, and 12 samples from GSE34394 dataset were selected, forming a total of 32 samples to be analyzed. From these, 7 samples belong to the control group,

7 samples belong to the wound healing group, and 18 belong to the regenerative group (Table 2).

3.2   Whole Gene Expression Data-based Principal Component Analysis

The principal component analysis performed on the z-scored, combined Microarray data having 4322 genes (Figure 4) shows that the first principal component (PC1) roughly separates between the samples based on their group types. This suggests that the source of variation is likely due to differential expression between the group types. The second principal component (PC2), however, separates the samples based on their study origin.

On the other hand, the principal component analysis performed on the voom-counts RNA-seq data having 7562 genes (Figure 5) shows that the first principal component tends to separate the samples based on their study origin, conspicuously between the GSE34394 and the rest. However, the second principal component seems to roughly separate the samples based on their group types. Overall, regarding this whole gene expression data-based principle component analysis approach, it seems that batch factor (study origin) is more important than the time points (group types) to separate the samples in both Microarray and RNA-seq data.
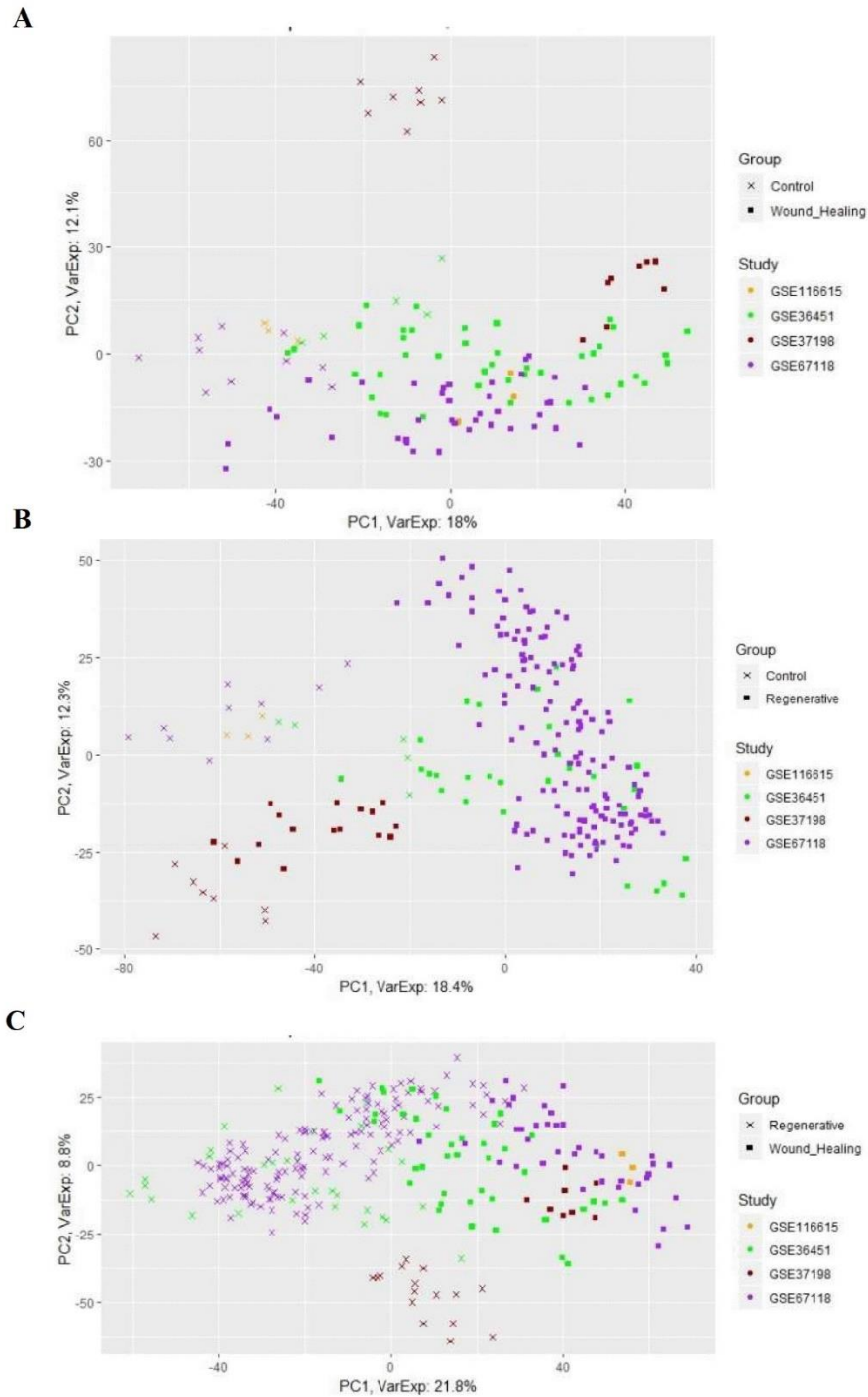
Figure 4: Principal component analysis for the Microarray quantile-normalized, log2-transformed, z-scored, combined data having 4322 genes. A) Control and Wound Healing. B) Control and Regenerative. C) Wound healing and Regenerative. The number of samples per group are: 26 Control, 93 Wound healing, and 194 Regenerative.
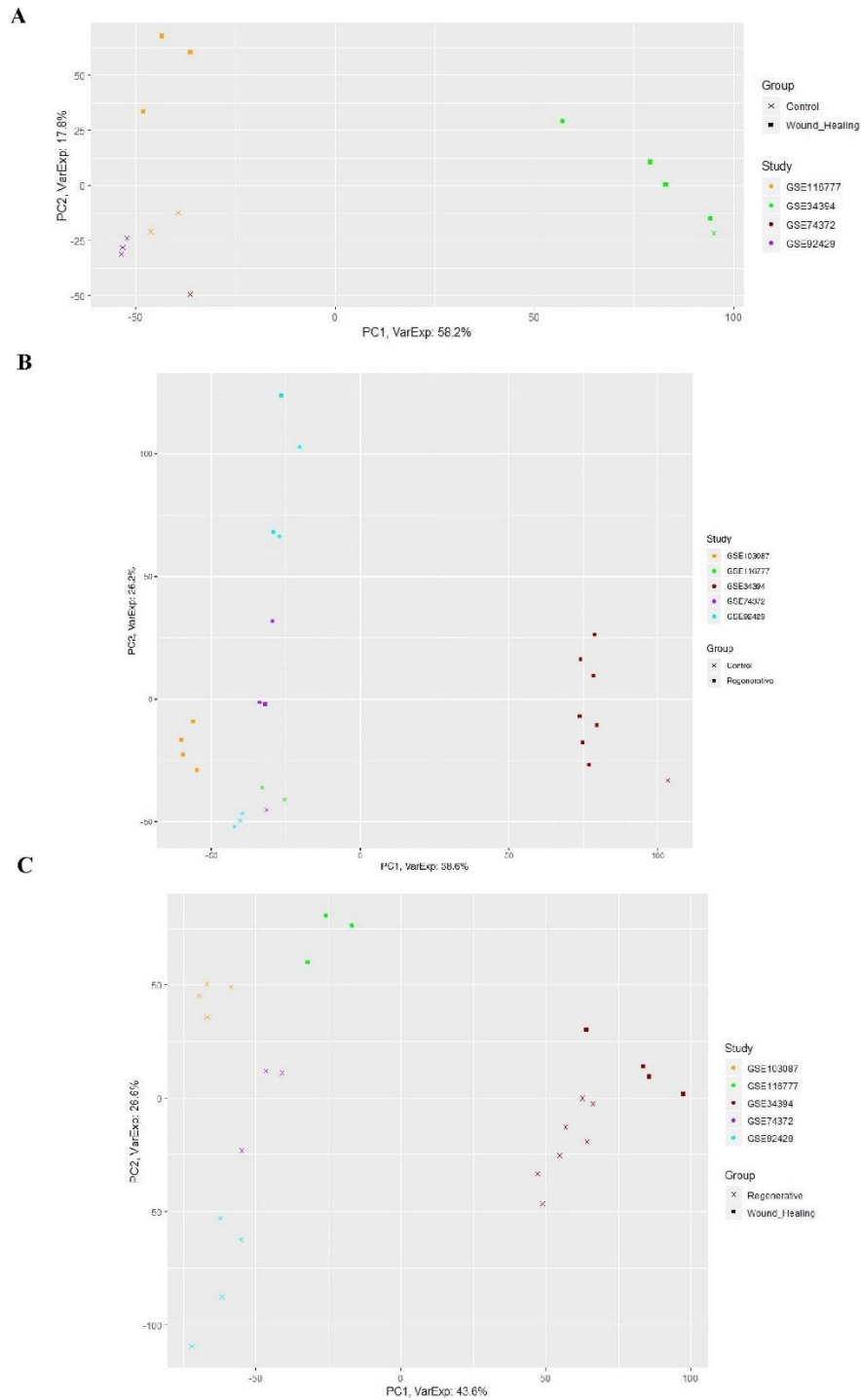
Figure 5: Principal component analysis for the RNA-seq logCPM (voom) counts, having 7562 genes. A) Control and Wound Healing. B) Control and Regenerative. C) Wound healing and Regenerative. The number of samples per group are: 7 Control, 7 Wound healing, and 18 Regenerative.

3.3   Distribution of Raw and Adjusted P-values

For both Microarray (Figure 6) and RNA-seq (Figure 7) DEA results, for every comparison, p-value and adjusted p-value histograms were plotted. Corresponding to true null hypotheses, a uniform distribution for the p-values is expected, with low p-values enrichment corresponding to differentially expressed genes at the near-zero peak. In line with the expectations, p-values of every comparisons from both microarray and RNA-Seq analyses show enrichment near-zero peak corresponding to differentially expressed genes.
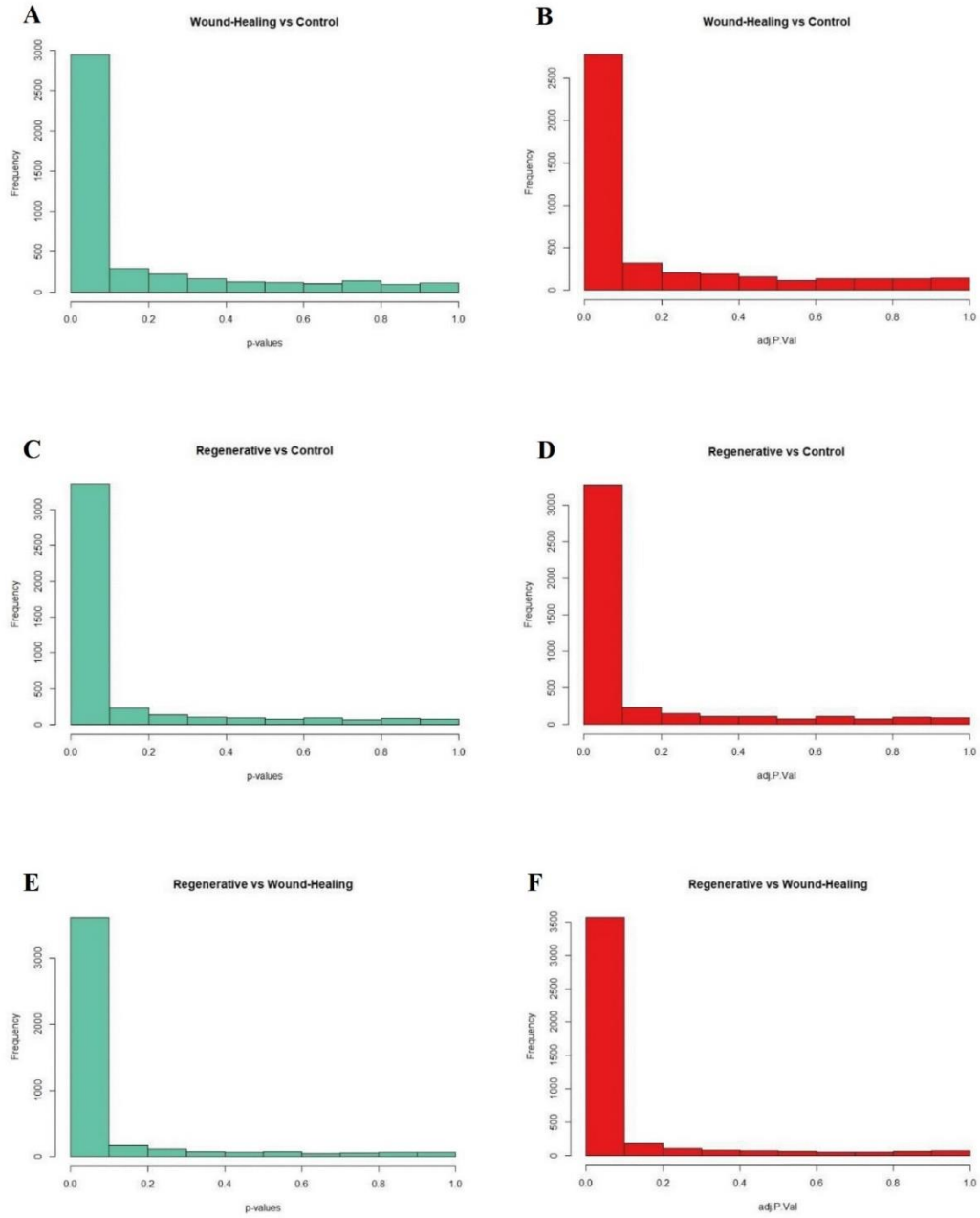
Figure 6: P and adjusted-P value distribution (microarray). p-value histogram (left) and adj.P.Value histogram (right) after DEA on Microarray data for the following comparisons A,B) wound healing vs. control, C,D) regenerative vs. control, E,F) regenerative vs. wound healing.
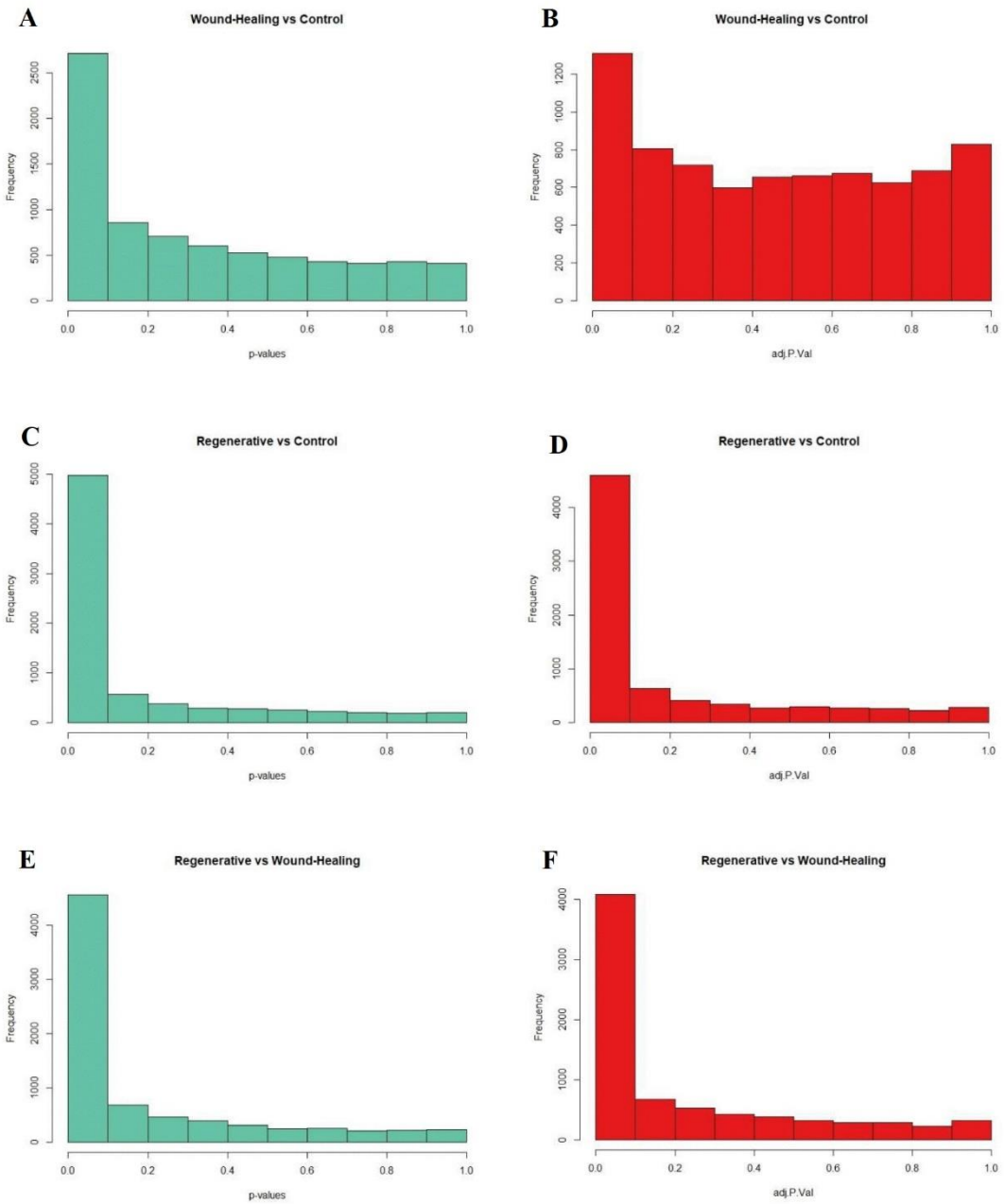
Figure 7: P and adjusted P-value distribution (RNA-Seq). p-value histogram (left) and adj.P.Value histogram (right) after DEA on RNA-seq data for the following comparisons A,B) wound healing vs. control, C,D) regenerative vs. control, E,F) regenerative vs. wound healing.

3.4   DEA-based Principal Component Analysis

The principal component analysis performed on the z-scored, combined Microarray data for the differentially expressed genes of each of the three comparisons (Figure 8) shows that the first principal component (PC1) clearly separates the samples based on their group types. This verifies that the source of variation is due to differential expression between the group types. The second principal component (PC2), however, doesn't seem to strongly indicate any particular type of separation. Wound healing vs. control comparison had 2092 DE genes (adj p-value < 0.01), while regenerative vs. control and regenerative vs. wound healing comparisons had 2748 and 3166 DE genes (adj p-value < 0.01), respectively.

On the other hand, the principal component analysis performed on the voom-counts RNA-seq data for the differentially expressed genes of each of three comparisons (Figure 9) shows that, unlike the whole gene expression data-based PCA, the first principal component (PC1) clearly separates the samples based on their group types, while the second principal component (PC2) seemingly indicate no specific separation of any type. Therefore, the high variation and separation that PC1 illustrates, proves that differential expression between group types is the dominant source of variation. The DEA-based PCA performed on both Microarray and RNA-seq data indicate a successful minimization of the batch effect among studies, making the observation that group types are separated due to differential expression the dominant one. Wound healing vs. control comparison had 423 DE genes (adj p-value < 0.01), while regenerative vs. control and regenerative vs. wound healing comparisons had 2992 and 2371 DE genes (adj p-value < 0.01), respectively.
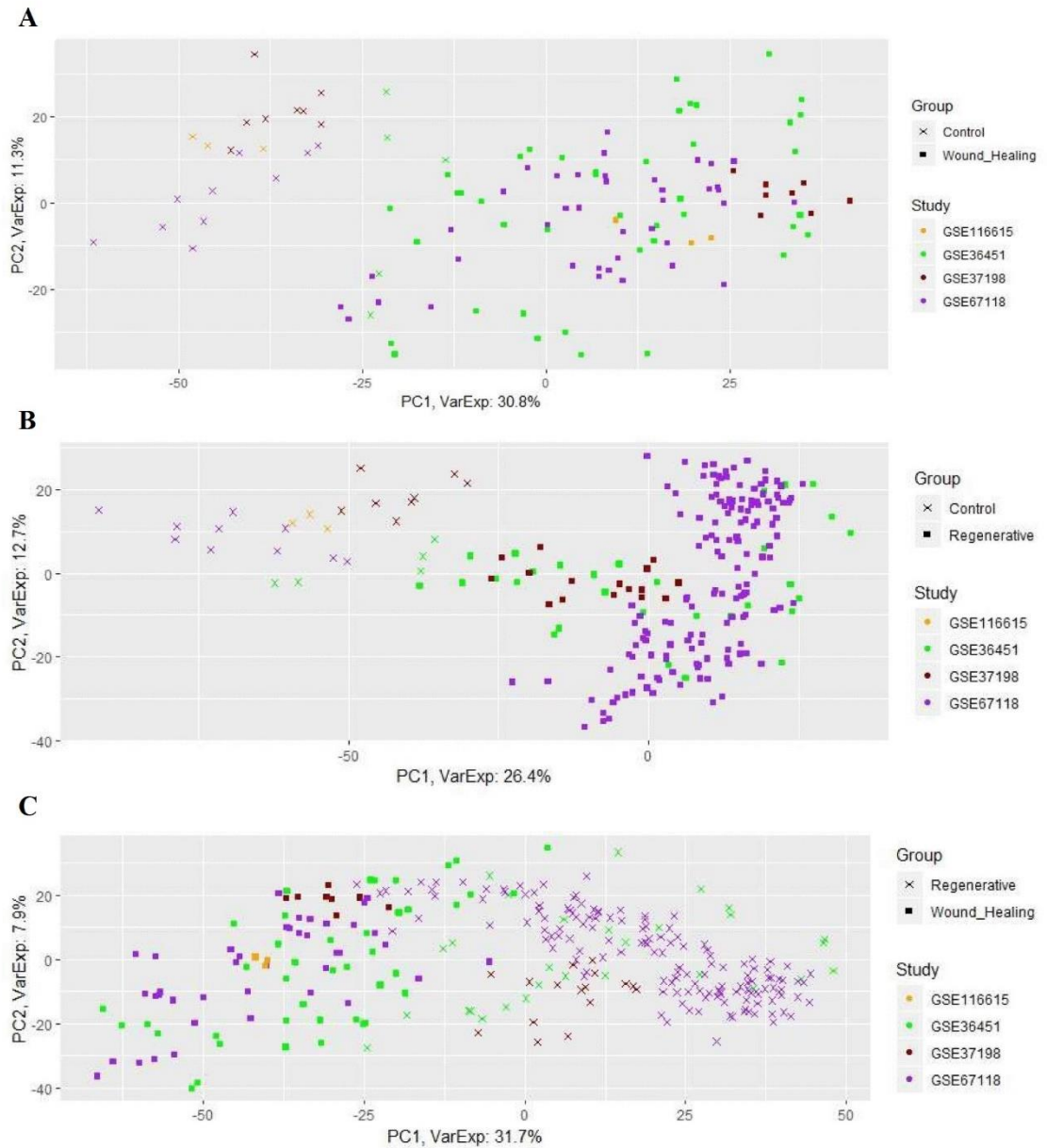
Figure 8: Principal component analysis for the Microarray quantile-normalized, log2-transformed, z-scored, combined data after DEA. A) wound healing vs. control (2092 DE genes, 119 samples). B) regenerative vs. control (2748 DE genes, 220 samples). C) regenerative vs. wound healing (3166 DE genes, 287 samples). The number of samples per group are: 26 Control, 93 Wound healing, and 194 Regenerative. The DE genes have an adjusted p-value < 0.01.
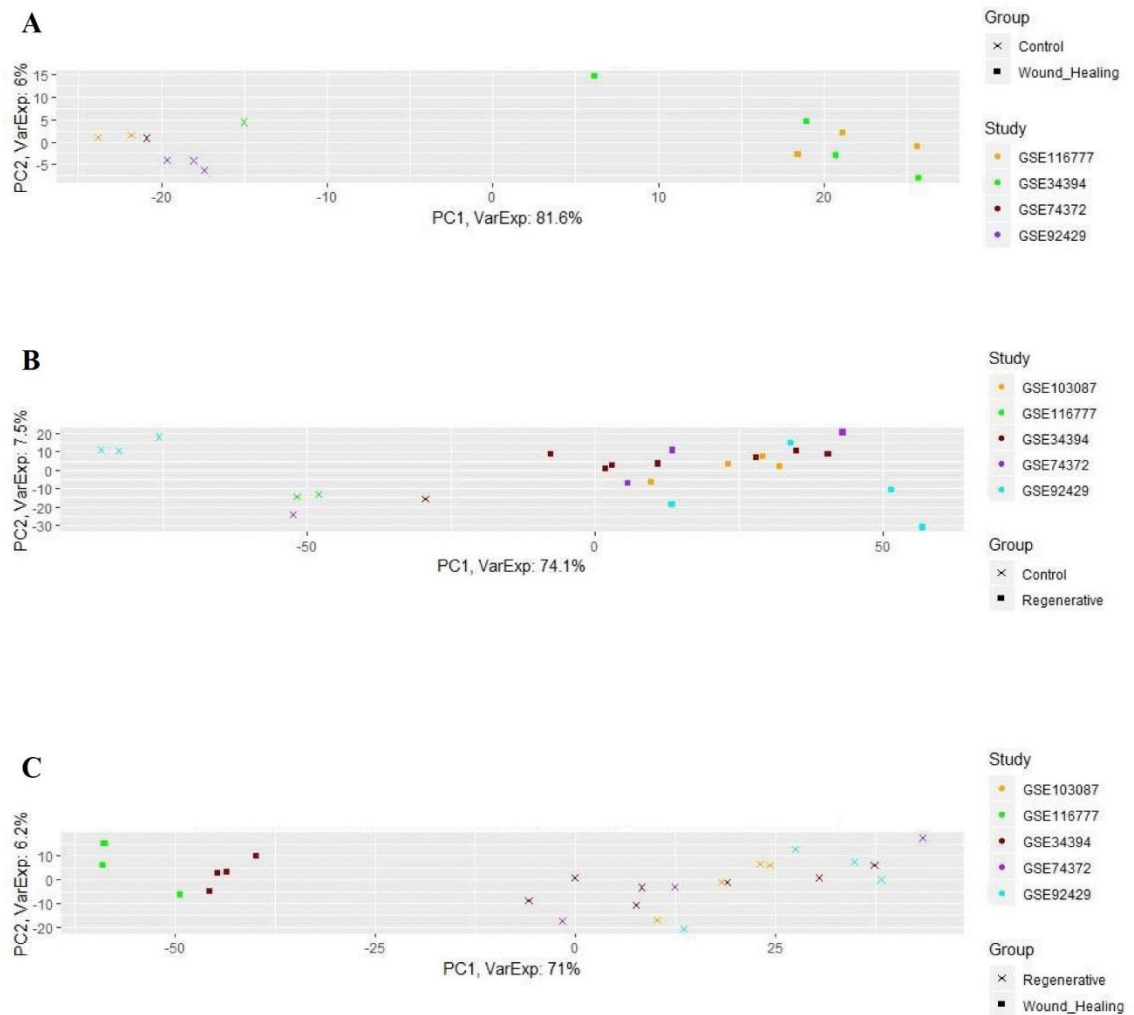
Figure 9: Principal component analysis for the RNA-seq logCPM (voom) counts, after DEA. A) wound healing vs. control (423 DE genes, 14 samples). B) regenerative vs. control (2992 DE genes, 25 samples). C) regenerative vs. wound healing (2371 DE genes, 25 samples). The number of samples per group are: 7 Control, 7 Wound healing, and 18 Regenerative. The DE genes have an adjusted p-value < 0.01.

3.5   Distribution of Differentially Expressed Genes

DE genes from Microarray data were found to be distributed among the three comparisons. I.e. genes may be differentially expressed in one, two, or all of the comparisons (Figure 10).
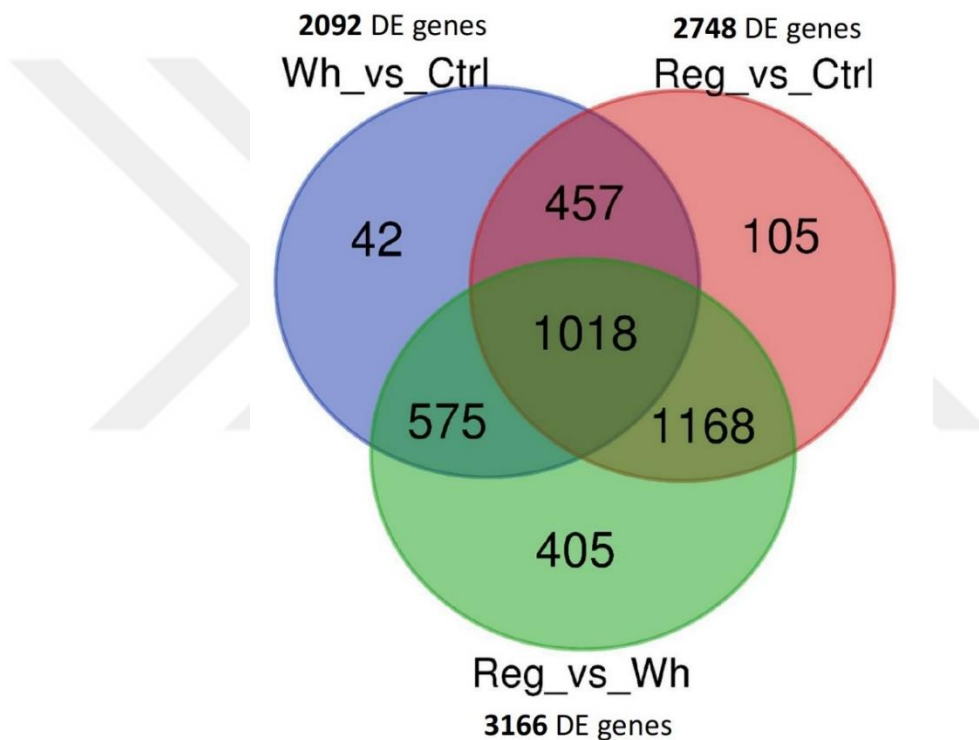
Figure 10: Venn Diagram of the distribution of significantly DE genes (adj.p <0.01) among the three comparisons, from Microarray data; Wound healing (Wh) vs. Control (Ctrl), Regenerative (Reg) vs. Control (Ctrl), and Regenerative (Reg) vs. Wound healing (Wh). Each complete circle represents the number of differentially expressed genes of a certain condition comparison as resulted by DEA.

There are 42 genes uniquely DE in wound healing vs. control comparison, 105 genes uniquely DE in regenerative vs. control comparison, and 405 genes uniquely DE in regenerative vs. wound healing comparison. There are 457 genes commonly DE in

regenerative vs. control and wound healing vs. control comparisons, 1168 genes commonly DE in regenerative vs. control and regenerative vs. wound healing comparisons, 575 genes commonly DE in wound healing vs. control and regenerative vs. wound healing comparisons, and 1018 genes commonly DE in all three comparisons. Those genes commonly DE among comparisons, however, may not necessarily share the same gene regulation status, i.e., a gene may be up-regulated in one comparison and down-regulated in another comparison. To test this notion, the correlation of the logFC of the genes common in two or more comparisons was calculated in a pair-wise manner and scatter plots were plotted to visualize the differential expression pattern for each gene.

The Spearman correlation coefficients for the logFC of the genes commonly DE in regenerative vs. control and regenerative vs. wound healing comparisons (Figure 11A) as well as in regenerative vs. control and wound healing vs. control comparisons (Figure 11C) are 0.85 and 0.96, respectively.

The positive correlation indicates that the DE genes common in those condition comparisons are mostly regulated in the same direction; meaning that they are mostly either up-regulated or down-regulated at the two different condition comparisons sharing those DE genes. However, the logFC of the 575 genes commonly DE in wound healing vs. control and regenerative vs. wound healing comparisons show a negative correlation, having a Spearman correlation coefficient of – 0.71, indicating that those genes are mostly oppositely regulated in these two different condition comparisons, i.e., most of those 575 genes are up-regulated in one of the two comparisons and down-regulated in the other comparison (Figure 11B).

The pair-wise correlation testing for the 1018 genes DE in all three comparisons shows that the genes shared by all three comparisons follow the same trend as when they are shared by only the two corresponding comparisons (Figure 11D-F), having a positive correlation for regenerative vs. control and regenerative vs. wound healing comparisons (0.52 Spearman correlation coefficient) and for regenerative vs. control and wound healing vs. control comparisons (0.77 Spearman correlation coefficient),

and a negative correlation, though very low magnitude, for regenerative vs. wound healing and wound healing vs. control (-0.02 Spearman correlation coefficient).
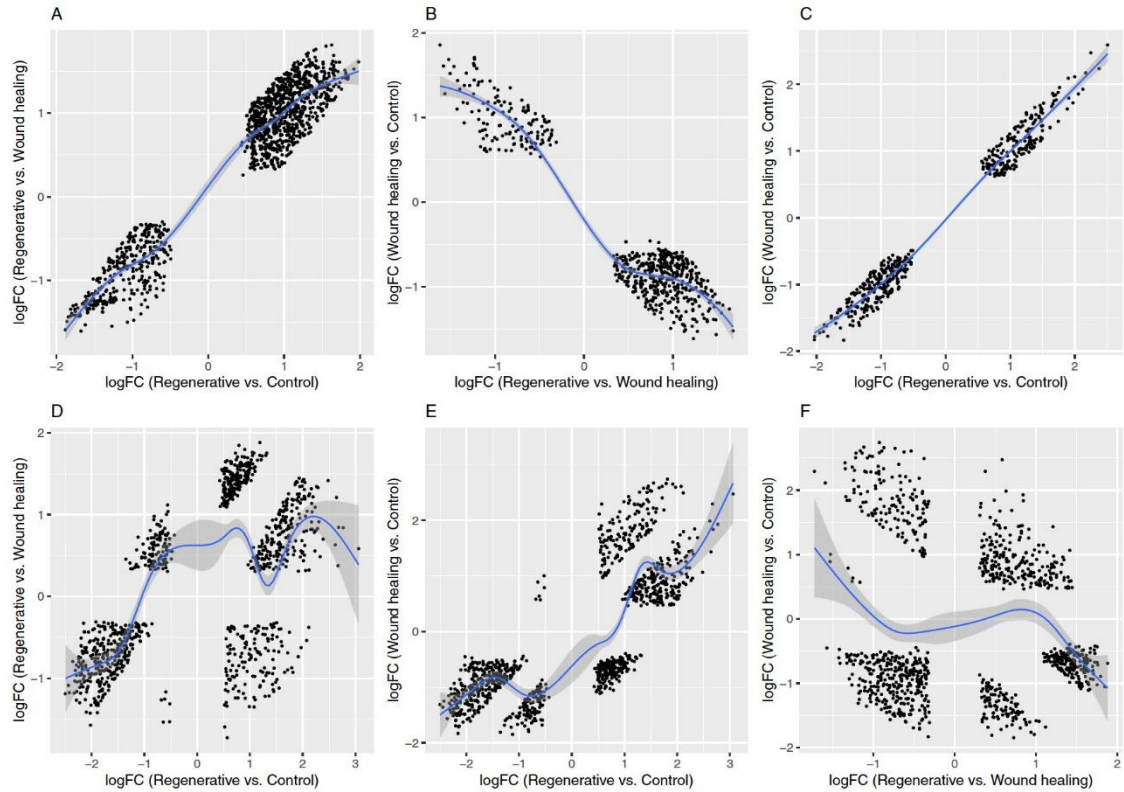
Figure 11: Scatter plot of the log-fold change of significant genes (adj.p <0.01) shared by two or more comparisons as shown in the Venn diagram (Figure 10), from Microarray data. A) Scatter plot of the logFC of the 1168 DE genes shared by Regenerative vs. Control and Regenerative vs. Wound healing comparisons. B) Scatter plot of the logFC of the 575 DE genes shared by Regenerative vs. Wound healing and Wound healing vs. Control comparisons. C) Scatter plot of the logFC of the 457 DE genes shared by Regenerative vs. Control and Wound healing vs. Control comparisons. D-F) Pair-wise scatter plots of the logFC of the 1018 DE genes shared by all three comparisons; D) Regenerative vs. Control and Regenerative vs. Wound healing, E) Regenerative vs. Control and Wound healing vs. Control, F) Regenerative vs. Wound healing and Wound healing vs. Control.

Additionally, DE genes from RNA-seq data were also found to be distributed among the three comparisons (Figure 12). There are 62 genes uniquely DE in wound healing vs. control comparison, 1226 genes uniquely DE in regenerative vs. control comparison, and 573 genes uniquely DE in regenerative vs. wound healing

comparison. There are 145 genes commonly DE in regenerative vs. control and wound healing vs. control comparisons, 1582 genes commonly DE in regenerative vs. control and regenerative vs. wound healing comparisons, 177 genes commonly DE in wound healing vs. control and regenerative vs. wound healing comparisons, and 39 genes commonly DE in all three comparisons.
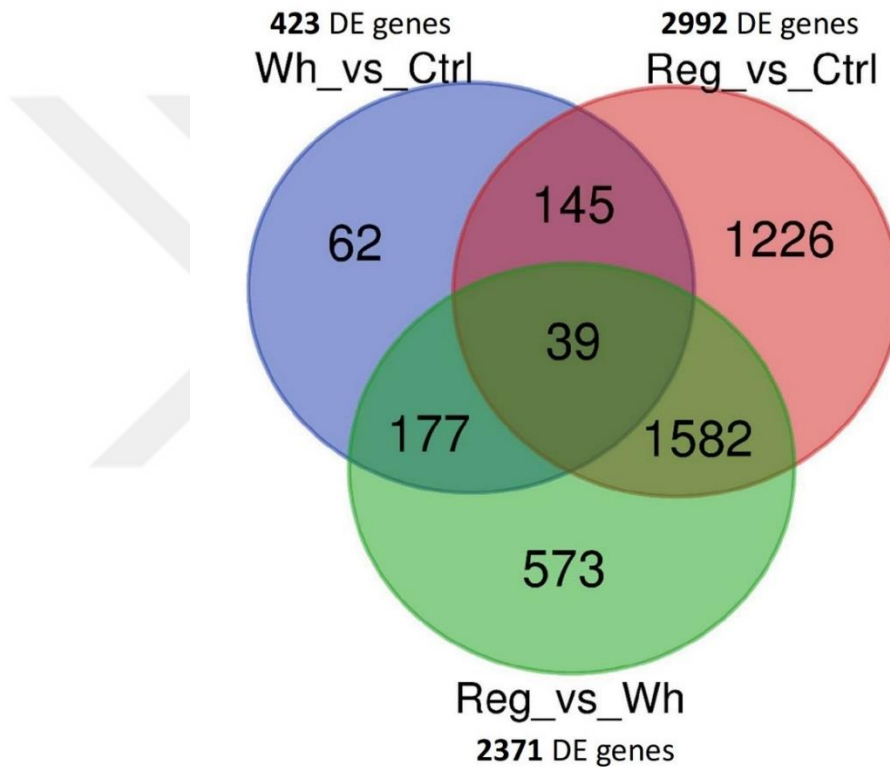
Figure 12: Venn Diagram of the distribution of significant genes (adj.p <0.01) among the three comparisons, from RNA-seq data; Woun -healing (Wh) vs. Control (Ctrl), Regenerative (Reg) vs. Control (Ctrl), and Regenerative (Reg) vs. Wound healing (Wh). Each complete circle represents the number of differentially expressed genes of a certain condition comparison as resulted by DEA.

The correlation of the logFC of the genes common in two or more comparisons was also calculated in a pair-wise manner, and interestingly, the same pattern of gene regulation directionality occurred as with those from Microarray data.

The Spearman correlation coefficients for the logFC of the genes commonly DE in regenerative vs. control and regenerative vs. wound healing comparisons (Figure 13A) as well as in regenerative vs. control and wound healing vs. control comparisons (Figure 13C) are 0.94 and 0.93, respectively.

The positive correlation, therefore, indicates that genes commonly DE in those condition comparisons are mostly either up-regulated or down-regulated. On the other hand, the logFC of the 177 genes commonly DE in wound healing vs. control and regenerative vs. wound healing comparisons have a negative correlation (-0.95 Spearman correlation coefficient), indicating that those genes are mostly up-regulated in one of the two different condition comparisons and down-regulated in the other (Figure 13B).

The 39 genes DE in all three comparisons follow the same gene regulation trend as when they are shared by only the two corresponding comparisons, as shown by pair-wise correlation testing of those genes (Figure 13D-F).
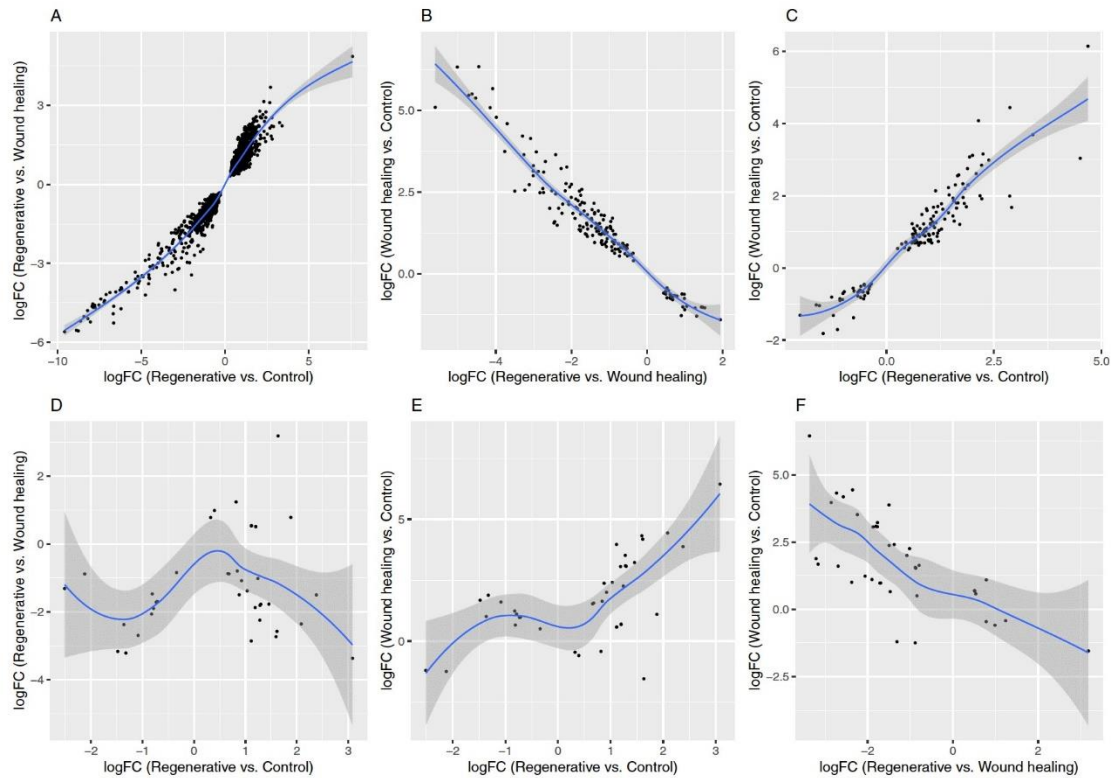
Figure 13: Scatter plot of the log-fold change of significant genes (adj.p <0.01) shared by two or more comparisons as shown in the Venn diagram (Figure 12), from RNA-seq data. A) Scatter plot of the logFC of the 1582 DE genes shared by Regenerative vs. Control and Regenerative vs. Wound healing comparisons. B) Scatter plot of the logFC of the 177 DE genes shared by Regenerative vs. Wound healing and Wound-healing vs. Control comparisons. C) Scatter plot of the logFC of the 145 DE genes shared by Regenerative vs. Control and Wound healing vs. Control comparisons. D-F) Pair-wise scatter plots of the logFC of the 39 DE genes shared by all three comparisons; D) Regenerative vs. Control and Regenerative vs. Wound healing, E) Regenerative vs. Control and Wound healing vs. Control, F) Regenerative vs. Wound healing and Wound healing vs. Control.

The correlation for regenerative vs. control and regenerative vs. wound healing comparisons (0.03 Spearman correlation coefficient) and for regenerative vs. control and wound healing vs. control comparisons (0.54 Spearman correlation coefficient) is positive, and for regenerative vs. wound healing and wound healing vs. control is negative (-0.71 Spearman correlation coefficient).

3.6 Comparison of DE Genes Identified Based on Microarray and RNA-Seq Data

The number of genes used for DEA from Microarray and RNA-seq data was 4322 and 7562, respectively. Because these genes share the same annotation source (AMBY_002a520748F probeset annotation file), there are 3653 genes common between the two technologies (Figure 14).
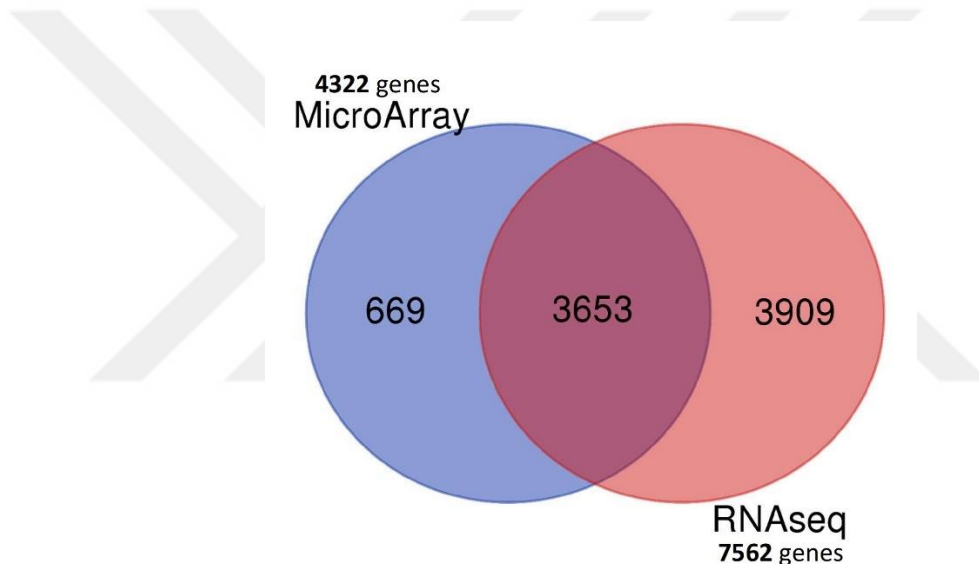
Figure 14: Venn Diagram of the initial number of genes used before differential expression analysis. This number for each platform is obtained just after the filtering and /or merging.

Therefore, there will naturally be varying number of common DE genes per condition comparison between the technologies. By merging the DE lists (adj p-value < 0.01) of both technologies together for each comparison, we found that 170, 1254, and 1047 genes that are DE in wound healing vs. control, regenerative vs. control, and regenerative vs. wound healing comparisons, respectively, are from both technologies (Figure 15A,C,E). The correlation of the logFC of the DE genes common between the technologies for each comparison was calculated and visualized by scatter plots. The

logFC of the 170, 1254, and 1047 genes identified as DE from both technologies in wound healing vs. control, regenerative vs. control, and regenerative vs. wound healing comparisons all have a positive correlation, with a Spearman correlation coefficient of 0.74, 0.71, and 0.77, respectively (Figure 15B,D,F).
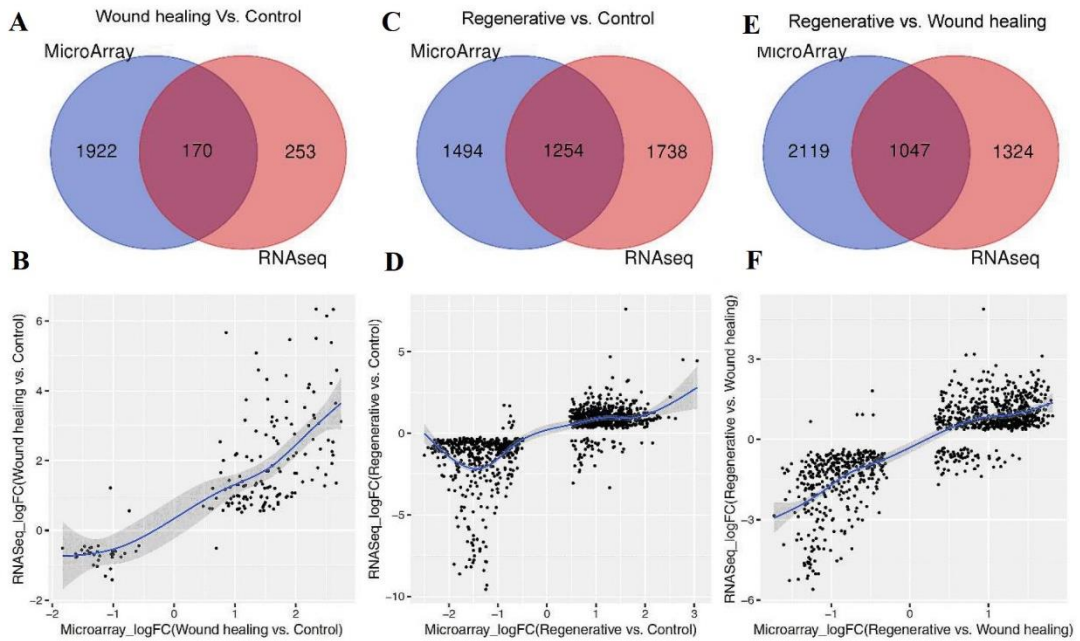
Figure 15: Venn diagrams of the distribution of DE genes (adj p-value < 0.01) between Microarray and RNA-seq data as well as scatter plots of the log-fold change of the common DE genes between the two technologies for A,B) wound healing vs. control, C,D) regenerative vs. control, and E,F) regenerative vs. wound healing

Although our lists of DE genes commonly identified by both technologies are significant (adjusted p-value < 0.01) for each condition comparison, there are many genes that have very low logarithmic fold change (logFC magnitudes < 1). Therefore, a more reliable attribution of "DE" genes would be to extract the top significant genes, by a criterion, from the list of DE genes commonly identified by both technologies. Even though the correlation coefficients of the DE genes between technologies for each comparison was positive with fairly high magnitude, an added benefit to extracting top DE genes would be to further decrease the number of genes with conflicting gene

expression directionality between technologies for each condition comparison. So, the criterion for extracting the top DE genes is as follows: first, genes with logFC magnitudes > 1 are extracted from both Microarray and RNA-Seq DE lists, independently. Then, the resulting two lists are merged together, yielding the top DE genes identified from both microarray and RNA-Seq. Consequently, the extracted top DE genes commonly identified by the two technologies are 91 genes in wound healing vs. control, 351 genes in regenerative vs. control, and 280 genes in regenerative vs. wound healing comparisons. The list of these genes along with their logFC from both technologies is provided in Table A.5. The correlation of the logFC of those top DE genes common between the technologies was also calculated and visualized by scatter plots. The logFC of the 91, 351, and 280 genes identified as the top DE genes from both technologies in wound healing vs. control, regenerative vs. control, and regenerative vs. wound healing comparisons all have an overall positive correlation, with a Spearman correlation coefficient of 0.44, 0.72, and 0.76, respectively (Figure 16).
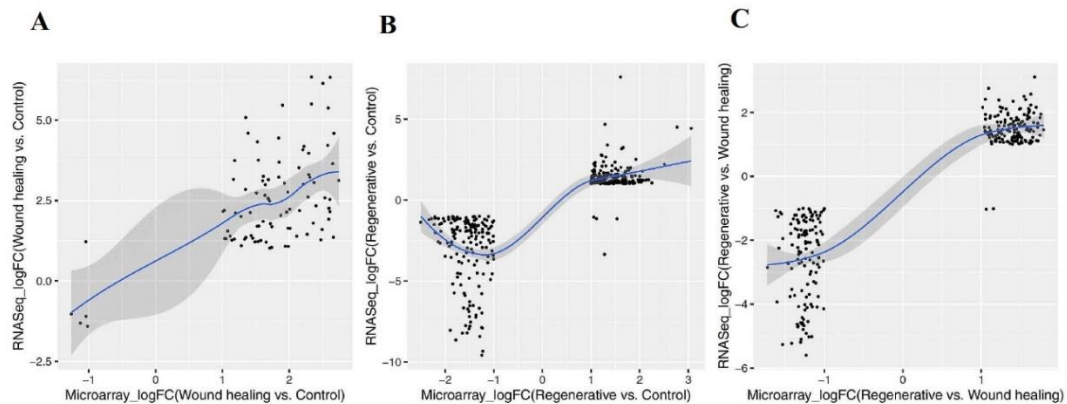
Figure 16: Scatter plots of the log-fold change of the top DE genes (adj p-value < 0.01, logFC magnitudes > 1) commonly identified by Microarray and RNA-seq technologies for A) wound healing vs. control (91 top DE genes), B) regenerative vs. control (351 top DE genes), and C) regenerative vs. wound healing (280 top DE genes).

3.7 Gene Ontology Enrichment Analysis of the Top DE Genes

By using the overrepresentation test, several different gene ontology terms of biological processes, cellular components, and molecular functions were reported to be enriched by the top DE genes commonly identified by both technologies' analyses, for the condition comparisons. The top 86 up-regulated and 4 down-regulated genes in wound healing vs. control comparison enriched 80 GO terms and 2 MF terms, respectively (Table A.6). Among the top biological processes enriched by the top 86 up-regulated genes in the latter comparison are found as: positive regulation of cell death, cytokine-mediated signaling pathway, collagen metabolic process, negative regulation of cell adhesion, positive regulation of cell proliferation, and regulation of cell migration (Figure 17A). The top 181 up-regulated and 166 down-regulated genes in regenerative vs. control comparison enriched 64 and 142 GO terms, respectively (Table A.7). Mitotic nuclear division, chromosome segregation, mitotic spindle organization, RNA splicing, regulation of cell cycle process, and regulation of mRNA metabolic process were seen as the top biological processes enriched by the top 181 up-regulated genes in the latter comparison (Figure 17B). On the other hand, muscle filament sliding, muscle contraction, heart contraction, generation of precursor metabolites and energy, regulation of muscle contraction, and muscle structure development were recognized as the top biological process enriched by the top 166 down-regulated genes in the latter comparison (Figure 17C). A total of 128 and 109 GO terms were enriched by the top 150 up-regulated and 128 down-regulated genes in regenerative vs. wound healing comparison (Table A.8).
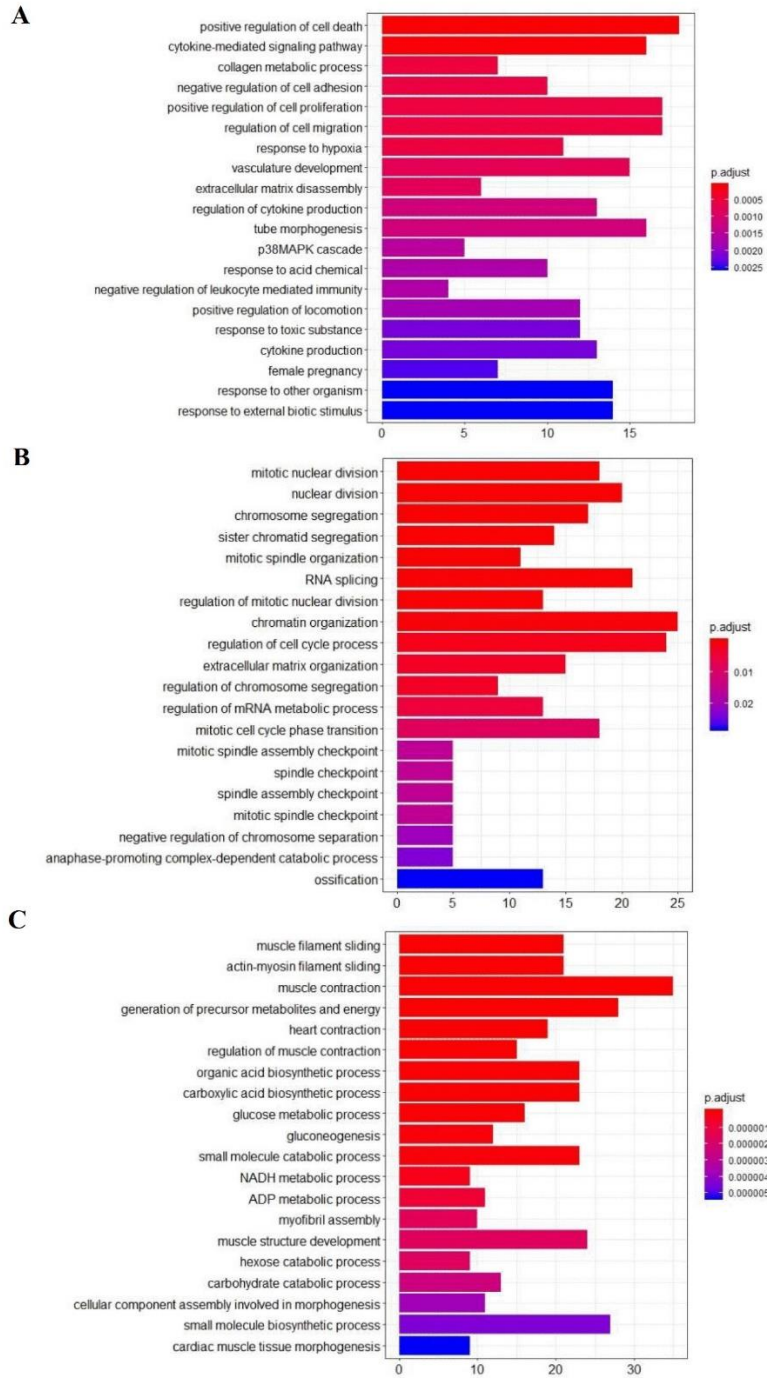
Figure 17: Bar plots showing the top 20 GO biological processes with their corresponding enriched gene counts. The bars are colored according to the adjusted p-value of the corresponding process. A) Top 20 GO processes for the top upregulated genes in wound Healing vs. control comparison. B) Top 20 GO processes for the top upregulated genes in regenerative vs. control comparison. C) Top 20 GO processes for the top downregulated genes in regenerative vs. control comparison. The genes used for the GO enrichment analysis are the top DE genes commonly identified by Microarray and RNA-seq analyses.

Chapter 4

Discussion

In this thesis, integrative data analysis was performed on axolotl gene-expression data. To the best of our current knowledge, this is the first study describing the investigation of differentially expressed genes implicated in the wound healing and regenerative mechanisms of the axolotl limb by integrative analysis of publicly available Microarray and RNA-Seq data.

Although the technical "meta-analysis" (late-stage data integration) method of integrative data analysis has more frequently been used in the literature compared to the early-stage data integration (merging) method [50], the latter method has been applied in multiple studies [50,83–85] and was particularly chosen for the aim of our study. It has been proposed that late-stage data integration performs worse that the direct-merging approach when the purpose is to identify robust biomarkers [50]. In other words, "deriving separate statistics and then averaging is often less powerful than directly computing statistics from aggregated data" [50,86]. For example, cross-platform normalization (early-stage data merging) yielded more differentially-expressed genes than meta-analysis as reported by Taminau *et al*. [53]. Furthermore, when prediction models are applied to a subset of studies, the data merging method can

facilitate the application of these models onto different studies from different platforms [48,50].

While samples from different datasets across different platforms are considered as a single dataset by the "data merging" method for testing the same hypothesis, systematic biases are a common issue [50,53,58,87], wherein they introduce undesirable non-biological differences (batch effects) in the downstream gene signature analysis which can mask the real biological differences among the conditions of interest. Many different intra-laboratory variables are not clearly specified by some labs when their datasets are deposited into GEO and, because of that, we had to presume the uniformity of such variables across different datasets. For example, amputation site, size, feeding, and maintenance protocols of Axolotls are among those factors that can influence the clustering among the investigated samples, especially if a limited number of samples is being analyzed. This could lead to some difficulty in the interpretation of whether samples are inherently different due to gene-expression differences between particular amputation timepoints or due to other kinds of factors which were unaccounted for during the data selection and processing. Therefore, those factors could play a critical role in interpreting the whole gene expression data-based PCA for each condition comparison (Figures 4 and 5). Nevertheless, since one of the major aims of this thesis was to increase sample size as much as possible for gaining more statistical power, those presumed biological variations can be neglected, provided that real biological differences among group types can be clearly observed following differential gene-expression analysis. Indeed, DEA-based PCA showed a clear separation between experimental groups indicating an indecisive role of those presumed factors (Figures 8 and 9). Importantly, the application of transformation and normalization techniques during the process of data merging [50,73] along with accounting for the experiment source (study origin) for each sample while applying DEA using the limma method [78], were the major approaches for minimizing the observation of batch effects and maximizing the observation of gene-expression differences between experiment groups.

The validity and accuracy of conducting DEA on the Microarray and RNA-Seq data can be realized from the consistency of the results obtained from each technology with one another. Firstly, as the Spearman coefficients indicate, every pair-wise distribution of the DE genes among the three condition comparisons from Microarray data (Figures 10 and 11) are consistent with those from RNA-Seq data (Figures 12 and 13). The genes that are commonly DE in regenerative vs. control and regenerative vs. wound healing comparisons always have a positive correlation (Figures 11A,D and 13A,D), as do those genes commonly DE in regenerative vs. control and wound healing vs. control comparisons (Figures 11B,E and 13B,E). Also, the genes that are commonly DE in regenerative vs. wound healing and wound healing vs. control comparisons always have a negative correlation (Figures 11C,F and 13C,F). These consistent correlations also strongly suggest a true biological behavior of those DE genes across the conditions. Secondly, the Spearman correlation coefficients show that the DE genes as well as the top DE genes commonly identified by both Microarray and RNA-Seq data analyses are positively correlated with fairly strong magnitude for each of the three condition comparisons (Figures 15 and 16). Such strong positive correlations between microarray and RNA-Seq data was found in several previous studies [88–91]. Despite having such a positive correlation for most of the DE genes, some genes have opposing gene expression directionality. This might be due to the artifacts of gene expression technologies. However, the number of those genes with opposite direction was found significantly low for the top DE genes (Figure 16). The lower Spearman coefficient which was observed for the top DE genes in wound healing vs. control ($r_s = 44$), despite having only a single inversely correlated gene out of 91, could be attributed to the difference between the logFC range of the DE genes from microarray data and those of RNA-Seq data. Consequently, the strength of the logFC magnitude for some genes might significantly differ, and thus, the whole pair-wise correlation would similarly be affected.

In response to limb amputation, the typical wound healing process is characterized by the induction of stress signals and damage-associated molecules [92]. During the first 6-8 hpa, epithelial cells migrate to and cover the amputation site [93], forming the "wound epithelium (WE)" beneath which are extracellular and cellular debris along

with a damaged vasculature [64]. We found thbs1 as the top up-regulated gene in wound healing vs. control comparison, which is specifically highly up-regulated in basal cells of the wound epidermis that lacks a basement membrane at 24 hpa [63,94]. We also found that metalloproteinases (mmp1, mmp3, mmp19) along with their regulator timp1 [63], which are important to regulate the extracellular matrix and enriched in the wound epidermis immediately after injury [95], to be amongst the top up-regulated wound healing vs. control genes, as were extracellular matrix-generating components such as tnc [63]. At the wound healing phase, innate immunity elements; neutrophils, macrophages, and granulocytes are infiltrated into the regenerating limb at around 24 hpa [17]. Our wound healing vs. control top up-regulated genes also enriched several immunological processes, such as tissue histolysis (mmp1, mmp3, mmp19, timp1), inflammation (ptgs2), and host-defense molecules at the site of injury (zyx, mpo, cybb) [63]. In addition to innate immunity components, some biomarkers of leukocytes (lgals9, mpo) were also up-regulated [63]. In response to leukocytes infiltration, chemokines are expected to be released [63], and our results confirmed that some of genes (arg1, bcl2l1, cxcr4, egr1, hmox1, junb, lmnb1, mmp1, mmp2, mmp3, peli1, ptgs2, socs1, sqstm1, timp1, ywhaz) were up-regulated in wound healing vs. control data and these genes were enriched in cytokine-mediated signaling pathway GO term. Many of those genes enriched a variety of other GO terms associated with tissue development, cell death, proliferation, migration, and immune responses, which is probably due to the fact that most of those processes are activated by the cytokine signaling pathway [63].

It's been previously shown that when the regeneration phase starts at 2 dpa onwards, genes that are up-regulated within this interval enrich terms associated with DNA replication, mitosis, and the cell cycle [25]. The majority of these genes are up-regulated during the 2-3 dpa interval, marking a transition phase in the limb regeneration program, after which they either gradually increase or sustain a relatively constant expression until the 28 dpa period [25]. We similarly found that the regenerative vs. control top up-regulated genes enriched many cell cycle related GO terms, such as positive regulation of cell cycle (apex1, aurka, aurkb, ccnj, fen1, hcfc1, kif23, mad2l1, mtbp, nipbl, pggt1b, rps6kb1, sfpq), mitotic nuclear division (aurka,

aurkb, ccnj, cdc20, cdca8, flna, kif11, kif22, kif23, mad2l1, mad2l1bp, mtbp, nek2, nipbl, plk1, prc1, rcc1, trip13), and DNA conformation change (asf1b, hells, hist3h2bb, hmgb2, nasp, nipbl, rpa2, sart3, top1, top2b). This indicates that the distal limb stump undergoes a remarkable change in the population of proliferative cells due the punctuated increase in the transcripts associated with cell cycle processes [25].

The expression of muscle-specific genes has previously been reported to be significantly reduced during limb regeneration [24,25,63,66,96]. Although muscle tissue remodeling is observed in the limb stump along with reduced muscle-specific transcripts during early response to limb amputation [63], by around 10 dpa the expression of those muscle-specific genes significantly drops, implying absence of muscle tissues [25]. It's been propounded that for progenitor cells to be recruited and for blastemal outgrowth to be initiated, muscle tissue depletion is necessary in the blastemal area [63]. Indeed, our top down-regulated regenerative vs. control genes enriched many muscle tissue-specific GO terms, including muscle filament sliding (acta1, actc1, actn3, des, mybpc2, mybpc3, myh2, myh4, myh7, myl1, myl2, myl3, myl4, tnnc1, tnnc2, tnni1, tnni2, tnnt1, tnnt3, tpm1, tpm3), regulation of muscle contraction (abat, actn3, anxa6, bin1, mybpc3, myh7, myl2, myl3, tnnc1, tnnc2, tnni1, tnni2, tnnt1, tnnt3, tpm1), and muscle cell development (acta1, actc1, bin1, mybpc2, mybpc3, myh10, myl2, myoz1, tnnt1, tnnt3, tpm1). In addition, it was previously documented that the regenerative phase, especially around 10 dpa, undergoes reduction in metabolic processes-associated transcripts [25,63]. Among the top down-regulated regenerative vs. control genes, we also found some genes that enriched a variety of cellular metabolic GO processes such as NADH metabolic process (actn3, gapdh, gpd1, gpi, mdh2, pfkm, pgk1, slc25a12, tpi1), ATP biosynthetic process (actn3, gapdh, gpd1, gpi, pfkm, pgk1, pgm1, prkag2, slc25a12, tpi1), and regulation of ATPase activity (atp1b2, gabarapl2, mybpc3, myl3, myl4, tnnc1, tnnt3, tpm1). It's been also shown that, although muscle-specific genes are significantly down-regulated over the regenerative phase, some of the metabolic genes do not drop in such an absolute manner, but instead they moderately drop during the regenerative phase [63]. It is suggested that, unlike the cells that die or undergo reprogramming, some other cells make up for the lost cellular metabolic genes, and thus, this moderate and incomplete

44

metabolic gene expression is observed [63]. Likewise, we did observe this kind of relationship between the muscle-specific genes (myh6, myh3, mybpc3, myl1, myl2, myl3, tpm1), most of which are among the top down-regulated regenerative vs. control genes, and some of the metabolic genes that function in the electron transport chain and locate to mitochondria (dld, ndufb9, ndufc2, ndufs7, ndufv2, slc25a12, uqcrc2, uqcrfs1), most of which are not among the top DE genes, but rather among the down-regulated regenerative vs. control genes. However, all of those metabolic genes are much less down-regulated than the muscle-specific genes over the regenerative phase. Notably, when our "top DE genes" is discussed, it's referring to those top DE genes commonly identified by the analyses of both Microarray and RNA-Seq. However, two of the aforementioned muscle-specific genes (myh6, myh3) and the metabolic gene (ndufv2) are actually found DE (adj p-value < 0.01) only in RNA-Seq DEA. In fact, those 3 genes were never part of the 4322-microarray gene list that was used for Microarray DEA. This is important to show that the reliability of our results may be extended to those DE genes identified specifically by RNA-Seq DEA, and not to be limited to those DE gene commonly identified by both technologies, because many genes that were used for RNA-Seq DEA were not represented in the final 4322 Microarray gene list due to the merging of Affymetrix gene list (whose annotation file was also used for RNA-Seq annotation) with that of Agilent's. One could argue that the use of Agilent dataset may not have been necessary. However, besides the obvious reason that including the Agilent dataset increases the sample size (which is one of the fundamental premises for a more successful integrative data analysis), another reason is that the results one might get from excluding the Agilent dataset might be biased towards the popularity of the Affymetrix platform. Therefore, by analyzing different platforms of Microarray technology as well as similar versions of the same Illumina RNA-Seq platform, we probably minimized any such bias.

While the utilized cross-platform normalization (merging) methodology works quite well for robust biomarker discovery, there are some inherent limitations to be recognized. Despite our successful efforts to minimize between-laboratory heterogeneity (batch effects) across experiments, the merging method cannot guarantee the complete removal of such effects. Moreover, integrative analysis methods may

provide power through increased sample size at the expense of the analyzed number of genes. Genes which are not common in all integrated platforms are lost, and consequently, a decline in the number of genes to be analyzed was observed. Although the results were concordant with the literature and consistent within and between both technologies, the quality of the deposited, original data may be a limiting factor for having the most accurate, statistically sound results.

Chapter 5

Conclusion

To our knowledge, this thesis describes the first technical approach for integrative publicly available Microarray and RNA-Seq axolotl data analyses, aiming at unraveling differentially expressed genes marking the wound healing and regenerative phases of the axolotl limb. The Microarray and RNA-Seq DEAs showed consistent results manifested in the same pattern of distribution of DE genes, as well as the positive correlation of the DE genes and the top DE genes commonly identified by both technologies, across the wound healing vs. control, regenerative vs. control, and regenerative vs. wound healing comparisons. Many of our top DE genes were previously identified as significantly differentially expressed, and their enrichment in a wide variety of biological processes was concordant with those described in previous studies. Some DE genes resulting from only RNA-Seq DEA also showed similar concordance. Future direction of this study would aim to functionally validate some of our top DE genes and perhaps identify some of them as biomarkers for the wound healing and regenerative phases of the axolotl limb. Besides, the described bioinformatic methodology can be further expanded to include various other statistical approaches, such as performing differential expression analysis among all experimental groups at once using the ANOVA test or the limma package, followed

by hierarchical clustering-based heatmap generation in order to have a unified visualization and interpretation of the data. We hope that our study provides enough confidence for researchers around the world to consider our DE lists for their functional studies and perhaps to integrate their data into our methodology in order to increase the sample size, and thereby obtaining even higher statistical confidence for biomarker discovery.

Bibliography

1. McCusker C, Bryant S V., Gardiner DM. The axolotl limb blastema: cellular and molecular mechanisms driving blastema formation and limb regeneration in tetrapods. Regeneration. 2015; doi:10.1002/reg2.32

2. Shaffer HB. Phylogenetics of model organisms: The laboratory axolotl, ambystoma mexicanum. Syst Biol. 1993; doi:10.1093/sysbio/42.4.508

3. Carlson BM. Principles of Regenerative Biology. Principles of Regenerative Biology. 2007. doi:10.1016/B978-0-12-369439-3.X5000-4

4. Tompkins R. Genie control of axolotl metamorphosis. Integr Comp Biol. 1978; doi:10.1093/icb/18.2.313

5. Galliot B, Ghila L. Cell plasticity in homeostasis and regeneration. Mol Reprod Dev. 2010; doi:10.1002/mrd.21206

6. Cano-Martínez A, Vargas-González A, Guarner-Lans V, Prado-Zayago E, León-Olea M, Nieto-Lima B. Functional and structural regeneration in the axolotl heart (Ambystoma mexicanum) after partial ventricular amputation. Archivos de Cardiologia de Mexico. 2010.

7. Nakamura R, Koshiba-Takeuchi K, Tsuchiya M, Kojima M, Miyazawa A, Ito K, et al. Expression analysis of Baf60c during heart regeneration in axolotls and neonatal mice. Dev Growth Differ. 2016; doi:10.1111/dgd.12281

8. Natarajan N, Abbas Y, Bryant DM, Gonzalez-Rosa JM, Sharpe M, Uygur A, et al.

Complement Receptor C5aR1 Plays an Evolutionarily Conserved Role in Successful Cardiac Regeneration. Circulation. 2018; doi:10.1161/CIRCULATIONAHA.117.030801

9. Tazaki A, Tanaka EM, Fei JF. Salamander spinal cord regeneration: The ultimate positive control in vertebrate spinal cord regeneration. Developmental Biology. 2017. doi:10.1016/j.ydbio.2017.09.034

10. Amamoto R, Huerta VGL, Takahashi E, Dai G, Grant AK, Fu Z, et al. Adult axolotls can regenerate original neuronal diversity in response to brain injury. Elife. 2016; doi:10.7554/eLife.13998

11. Monaghan JR, Stier AC, Michonneau F, Smith MD, Pasch B, Maden M, et al. Experimentally induced metamorphosis in axolotls reduces regenerative rate and fidelity. Regeneration. 2014; doi:10.1002/reg2.8

12. Demircan T, Ovezmyradov G, Yıldırım B, Keskin İ, İlhan AE, Fesçioğlu EC, et al. Experimentally induced metamorphosis in highly regenerative axolotl (ambystoma mexicanum) under constant diet restructures microbiota. Sci Rep. 2018; doi:10.1038/s41598-018-29373-y

13. Tompkins R, Townsend JK. Control of metamorphic events in a neotenous urodele Ambystoma mexicanum. J Exp Zool. 1977; doi:10.1002/jez.1402000124

14. Mescher AL, Neff AW. Regenerative capacity and the developing immune system. Advances in Biochemical Engineering/Biotechnology. 2005. doi:10.1007/b99966

15. Campbell LJ, Crews CM, Sciences ML. Wound epidermis formation and function in urodele amphibian limb regeneration. Cell Mol Life Sci. 2008; doi:10.1007/s00018-007-7433-z

16. Haas BJ, Whited JL. Advances in Decoding Axolotl Limb Regeneration. Trends in Genetics. 2017. doi:10.1016/j.tig.2017.05.006

17. Godwin JW, Pinto AR, Rosenthal NA. Macrophages are required for adult salamander limb regeneration. Proc Natl Acad Sci. 2013; doi:10.1073/pnas.1300290110

18. Kragl M, Knapp D, Nacu E, Khattak S, Maden M, Epperlein HH, et al. Cells keep a memory of their tissue origin during axolotl limb regeneration. Nature. 2009. doi:10.1038/nature08152

19. Knapp D, Schulz H, Rascon CA, Volkmer M, Scholz J, Nacu E, et al. Comparative Transcriptional Profiling of the Axolotl Limb Identifies a Tripartite Regeneration-Specific Gene Program. PLoS One. 2013; doi:10.1371/journal.pone.0061352

20. Nacu E, Gromberg E, Oliveira CR, Drechsel D, Tanaka EM. FGF8 and SHH substitute for anterior-posterior tissue interactions to induce limb regeneration. Nature. 2016; doi:10.1038/nature17972

21. Han MJ, An JY, Kim WS. Expression patterns of Fgf-8 during development and limb regeneration of the axolotl. Dev Dyn. 2001; doi:10.1002/1097-0177(2000)9999:9999<::AID-DVDY1085>3.0.CO;2-8

22. Sugiura T, Wang H, Barsacchi R, Simon A, Tanaka EM. MARCKS-like protein is an initiating molecule in axolotl appendage regeneration. Nature. 2016; doi:10.1038/nature16974

23. Gorsic M, Majdic G, Komel R. Identification of differentially expressed genes in 4-day axolotl limb blastema by suppression substractive hybridization. J Physiol Biochem. 2008; doi:10.1007/BF03168233

24. Monaghan JR, Epp LG, Putta S, Page RB, Walker JA, Beachy CK, et al. Microarray and cDNA sequence analysis of transcription during nerve-dependent limb regeneration. BMC Biol. 2009; doi:10.1186/1741-7007-7-1

25. Voss SR, Palumbo A, Nagarajan R, Gardiner DM, Muneoka K, Stromberg AJ, et al. Gene expression during the first 28 days of axolotl limb regeneration I: Experimental design and global analysis of gene expression. Regeneration. 2015; doi:10.1002/reg2.37

26. Koshiba K, Kuroiwa A, Yamamoto H, Tamura K, Ide H. Expression of Msx genes in regenerating and developing limbs of axolotl. Journal of Experimental Zoology. 1998. doi:10.1002/(SICI)1097-010X(19981215)282:6<703::AID-JEZ6>3.0.CO;2-P

27. Carlson MRJ, Bryant S V., Gardiner DM. Expression of Msx-2 during development, regeneration, and wound healing in axolotl limbs. Journal of Experimental Zoology. 1998. doi:10.1002/(SICI)1097-010X(19981215)282:6<715::AID-JEZ7>3.0.CO;2-F

28. Ghosh S, Roy S, Séguin C, Bryant S V., Gardiner DM. Analysis of the expression and function of Wnt-5a and Wnt-5b in developing and regenerating axolotl (Ambystoma mexicanum) limbs. Dev Growth Differ. 2008; doi:10.1111/j.1440-169X.2008.01000.x

29. Kawakami Y, Esteban CR, Raya M, Kawakami H, Martí M, Dubova I, et al. Wnt/β-catenin signaling regulates vertebrate limb regeneration. Genes Dev. 2006; doi:10.1101/gad.1475106

30. Bryant DM, Johnson K, DiTommaso T, Tickle T, Couger MB, Payzin-Dogru D, et al. A Tissue-Mapped Axolotl De Novo Transcriptome Enables Identification of Limb Regeneration Factors. Cell Rep. 2017; doi:10.1016/j.celrep.2016.12.063

31. Yun MH, Gates PB, Brockes JP. Regulation of p53 is critical for vertebrate limb regeneration. Proc Natl Acad Sci. 2013; doi:10.1073/pnas.1310519110

32. Villiard É, Brinkmann H, Moiseeva O, Mallette FA, Ferbeyre G, Roy S. Urodele p53 tolerates amino acid changes found in p53 variants linked to human cancer. BMC Evol Biol. 2007; doi:10.1186/1471-2148-7-180

33. Gatien S, Sader F, Villiard É, Philip A, Denis J-F, Roy S. Activation of Smad2 but not Smad3 is required to mediate TGF-β signaling during axolotl limb regeneration. Development. 2016; doi:10.1242/dev.131466

34. Khattak S, Murawala P, Andreas H, Kappert V, Schuez M, Sandoval-Guzmán T, et al. Optimized axolotl (Ambystoma mexicanum) husbandry, breeding, metamorphosis, transgenesis and tamoxifen-mediated recombination. Nat Protoc. 2014; doi:10.1038/nprot.2014.040

35. Sobkow L, Epperlein HH, Herklotz S, Straube WL, Tanaka EM. A germline GFP transgenic axolotl and its use to track cell fate: Dual origin of the fin mesenchyme during development and the fate of blood cells during regeneration. Dev Biol. 2006;

doi:10.1016/j.ydbio.2005.11.037

36. Crews CM, Flowers GP, Timberlake AT, Monaghan JR, Mclean KC. Highly efficient targeted mutagenesis in axolotl using Cas9 RNA-guided nuclease. Development. 2014; doi:10.1242/dev.105072

37. Fei JF, Schuez M, Tazaki A, Taniguchi Y, Roensch K, Tanaka EM. CRISPR-mediated genomic deletion of Sox2 in the axolotl shows a requirement in spinal cord neural stem cell amplification during tail regeneration. Stem Cell Reports. 2014; doi:10.1016/j.stemcr.2014.06.018

38. Kuo T-H, Kowalko JE, DiTommaso T, Nyambi M, Montoro DT, Essner JJ, et al. TALEN-mediated gene editing of the thrombospondin-1 locus in axolotl. Regeneration. 2015; doi:10.1002/reg2.29

39. Ryan Woodcock M, Vaughn-Wolfe J, Elias A, Kevin Kump D, Kendall KD, Timoshevskaya N, et al. Identification of mutant genes and introgressed tiger salamander DNA in the laboratory axolotl, ambystoma mexicanum. Sci Rep. 2017; doi:10.1038/s41598-017-00059-1

40. Smith JJ, Putta S, Zhu W, Pao GM, Verma IM, Hunter T, et al. Genic regions of a large salamander genome contain long introns and novel genes. BMC Genomics. 2009; doi:10.1186/1471-2164-10-19

41. Nowoshilow S, Schloissnig S, Fei JF, Dahl A, Pang AWC, Pippel M, et al. The axolotl genome and the evolution of key tissue formation regulators. Nature. 2018; doi:10.1038/nature25458

42. Jiang P, Nelson JD, Leng N, Collins M, Swanson S, Dewey CN, et al. Analysis of embryonic development in the unsequenced axolotl: Waves of transcriptomic upheaval and stability. Dev Biol. 2017; doi:10.1016/j.ydbio.2016.05.024

43. Demircan T, Keskin I, Dumlu SN, Aytürk N, Avşaroğlu ME, Akgün E, et al. Detailed tail proteomic analysis of axolotl (Ambystoma mexicanum) using an mRNA-seq reference database. Proteomics. 2017; doi:10.1002/pmic.201600338

44. Rao N, Jhamb D, Milner DJ, Li B, Song F, Wang M, et al. Proteomic analysis of

blastema formation in regenerating axolotl limbs. BMC Biol. 2009; doi:10.1186/1741-7007-7-83

45. King BL, Yin VP. A conserved microRNA regulatory circuit is differentially controlled during limb/appendage regeneration. PLoS One. 2016; doi:10.1371/journal.pone.0157106

46. Gerber T, Murawala P, Knapp D, Masselink W, Schuez M, Hermann S, et al. Single-cell analysis uncovers convergence of cell identities during axolotl limb regeneration. Science (80-). 2018; doi:10.1126/science.aaq0681

47. Brown LA, Peirson SN. Improving Reproducibility and Candidate Selection in Transcriptomics Using Meta-analysis. J Exp Neurosci. 2018; doi:10.1177/1179069518756296

48. Tseng GC, Ghosh D, Feingold E. Comprehensive literature review and statistical considerations for microarray meta-analysis. Nucleic Acids Research. 2012. doi:10.1093/nar/gkr1265

49. Hu P, Wang X, Haitsma JJ, Furmli S, Masoom H, Liu M, et al. Microarray Meta-Analysis Identifies Acute Lung Injury Biomarkers in Donor Lungs That Predict Development of Primary Graft Failure in Recipients. PLoS One. 2012; doi:10.1371/journal.pone.0045506

50. Walsh C, Hu P, Batt J, Santos C. Microarray Meta-Analysis and Cross-Platform Normalization: Integrative Genomics for Robust Biomarker Discovery. Microarrays. 2015; doi:10.3390/microarrays4030389

51. Nadon R, Shoemaker J. Statistical issues with microarrays: Processing and analysis. Trends in Genetics. 2002. doi:10.1016/S0168-9525(02)02665-3

52. Hamid JS, Beyene J, Ling V, Greenwood CMT, Hu P, Roslin NM. Data Integration in Genetics and Genomics: Methods and Challenges. Hum Genomics Proteomics. 2009; doi:10.4061/2009/869093

53. Taminau J, Lazar C, Meganck S, Nowé A. Comparison of Merging and Meta-Analysis as Alternative Approaches for Integrative Gene Expression Analysis. ISRN

Bioinforma. 2014; doi:10.1155/2014/345106

54. Ramasamy A, Mondry A, Holmes CC, Altman DG. Key Issues in Conducting a Meta-Analysis of Gene Expression Microarray Datasets. PLoS Med. 2008; doi:10.1371/journal.pmed.0050184

55. Hu P, Greenwood CMT, Beyene J. Integrative analysis of multiple gene expression profiles with quality-adjusted effect size models. BMC Bioinformatics. 2005; doi:10.1186/1471-2105-6-128

56. Shabalin AA, Tjelmeland H, Fan C, Perou CM, Nobel AB. Merging two gene-expression studies via cross-platform normalization. Bioinformatics. 2008; doi:10.1093/bioinformatics/btn083

57. Sun Y V., Hu YJ. Integrative Analysis of Multi-omics Data for Discovery and Functional Studies of Complex Human Diseases. Adv Genet. 2016; doi:10.1016/bs.adgen.2015.11.004

58. Turnbull AK, Kitchen RR, Larionov AA, Renshaw L, Dixon JM, Sims AH. Direct integration of intensity-level data from Affymetrix and Illumina microarrays improves statistical power for robust reanalysis. BMC Med Genomics. 2012; doi:10.1186/1755-8794-5-35

59. Edgar R. Gene Expression Omnibus: NCBI gene expression and hybridization array data repository. Nucleic Acids Res. 2002; doi:10.1093/nar/30.1.207

60. Barrett T, Wilhite SE, Ledoux P, Evangelista C, Kim IF, Tomashevsky M, et al. NCBI GEO: Archive for functional genomics data sets - Update. Nucleic Acids Res. 2013; doi:10.1093/nar/gks1193

61. Leinonen R, Akhtar R, Birney E, Bower L, Cerdeno-Tárraga A, Cheng Y, et al. The European nucleotide archive. Nucleic Acids Res. 2011; doi:10.1093/nar/gkq967

62. Moher D, Liberati A, Tetzlaff J, Altman DG, The PRISMA Group. PRISMA 2009 Flow Diagram. PLoS Med. 2009; doi:10.1371/journal.pmed1000097

63. Dwaraka VB, Smith JJ, Woodcock MR, Voss SR. Comparative transcriptomics of

limb regeneration: Identification of conserved expression changes among three species of Ambystoma. Genomics. 2018. doi:10.1016/j.ygeno.2018.07.017

64. Monaghan JR, Athippozhy A, Maden M, Gardiner DM, Seifert AW, Voss SR, et al. Gene expression patterns specific to the regenerating limb of the Mexican axolotl. Biol Open. 2012; doi:10.1242/bio.20121594

65. Bryant DM, Sousounis K, Payzin-Dogru D, Bryant S, Sandoval AGW, Martinez Fernandez J, et al. Identification of regenerative roadblocks via repeat deployment of limb regeneration in axolotls. npj Regen Med. 2017; doi:10.1038/s41536-017-0034-z

66. Stewart R, Rascón CA, Tian S, Nie J, Barry C, Chu LF, et al. Comparative RNA-seq Analysis in the Unsequenced Axolotl: The Oncogene Burst Highlights Early Gene Expression in the Blastema. PLoS Comput Biol. 2013; doi:10.1371/journal.pcbi.1002936

67. Team RC. R: A Language and Environment for Statistical Computing. In: Vienna, Austria. 2018.

68. Huber W, Carey VJ, Gentleman R, Anders S, Carlson M, Carvalho BS, et al. Orchestrating high-throughput genomic analysis with Bioconductor. Nat Methods. 2015; doi:10.1038/nmeth.3252

69. Gentleman RC, Carey VJ, Bates DM, Bolstad BM, Dettling M, Dudoit S, et al. Bioconductor: open software development for computational biology and bioinformatics. Genome Biol. 2004; doi:10.1186/gb-2004-5-10-r80

70. Klaus B. An end to end workflow for differential gene expression using Affymetrix microarrays. F1000Research. 2016; doi:10.12688/f1000research.8967.1

71. Gautier L, Cope L, Bolstad BM, Irizarry RA. Affy - Analysis of Affymetrix GeneChip data at the probe level. Bioinformatics. 2004; doi:10.1093/bioinformatics/btg405

72. Langfelder P, Horvath S. WGCNA: An R package for weighted correlation network analysis. BMC Bioinformatics. 2008; doi:10.1186/1471-2105-9-559

73. Cheadle C, Vawter MP, Freed WJ, Becker KG. Analysis of microarray data using Z

score transformation. J Mol Diagnostics. 2003; doi:10.1016/S1525-1578(10)60455-2

74. Patro R, Duggal G, Love MI, Irizarry RA, Kingsford C. Salmon provides fast and bias-aware quantification of transcript expression. Nat Methods. 2017; doi:10.1038/nmeth.4197

75. Soneson C, Love MI, Robinson MD. Differential analyses for RNA-seq: transcript-level estimates improve gene-level inferences. F1000Research. 2016; doi:10.12688/f1000research.7563.2

76. Robinson MD, McCarthy DJ, Smyth GK. edgeR: a Bioconductor package for differential expression analysis of digital gene expression data. Bioinformatics. 2010; doi:10.1093/bioinformatics/btp616

77. McCarthy DJ, Chen Y, Smyth GK. Differential expression analysis of multifactor RNA-Seq experiments with respect to biological variation. Nucleic Acids Res. 2012; doi:10.1093/nar/gks042

78. Ritchie ME, Phipson B, Wu D, Hu Y, Law CW, Shi W, et al. Limma powers differential expression analyses for RNA-sequencing and microarray studies. Nucleic Acids Res. 2015; doi:10.1093/nar/gkv007

79. Phipson B, Lee S, Majewski IJ, Alexander WS, Smyth GK. Robust hyperparameter estimation protects against hypervariable genes and improves power to detect differential expression. Ann Appl Stat. 2016; doi:10.1214/16-AOAS920

80. Law CW, Chen Y, Shi W, Smyth GK. Voom: Precision weights unlock linear model analysis tools for RNA-seq read counts. Genome Biol. 2014; doi:10.1186/gb-2014-15-2-r29

81. Wickham H. ggplot2: Elegant Graphics for Data Analysis. Journeal Stat Softw. 2017; doi:10.18637/jss.v080.b01

82. Yu G, Wang L-G, Han Y, He Q-Y. clusterProfiler: an R Package for Comparing Biological Themes Among Gene Clusters. Omi A J Integr Biol. 2012; doi:10.1089/omi.2011.0118

83.   Warnat P, Eils R, Brors B. Cross-platform analysis of cancer microarray data improves gene expression based classification of phenotypes. BMC Bioinformatics. 2005; doi:10.1186/1471-2105-6-265

84.   Fielden MR, Nie A, Mcmillian M, Elangbam CS, Trela BA, Yang Y, et al. Forum: Interlaboratory evaluation of genomic signatures for predicting carcinogenicity in the rat. Toxicol Sci. 2008; doi:10.1093/toxsci/kfn022

85.   Lu Y, Lemon W, Liu PY, Yi Y, Morrison C, Yang P, et al. A gene expression signature predicts survival of patients with stage I non-small cell lung cancer. PLoS Med. 2006; doi:10.1371/journal.pmed.0030467

86.   Xu L, Tan AC, Winslow RL, Geman D. Merging microarray data from separate breast cancer studies provides a robust prognostic test. BMC Bioinformatics. 2008; doi:10.1186/1471-2105-9-125

87.   Sims AH, Smethurst GJ, Hey Y, Okoniewski MJ, Pepper SD, Howell A, et al. The removal of multiplicative, systematic bias allows integration of breast cancer gene expression datasets – improving meta-analysis and prediction of prognosis. BMC Med Genomics. 2008; doi:10.1186/1755-8794-1-42

88.   Rao MS, Van Vleet TR, Ciurlionis R, Buck WR, Mittelstadt SW, Blomme EAG, et al. Comparison of RNA-Seq and Microarray Gene Expression Platforms for the Toxicogenomic Evaluation of Liver From Short-Term Rat Toxicity Studies. Front Genet. Frontiers Media S.A.; 2019;9: 636. doi:10.3389/fgene.2018.00636

89.   Kogenaru S, Qing Y, Guo Y, Wang N. RNA-seq and microarray complement each other in transcriptome profiling. BMC Genomics. 2012; doi:10.1186/1471-2164-13-629

90.   Wolff A, Bayerlová M, Gaedcke J, Kube D, Beißbarth T. A comparative study of RNA-Seq and microarray data analysis on the two examples of rectal-cancer patients and Burkitt Lymphoma cells. PLoS One. 2018; doi:10.1371/journal.pone.0197162

91.   Zhao S, Fung-Leung WP, Bittner A, Ngo K, Liu X. Comparison of RNA-Seq and microarray in transcriptome profiling of activated T cells. PLoS One. 2014;

doi:10.1371/journal.pone.0078644

92.   Niethammer P. The early wound signals. Current Opinion in Genetics and Development. 2016. doi:10.1016/j.gde.2016.05.001

93.   Endo T, Bryant S V., Gardiner DM. A stepwise model system for limb regeneration. Dev Biol. 2004; doi:10.1016/j.ydbio.2004.02.016

94.   Whited JL, Lehoczky JA, Austin CA, Tabin CJ. Dynamic expression of two thrombospondins during axolotl limb regeneration. Dev Dyn. 2011; doi:10.1002/dvdy.22548

95.   Yang E V., Gardiner DM, Carlson MRJ, Nugas CA, Bryant S V. Expression of Mmp-9 and related matrix metalloproteinase genes during axolotl limb regeneration. Dev Dyn. 1999; doi:10.1002/(SICI)1097-0177(199909)216:1<2::AID-DVDY2>3.0.CO;2-P

96.   Randal Voss S, Murrugarra D, Jensen TB, Monaghan JR. Transcriptional correlates of proximal-distal identify and regeneration timing in axolotl limbs. Comp Biochem Physiol Part - C Toxicol Pharmacol. 2018; doi:10.1016/j.cbpc.2017.10.010

Appendix

Appendix A

A.1   Microarray Axolotl Dataset Selection

GSE Accession	Year	Title	Publication	# of samples used for analysis
GSE116615	2018	Comparative Transcriptomics of Limb Regeneration: Identification of Conserved Expression Changes Among Three Species of Ambystoma [microarray]	Dwaraka VB, Smith JJ, Woodcock MR, Voss SR. Comparative transcriptomics of limb regeneration: Identification of conserved expression changes among three species of Ambystoma. Genomics 2018 Aug 6. PMID: 30092345	6
GSE67118	2015	Gene Expression During the First 28 Days of Axolotl Limb Regeneration	Voss SR, Palumbo A, Nagarajan R, Gardiner DM et al. Gene expression during the first 28 days of axolotl limb regeneration I: Experimental design and global analysis of gene expression. Regeneration (Oxf) 2015 Jun;2(3):120-136. PMID: 27168937	198
GSE36451	2013	Comparative Transcriptional Profiling of the Axolotl Limb Identifies a Tripartite Regeneration-Specific Gene Program	Knapp D, Schulz H, Rascon CA, Volkmer M et al. Comparative transcriptional profiling of the axolotl limb identifies a tripartite regeneration-specific gene program. PLoS One	77

GSE Accession	Platform	Study design as reported in GEO	Type of raw/processed data used for analysis	Link GEO
GSE37198	2012	Expression data from aquatic axolotl full thickness epithelial flank wounds, innervated limbs, and denervated limbs collected over seven days	James R. Monaghan, Antony Athippozhy, Ashley W. Seifert, Sri Putta, Arnold J. Stromberg, Malcolm Maden, David M. Gardiner, and S. Randal Voss. Gene expression patterns specific to the regenerating limb of the Mexican axolotl. Biology Open 2012 BIO20121594; Advance Online Publication August 8, 2012, doi:10.1242/bio.20121594.	32
GSE116615	GPL25286 [AMBY_002a520748F] Affymetrix Ambystoma mexicanum	Forelimbs were amputated mid-zeugopod. 1.0mm samples of heterogeneous tissue from regenerating limb tip were removed and used for RNA extraction. Three replicates samples were collected for each time point, with each replicate formed by pooling tissue from 5 different larvae.	CEL	https://www.ncbi.nlm.nih.gov/geo/query/acc.cgi?acc=GSE116615
GSE67118	GPL15153 Affymetrix Ambystoma mexicanum AMBY_002 20k array [CDF: AMBY_002a520748F]	The distal 1.0mm of heterogeneous tissue from regenerating limb tip were removed and used for RNA extraction. 10 samples were collected for each of 20 time points.	CEL	https://www.ncbi.nlm.nih.gov/geo/query/acc.cgi?acc=GSE67118
GSE36451	GPL15342 Agilent-019788 Ambystoma mexicanum 44k_v3_20080327	Regeneration of the axolotl forelimb lower arm was compared with the healing of a deep lateral injury in a high density timecourse (uncut, 3h, 6h, 9h, 12h, 24h, 36h, 52h, 72h, 120h, 168h, 288h and 528h after injury). Three independent biological replicates were performed using separate clutches of animals. Amputated and lateral wound samples were made as matched contralateral samples of four pooled animals per timepoint.	TXT	https://www.ncbi.nlm.nih.gov/geo/query/acc.cgi?acc=GSE36451
GSE37198	GPL15153 Affymetrix Ambystoma mexicanum AMBY_002 20k array [CDF:	To determine the gene expression changes that take place during limb regeneration, flank wound healing, and an denervated amputated limb. Epidermal tissue and cells adhered to the epidermis were	CEL	https://www.ncbi.nlm.nih.gov/geo/query/acc.cgi?acc=GSE37198

	AMBY_002a52 0748F]	collected as samples. Two harvested samples was pooled for each animal. Four biological replicates were collected from uninjured epidermis (D0) and at 1, 3, and 7 days post injury.		

Table A.1: Description of the selected microarray datasets for integrative analysis

A.2 RNA-Seq Axolotl Dataset Selection

GSE Accession	Year	Title	Publication	# of samples used for analysis	Total # of samples
GSE116777	2018	Comparative Transcriptomics of Limb Regeneration:Identification of Conserved Expression Changes Among Three Species of Ambystoma [RNA-Seq]	Dwaraka VB, Smith JJ, Woodcock MR, Voss SR. Comparative transcriptomics of limb regeneration: Identification of conserved expression changes among three species of Ambystoma. Genomics 2018 Aug 6. PMID: 30092345	5	18
GSE103087	2017	Identification of regenerative roadblocks via repeat deployment of limb regeneration in axolotls	Donald M. Bryant, Konstantinos Sousounis, Duygu Payzin-Dogru, Sevara Bryant, Aaron Gabriel W. Sandoval, Jose Martinez Fernandez, Rachelle Mariano, Rachel Oshiro, Alan Y. Wong, Nicholas D. Leigh, Kimberly Johnson & Jessica L. Whited. Identification of regenerative roadblocks via repeat deployment of limb regeneration in axolotls. npj Regenerative Medicine, 2, 30 (2017). doi:10.1038/s41536-017-0034-z	4	8
GSE92429	2016	A tissue-mapped axolotl de novo transcriptome enables identification of limb regeneration factors	Bryant DM, Johnson K, DiTommaso T, Tickle T et al. A Tissue-Mapped Axolotl De Novo Transcriptome Enables Identification of Limb Regeneration Factors. Cell Rep 2017 Jan 17;18(3):762-776. PMID: 28099853	7	42
GSE74372	2016	Small RNA and mRNA expression profiling during axolotl forelimb regeneration	King BL, Yin VP. A Conserved MicroRNA Regulatory Circuit Is Differentially Controlled during Limb/Appendage Regeneration. PLoS One 2016;11(6):e0157106. PMID: 27355827	4	8
GSE34394	2013	Three Distinct Phases of Regeneration-Specific Gene Expression in the Axolotl Blastema	Stewart R, Rascón CA, Tian S, Nie J et al. Comparative RNA-seq analysis in the unsequenced axolotl: the oncogene burst highlights early gene expression in the blastema. PLoS Comput Biol 2013;9(3):e1002936. PMID: 23505351	12	20
GSE Accession	Platform	Study design as reported in GEO	Type of raw data used for analysis	GEO Link	ENA Link
GSE116777	GPL21473 Illumina HiSeq 2000 (Ambystoma mexicanum)	Forelimbs were amputated mid-zeugopod in all animals. 1.0mm samples of heterogeneous tissue from regenerating limb tips were removed and used for RNA extraction. Three replicates samples were collected for each time point, with each replicate formed by pooling tissue from 5 different larvae.	Fastq	https://www.ncbi.nlm.nih.gov/geo/query/acc.cgi?acc=GSE116777	https://www.ebi.ac.uk/ena/data/view/PRJNA480225

GSE1 03087	GPL22800 Illumina HiSeq 2500 (Ambysto ma mexicanu m)	There are two conditions, with four biological replicates per condition. Condition 1 samples, "Multi-amp" in the sample names, are derived from axolotl limbs that have undergone six rounds of amputation-regeneration and mRNA was extracted at three days following the last amputation. Condition 2 samples, "Contol" in the sample names, are age- and size-matched sibling animals that have undergone a single amputation and mRNA was extracted at three days following this amputation.	Fastq	https://www.ncbi.nlm.nih.gov/geo/query/acc.cgi?acc=GSE103087	https://www.ebi.ac.uk/ena/data/view/PRJNA400170
GSE9 2429	GPL22800 Illumina HiSeq 2500 (Ambysto ma mexicanu m)	Profiled 42 samples across 16 tissues, from distinct locations among intact and regenerating limbs, relevant cell types, and other progenitor-rich samples using RNA-sequencing	Fastq	https://www.ncbi.nlm.nih.gov/geo/query/acc.cgi?acc=GSE92429	https://www.ebi.ac.uk/ena/data/view/PRJNA300706
GSE7 4372	GPL14997 Illumina Genome Analyzer IIx (Ambysto ma mexicanu m)	Characterized microRNA expression during Axolotl forelimb regeneration using small RNA sequencing. The same samples were assayed for mRNA expression using mRNA sequencing. Small RNA and mRNA gene expression profiling during 0, 3, 6 and 14 days post amputation.	Fastq	https://www.ncbi.nlm.nih.gov/geo/query/acc.cgi?acc=GSE74372	https://www.ebi.ac.uk/ena/data/view/PRJNA299879
GSE3 4394	GPL14997 Illumina Genome Analyzer IIx (Ambysto ma mexicanu m)	performed deep RNA sequencing of the blastema over a time course.Then, compare the expression patterns to those in a mouse digit amputation model to identify genes specific to the regenerative response	Fastq	https://www.ncbi.nlm.nih.gov/geo/query/acc.cgi?acc=GSE34394	https://www.ebi.ac.uk/ena/data/view/PRJNA149573

Table A.2: Description of the selected RNA-Seq datasets for integrative analysis

A.3 Detailed Information on Microarray Axolotl Data

GSE Study	1. **Control**: Intact (forelimb or hindlimb)-zero time point
GSE116615	GSM3243805 forelimb 0hpa replicate 1
	GSM3243806 forelimb 0hpa replicate 2
	GSM3243807 forelimb 0hpa replicate 3
GSE67118	GSM1639337 forelimb T0 replicate 1
	GSM1639338 forelimb T0 replicate 2
	GSM1639339 forelimb T0 replicate 3
	GSM1639340 forelimb T0 replicate 4
	GSM1639341 forelimb T0 replicate 5
	GSM1639342 forelimb T0 replicate 6
	GSM1639343 forelimb T0 replicate 7
	GSM1639344 forelimb T0 replicate 8
	GSM1639345 forelimb T0 replicate 9
	GSM1639346 forelimb T0 replicate 10
GSE36451	GSM893962 mat-1_rep1
	GSM893963 mat-2_rep1
	GSM894016 mat-2_rep3
	GSM894015 mat-1_rep3
	GSM893989 mat_rep2
GSE37198	GSM913369 Flank wound at D0, biological rep1
	GSM913370 Flank wound at D0, biological rep2
	GSM913371 Flank wound at D0, biological rep3
	GSM913372 Flank wound at D0, biological rep4
	GSM913373 Innervated limb at D0, biological rep1
	GSM913374 Innervated limb at D0, biological rep2
	GSM913375 Innervated limb at D0, biological rep3
	GSM913376 Innervated limb at D0, biological rep4
GSE Study	2. **Wound Healing**: injuries or amputations up to 48 hrs
GSE116615	GSM3243808 forelimb 24hpa replicate 1
	GSM3243809 forelimb 24hpa replicate 2

	GSM3243810 forelimb 24hpa replicate 3
GSE67118	GSM1639347 forelimb T0.5 replicate 1
	GSM1639348 forelimb T0.5 replicate 2
	GSM1639349 forelimb T0.5 replicate 3
	GSM1639350 forelimb T0.5 replicate 4
	GSM1639351 forelimb T0.5 replicate 5
	GSM1639352 forelimb T0.5 replicate 6
	GSM1639353 forelimb T0.5 replicate 7
	GSM1639354 forelimb T0.5 replicate 8
	GSM1639355 forelimb T0.5 replicate 9
	GSM1639356 forelimb T0.5 replicate 10
	GSM1639357 forelimb T1 replicate 1
	GSM1639358 forelimb T1 replicate 2
	GSM1639359 forelimb T1 replicate 3
	GSM1639360 forelimb T1 replicate 4
	GSM1639361 forelimb T1 replicate 5
	GSM1639362 forelimb T1 replicate 6
	GSM1639363 forelimb T1 replicate 7
	GSM1639364 forelimb T1 replicate 8
	GSM1639365 forelimb T1 replicate 9
	GSM1639366 forelimb T1 replicate 10
	GSM1639367 forelimb T1.5 replicate 1
	GSM1639368 forelimb T1.5 replicate 2
	GSM1639369 forelimb T1.5 replicate 3
	GSM1639370 forelimb T1.5 replicate 4
	GSM1639371 forelimb T1.5 replicate 5
	GSM1639372 forelimb T1.5 replicate 6
	GSM1639373 forelimb T1.5 replicate 7
	GSM1639374 forelimb T1.5 replicate 8
	GSM1639375 forelimb T1.5 replicate 9
	GSM1639376 forelimb T1.5 replicate 10
	GSM1639377 forelimb T2 replicate 1
	GSM1639378 forelimb T2 replicate 2

		GSM1639379 forelimb T2 replicate 3
		GSM1639380 forelimb T2 replicate 4
		GSM1639381 forelimb T2 replicate 5
		GSM1639382 forelimb T2 replicate 6
		GSM1639383 forelimb T2 replicate 7
		GSM1639384 forelimb T2 replicate 8
		GSM1639385 forelimb T2 replicate 9
		GSM1639386 forelimb T2 replicate 10
	GSE36451	GSM893964 3h_amp_rep1
		GSM893965 6h_amp_rep1
		GSM893966 9h_amp_rep1
		GSM893967 12h_amp_rep1
		GSM893968 24h_amp_rep1
		GSM893969 36h_amp_rep1
		GSM893970 52h_amp_rep1 GSM893990 3h_amp_rep2
		GSM893990 3h_amp_rep2
		GSM893991 6h_amp_rep2
		GSM893992 9h_amp_rep2
		GSM893993 12h_amp_rep2
		GSM893994 24h_amp_rep2
		GSM893995 36h_amp_rep2
		GSM893996 52h_amp_rep2
		GSM894017 3h_amp_rep3
		GSM894018 6h_amp_rep3
		GSM894019 9h_amp_rep3
		GSM894020 12h_amp_rep3
		GSM894021 24h_amp_rep3
		GSM894022 36h_amp_rep3
		GSM894023 52h_amp_rep3
		GSM893976 3h_lwp_rep1
		GSM893977 6h_lwp_rep1
		GSM893978 9h_lwp_rep1

	GSM893979 12h_lwp_rep1
	GSM893980 24h_lwp_rep1
	GSM893981 36h_lwp_rep1
	GSM893982 52h_lwp_rep1
	GSM894002 3h_lwp_rep2
	GSM894003 6h_lwp_rep2
	GSM894004 9h_lwp_rep2
	GSM894005 12h_lwp_rep2
	GSM894006 24h_lwp_rep2
	GSM894007 36h_lwp_rep2
	GSM894008 52h_lwp_rep2
	GSM894029 3h_lwp_rep3
	GSM894030 6h_lwp_rep3
	GSM894031 9h_lwp_rep3
	GSM894032 12h_lwp_rep3
	GSM894033 24h_lwp_rep3
	GSM894034 36h_lwp_rep3
	GSM894035 52h_lwp_rep3
GSE37198	GSM913381 Innervated limb at D1, biological rep1
	GSM913382 Innervated limb at D1, biological rep2
	GSM913383 Innervated limb at D1, biological rep3
	GSM913384 Innervated limb at D1, biological rep4
	GSM913385 Flank wound at D1, biological rep1
	GSM913386 Flank wound at D1, biological rep2
	GSM913387 Flank wound at D1, biological rep3
	GSM913388 Flank wound at D1, biological rep4
GSE Study	**3. Regeneration**: amputations later than 48 hrs
GSE67118	GSM1639387 forelimb T3 replicate 1
	GSM1639388 forelimb T3 replicate 2
	GSM1639389 forelimb T3 replicate 3
	GSM1639390 forelimb T3 replicate 4
	GSM1639391 forelimb T3 replicate 5
	GSM1639392 forelimb T3 replicate 6

GSM1639393 forelimb T3 replicate 7
GSM1639394 forelimb T3 replicate 8
GSM1639395 forelimb T3 replicate 9
GSM1639396 forelimb T3 replicate 10
GSM1639397 forelimb T4 replicate 1
GSM1639398 forelimb T4 replicate 2
GSM1639399 forelimb T4 replicate 3
GSM1639400 forelimb T4 replicate 4
GSM1639401 forelimb T4 replicate 5
GSM1639402 forelimb T4 replicate 6
GSM1639403 forelimb T4 replicate 7
GSM1639404 froelimb T4 replicate 8
GSM1639405 forelimb T4 replicate 9
GSM1639406 forelimb T4 replicate 10
GSM1639407 forelimb T5 replicate 1
GSM1639408 forelimb T5 replicate 2
GSM1639409 forelimb T5 replicate 3
GSM1639410 forelimb T5 replicate 4
GSM1639411 forelimb T5 replicate 5
GSM1639412 forelimb T5 replicate 6
GSM1639413 forelimb T5 replicate 7
GSM1639414 forelimb T5 replicate 8
GSM1639415 forelimb T5 replicate 9
GSM1639416 forelimb T5 replicate 10
GSM1639417 forelimb T7 replicate 1
GSM1639418 forelimb T7 replicate 2
GSM1639419 forelimb T7 replicate 3
GSM1639420 forelimb T7 replicate 4
GSM1639421 forelimb T7 replicate 5
GSM1639422 forelimb T7 replicate 6
GSM1639423 forelimb T7 replicate 7
GSM1639424 forelimb T7 replicate 8
GSM1639425 forelimb T7 replicate 9

GSM1639426 forelimb T7 replicate 10
GSM1639427 forelimb T9 replicate 1
GSM1639428 forelimb T9 replicate 2
GSM1639429 forelimb T9 replicate 3
GSM1639430 forelimb T9 replicate 4
GSM1639431 forelimb T9 replicate 5
GSM1639432 forelimb T9 replicate 6
GSM1639433 forelimb T9 replicate 7
GSM1639434 forelimb T9 replicate 8
GSM1639435 forelimb T9 replicate 9
GSM1639436 forelimb T9 replicate 10
GSM1639437 forelimb T10 replicate 1
GSM1639438 forelimb T10 replicate 2
GSM1639439 forelimb T10 replicate 3
GSM1639440 forelimb T10 replicate 4
GSM1639441 forelimb T10 replicate 5
GSM1639442 forelimb T10 replicate 6
GSM1639443 forelimb T10 replicate 7
GSM1639444 forelimb T10 replicate 8
GSM1639445 forelimb T10 replicate 9
GSM1639446 forelimb T10 replicate 10
GSM1639447 forelimb T12 replicate 1
GSM1639448 forelimb T12 replicate 2
GSM1639449 forelimb T12 replicate 3
GSM1639450 forelimb T12 replicate 4
GSM1639451 forelimb T12 replicate 5
GSM1639452 forelimb T12 replicate 6
GSM1639453 forelimb T12 replicate 7
GSM1639454 forelimb T12 replicate 8
GSM1639455 forelimb T12 replicate 9
GSM1639456 forelimb T12 replicate 10
GSM1639457 forelimb T14 replicate 1
GSM1639458 forelimb T14 replicate 2

GSM1639459 forelimb T14 replicate 3
GSM1639460 forelimb T14 replicate 4
GSM1639461 forelimb T14 replicate 5
GSM1639462 forelimb T14 replicate 6
GSM1639463 forelimb T14 replicate 7
GSM1639464 forelimb T14 replicate 8
GSM1639465 forelimb T14 replicate 9
GSM1639466 forelimb T14 replicate 10
GSM1639467 forelimb T16 replicate 1
GSM1639468 forelimb T16 replicate 2
GSM1639469 forelimb T16 replicate 3
GSM1639470 forelimb T16 replicate 4
GSM1639471 forelimb T16 replicate 5
GSM1639472 forelimb T16 replicate 6
GSM1639473 forelimb T16 replicate 7
GSM1639474 forelimb T16 replicate 8
GSM1639475 forelimb T16 replicate 9
GSM1639476 forelimb T18 replicate 1
GSM1639477 forelimb T18 replicate 2
GSM1639478 forelimb T18 replicate 3
GSM1639479 forelimb T18 replicate 4
GSM1639480 forelimb T18 replicate 5
GSM1639481 forelimb T18 replicate 6
GSM1639482 forelimb T18 replicate 7
GSM1639483 forelimb T18 replicate 8
GSM1639484 forelimb T18 replicate 9
GSM1639485 forelimb T18 replicate 10
GSM1639486 forelimb T20 replicate 1
GSM1639487 forelimb T20 replicate 2
GSM1639488 forelimb T20 replicate 3
GSM1639489 forelimb T20 replicate 4
GSM1639490 forelimb T20 replicate 5
GSM1639491 forelimb T20 replicate 6

GSM1639492 forelimb T20 replicate 7
GSM1639493 forelimb T20 replicate 8
GSM1639494 forelimb T20 replciate 9
GSM1639495 forelimb T20 replicate 10
GSM1639496 forelimb T22 replicate 1
GSM1639497 forelimb T22 replicate 2
GSM1639498 forelimb T22 replicate 3
GSM1639499 forelimb T22 replicate 4
GSM1639500 forelimb T22 replicate 5
GSM1639501 forelimb T22 replicate 6
GSM1639502 forelimb T22 replicate 7
GSM1639503 forelimb T22 replicate 8
GSM1639504 forelimb T22 replicate 9
GSM1639505 forelimb T22 replicate 10
GSM1639506 forelimb T24 replicate 1
GSM1639507 forelimb T24 replicate 2
GSM1639508 forelimb T24 replicate 3
GSM1639509 forelimb T24 replicate 4
GSM1639510 forelimb T24 replicate 5
GSM1639511 forelimb T24 replicate 6
GSM1639512 forelimb T24 replicate 7
GSM1639513 forelimb T24 replicate 8
GSM1639514 forelimb T24 replicate 9
GSM1639515 forelimb T24 replicate 10
GSM1639516 forelimb T26 replicate 1
GSM1639517 forelimb T26 replicate 2
GSM1639518 forelimb T26 replicate 3
GSM1639519 forelimb T26 replicate 4
GSM1639520 forelimb T26 replicate 5
GSM1639521 forelimb T26 replicate 6
GSM1639522 forelimb T26 replicate 7
GSM1639523 forelimb T26 replicate 8
GSM1639524 forelimb T26 replicate 9

		GSM1639525 forelimb T26 replicate 10
		GSM1639526 forelimb T28 replicate 1
		GSM1639527 forelimb T28 replicate 2
		GSM1639528 forelimb T28 replicate 3
		GSM1639529 forelimb T28 replicate 4
		GSM1639530 forelimb T28 replicate 5
		GSM1639531 forelimb T28 replicate 6
		GSM1639532 forelimb T28 replicate 7
		GSM1639533 forelimb T28 replicate 8
		GSM1639534 forelimb T28 replicate 9
	GSE36451	GSM893971 72h_amp_rep1
		GSM893972 120h_amp_rep1
		GSM893973 168h_amp_rep1
		GSM893974 288h_amp_rep1
		GSM893975 528h_amp_rep1
		GSM893997 72h_amp_rep2
		GSM893998 120h_amp_rep2
		GSM893999 168h_amp_rep2
		GSM894000 288h_amp_rep2
		GSM894001 528h_amp_rep2
		GSM894024 72h_amp_rep3
		GSM894025 120h_amp_rep3
		GSM894026 168h_amp_rep3
		GSM894027 288h_amp_rep3
		GSM894028 528h_amp_rep3
		GSM893983 72h_lwp_rep1
		GSM893984 120h_lwp_rep1
		GSM893985 168h_lwp_rep1
		GSM893986 288h_lwp_rep1
		GSM893987 528h_lwp_rep1
		GSM894009 72h_lwp_rep2
		GSM894010 120h_lwp_rep2
		GSM894011 168h_lwp_rep2

		GSM894012 288h_lwp_rep2
		GSM894013 528h_lwp_rep2
		GSM894036 72h_lwp_rep3
		GSM894037 120h_lwp_rep3
		GSM894038 168h_lwp_rep3
		GSM894039 288h_lwp_rep3
		GSM894040 528h_lwp_rep3
	GSE37198	GSM913393 Innervated limb at D3, biological rep1
		GSM913394 Innervated limb at D3, biological rep2
		GSM913395 Innervated limb at D3, biological rep3
		GSM913396 Innervated limb at D3, biological rep4
		GSM913405 Innervated limb at D7, biological rep1
		GSM913406 Innervated limb at D7, biological rep2
		GSM913407 Innervated limb at D7, biological rep3
		GSM913408 Innervated limb at D7, biological rep4
		GSM913397 Flank wound at D3, biological rep1
		GSM913398 Flank wound at D3, biological rep2
		GSM913399 Flank wound at D3, biological rep3
		GSM913400 Flank wound at D3, biological rep4
		GSM913409 Flank wound at D7, biological rep1
		GSM913410 Flank wound at D7, biological rep2
		GSM913411 Flank wound at D7, biological rep3
		GSM913412 Flank wound at D7, biological rep4

Table A.3: Detailed information on possible GSM accession, timepoint, amputation/injury site, and replicate number of each sample from Microarray data as reported in GEO

74

A.4 Detailed Information on RNA-Seq Axolotl Data

GSE Study	1. **Control**: Intact (forelimb or hindlimb)-zero time point
GSE116777	GSM3261803 SRV-0041 0hpa
	GSM3261804 SRV-0042 0hpa
GSE34394	GSM848198 Axolotl limb blastemal 0hr
GSE74372	GSM1919057 0dpa mRNA
GSE92429	GSM2429608 upperarm_10329_GTGAAA
	GSM2429609 upperarm_10326_ATGTCA
	GSM2429610 upperarm_10322_CAGATC
GSE Study	2. **Wound Healing**: injuries or amputations up to 48 hrs
GSE116777	GSM3261812 SRV-0044 24hpa
	GSM3261813 SRV-0045 24hpa
	GSM3261814 SRV-0046 24hpa
GSE34394	GSM848199 Axolotl limb blastemal 3hr
	GSM848200 Axolotl limb blastemal 6hr
	GSM848201 Axolotl limb blastemal 12hr
	GSM848202 Axolotl limb blastemal 1d
GSE Study	3. **Regeneration**: amputations later than 48 hrs
GSE34394	GSM848203 Axolotl limb blastemal 3d
	GSM848204 Axolotl limb blastemal 5d
	GSM848205 Axolotl limb blastemal 7d
	GSM848206 Axolotl limb blastemal 10d
	GSM848207 Axolotl limb blastemal 14d
	GSM848208 Axolotl limb blastemal 21d
	GSM848209 Axolotl limb blastemal 28d
GSE74372	GSM1919058 3dpa mRNA
	GSM1919059 6dpa mRNA
	GSM1919060 14dpa mRNA
GSE92429	GSM2429615 proximal_TGACCA_L008
	GSM2429616 proximal_CAGATC_L006
	GSM2429628 distal_GCCAAT_L006

	GSM2429629 distal_CGATGT_L008
GSE103087	GSM2753452 LIB014416_TRA00035334
	GSM2753453 LIB014416_TRA00035335
	GSM2753454 LIB014416_TRA00035336
	GSM2753455 LIB014416_TRA00035337

Table A.4: Detailed information on possible GSM accession, timepoint, amputation/injury site, and replicate number of each sample from RNA-Seq data as reported in GEO

A.5 Top DE Genes from Both Technologies

Wound Healing vs. Control		
Symbol	logFC_Microarray	logFC_RNAseq
MMP1	2.334361424	6.338005577
MMP3	2.613784506	6.326727984
MMP13	2.505942171	6.142324809
SERPINE1	2.33448261	5.499983443
DUSP5	1.900733092	5.461830138
SLC2A1	2.583964126	5.376636756
PTGS2	1.349113221	5.081598276
DUSP1	1.384630072	4.592839444
TCN1	2.6701994	4.586502325
MMP19	1.842536588	4.438045568
CYR61	1.524675274	4.323121128
TFPI2	2.577931481	4.213641401
JUNB	2.221756685	4.18203071
HMOX1	2.20457087	4.078211279
GADD45B	2.292961256	3.967008368
MPO	1.539231455	3.754991511
EGR1	1.183623733	3.741661794
PLBD1	1.849523153	3.690513073
TIMP1	2.651597185	3.640411179
TUBB6	2.145998088	3.51921625
ARG1	2.294109452	3.303208849
DGAT2	1.612931003	3.252060638
ANTXR2	1.844975053	3.223922826
SCG2	2.309067267	3.218333481
MMP2	1.166588789	3.157313017
DDIT4	1.689073456	3.148257645
THBS1	2.741572843	3.119318838
FGL2	1.603042676	3.109661211

ODC1	2.371673142	3.059811212
TNC	1.928430829	3.038263794
TGM1	2.211429497	3.001913471
SPSB4	1.643229066	2.987181157
CXCR4	1.345824199	2.844759447
SOCS1	1.979271742	2.757441497
CHIT1	1.50988719	2.735948537
SGK1	1.63809861	2.65765517
ARL4D	2.282158023	2.607778471
UGDH	2.534200029	2.581818431
GADD45G	1.684827707	2.561964354
GLUL	2.61045621	2.530108807
PHLDA2	1.707124853	2.483842377
OBFC2A	2.403141247	2.330756238
DLGAP4	2.594097381	2.257749664
CYBB	2.007559993	2.22545569
SMAD7	1.029288045	2.196126161
ZFAND5	2.153701831	2.183211463
RHOB	1.00919381	2.160984515
PPP1R14B	2.610945966	2.154678459
ARHGEF2	1.961960934	2.137000929
G0S2	1.41786803	2.11914662
MAT2A	1.194248207	2.109284438
UGCG	1.874832507	2.036689675
SQSTM1	1.277666454	2.001438828
MAPK6	2.591000214	1.915050242
LARP6	1.608874063	1.849560081
FAM110B	2.360501041	1.79436392
LGALS9	1.717625991	1.776964321
BMP2	1.548472922	1.703815048
SLC16A1	1.520238061	1.699210532
KIAA1737	1.741476731	1.685631249
SNX18	1.98102521	1.638333222

Symbol	logFC_Microarray	logFC_RNAseq
ZNRF1	2.012149822	1.633122284
ZYX	2.492173002	1.597628818
SEMA3F	1.079471461	1.544727872
SLC30A1	2.26847655	1.446118762
RND3	1.431083506	1.406607239
FAM108A1	1.115918282	1.391500219
BCL2L1	2.112853034	1.388564269
ZC3H11A	2.662591672	1.355679812
MXI1	1.350166451	1.346243753
TMEM63B	1.453640867	1.323548748
SLC20A1	1.035372778	1.314067927
CDKN1C	1.054397908	1.308419045
BASP1	1.178196837	1.297370601
KEAP1	1.333360173	1.295536181
ERO1L	2.473193008	1.274935767
CCNL1	1.141953243	1.265750639
CHD7	1.575588305	1.256585758
UBE2J1	1.535279	1.219634011
ACCS	-1.044734647	1.216692098
LMNB1	1.488273056	1.210726837
PELI1	1.655103458	1.20294839
SKI	1.282945387	1.093195775
ACTB	1.941734833	1.076181244
YWHAZ	1.987227655	1.071105742
TOP1	1.737250792	1.041115392
RRAS2	1.708469955	1.017611445
RMI1	-1.262418344	-1.029607406
CENPO	-1.042610701	-1.102455378
SLC25A12	-1.127310982	-1.310792154
ZNF367	-1.017944133	-1.411253607
Regenerative vs. Control		
Symbol	**logFC_Microarray**	**logFC_RNAseq**
KAZALD1	1.60584757	7.606392103

79

MMP13	1.28751864	4.684782882
TNC	2.76899951	4.507054818
KRT17	3.059656959	4.433341211
PLBD1	1.335313996	3.405004145
TGFBI	1.65973202	3.250979687
PAMR1	1.629254917	3.170848422
F13A1	1.212030503	2.78544746
HIST3H2BB	1.226535435	2.752726323
LAMA1	1.304306191	2.670020033
CRABP2	1.922354318	2.519907225
SPSB4	1.255390854	2.378661784
MSI1	1.49324911	2.349822341
HAS2	1.086876414	2.327763108
MMP2	1.059033428	2.246131184
MAPK6	2.50893046	2.216563294
CXCR4	1.067219183	2.212249173
HMOX1	1.435034277	2.140113427
RCC1	1.305262112	2.114316205
MDK	1.084822228	2.110868401
TMEM35	1.227274134	2.093854739
CCNJ	1.613608596	2.024962826
THBS1	1.815119729	2.000311495
CALD1	1.755608975	1.986202794
B9D1	1.505093553	1.947534205
FAT1	1.066795372	1.877197689
ENTPD1	1.775105449	1.84689419
FN1	1.553184389	1.835956044
SMAD7	1.194322149	1.825610643
NEK2	1.02745336	1.813303252
KPNA2	1.427076531	1.813037336
MYO10	2.056775205	1.790043557
OBFC2A	1.71516334	1.776729504
COL12A1	1.074030507	1.763226013

KIF11	1.050111115	1.751192362
AURKA	1.072344938	1.742388078
ID3	1.697729526	1.7032721
FAM54A	1.257628986	1.687796398
SAFB	1.346742416	1.670871889
MBD3	1.328615086	1.655521106
PLK1	1.293625144	1.640839096
TFPI	1.169997882	1.633649003
JUNB	1.546643627	1.612122395
APEX1	1.513003124	1.592478909
BASP1	1.407396377	1.574297323
MTBP	1.341226826	1.558447412
RRM2	1.047933537	1.557171033
FEN1	1.260591674	1.548648846
CCDC112	1.488899459	1.547224799
HCFC1	1.091418951	1.543500584
KIF23	1.096763883	1.535794098
ETF1	1.907804983	1.523316608
TRIP13	1.329294518	1.519313346
RBMXL1	1.83538259	1.511374069
LOXL2	1.683217659	1.511148649
FUS	1.627373752	1.506398904
RPS6KB1	1.998922288	1.482751914
ANP32E	1.013212638	1.482296354
PPRC1	1.55319949	1.472802156
PCDHGC3	1.194529635	1.472670083
RRM1	1.186622498	1.466832234
KIF22	1.05279908	1.463444434
ANTXR2	1.157689592	1.455954835
CYBB	1.513514029	1.440987907
SLTM	1.839913086	1.423609321
DCTPP1	1.30169385	1.409175524
SLC37A2	1.2743202	1.407601065

CTHRC1	1.707279363	1.406558193
STMN1	1.044853214	1.39860325
TOP2B	1.315825097	1.398436393
MAD2L1	1.011679519	1.394810466
CSE1L	1.199614525	1.391365394
CNN2	1.458270201	1.379938557
BRD3	1.519527072	1.372571943
NOLC1	1.529308157	1.367652936
RHEBL1	1.216393753	1.360763512
PTBP1	1.3152891	1.35916821
TCF7L1	1.045569514	1.358976143
SULF1	1.663460656	1.347564214
POLR1C	1.133310331	1.310366692
TMPO	1.711141104	1.287855374
CLK3	1.702902437	1.28495491
IFNAR1	1.218780517	1.279103087
TUBB6	1.274342008	1.278964851
LGALS9	1.517271279	1.27866492
METTL9	1.64659179	1.276069061
MPHOSPH10	1.188343856	1.275420823
HSPD1	1.170583865	1.267641238
CTPS	1.275947639	1.266660019
RRP9	1.171714652	1.264018926
RBM14	2.182063802	1.261296776
VKORC1L1	1.265380317	1.26102556
IQCB1	1.090665177	1.258186512
CBX3	2.00281647	1.249126017
AURKB	1.073467612	1.249033698
HELLS	1.006017115	1.248658128
NASP	1.211429737	1.243353349
DLGAP4	1.97032316	1.242348426
HNRNPM	2.129523597	1.239922224
RANBP1	2.053316532	1.233057498

TNFAIP1	1.474680898	1.230858043
TOP1	2.055539401	1.223524047
CDC20	1.222147319	1.217938645
SNRPA1	2.014592306	1.207469543
SNRPA	2.072271658	1.206671475
PLOD1	1.136888509	1.205371696
ABCF3	1.410062591	1.204513445
OSGIN2	1.679516823	1.201526877
TRA2B	1.863140128	1.201250461
DOCK7	1.171588948	1.199925219
BMP2	1.254383717	1.194350684
ODC1	1.429935845	1.188706636
MOSPD1	1.161348584	1.188387736
BAZ1B	1.067569702	1.18746786
RBM45	1.561955186	1.185808293
GART	1.512272912	1.177148744
HAUS1	1.061849766	1.1738079
RBMX	1.652647418	1.16925224
BICD2	1.135499607	1.168321326
ITGB1	1.120346445	1.167621019
HMGB2	1.574797886	1.164390471
MRTO4	1.713486271	1.162133672
PRC1	1.053242679	1.160453632
PWP2	1.276759182	1.15994105
ZRANB2	1.062857067	1.157887282
NIPBL	1.42940232	1.150073674
CHD7	1.250149626	1.14663182
FBL	1.719161401	1.146031477
EWSR1	1.674695735	1.141187012
FILIP1L	1.368991093	1.139620733
CTTNBP2NL	1.090690398	1.138005977
SFPQ	1.783635615	1.136416749
MFAP2	1.651450121	1.135887019

PRPF39	1.593177148	1.133896893
SNRNP40	1.845539179	1.132316844
THAP6	1.984875967	1.131816827
VIM	1.241452154	1.13048239
CDCA8	1.007398768	1.126471673
DHX15	1.798987664	1.125904559
PSPC1	1.98185145	1.123943803
MAD2L1BP	1.630793821	1.114912413
FLNA	1.826421336	1.11478458
TARDBP	2.028328068	1.113076138
NOL11	1.662138781	1.113013553
NUP160	1.112650114	1.104068885
SPATS2L	1.246248719	1.103367499
CIRH1A	1.370557103	1.101662692
PTCD3	1.481629023	1.100268844
NUP85	1.173534131	1.09527314
GPNMB	1.355905264	1.091575357
IPO11	1.703512458	1.09072166
COIL	1.125811926	1.087814235
ASF1B	1.045023567	1.082578269
PRR11	1.020036112	1.082327308
SART3	1.019727892	1.08211025
TMEM138	1.524606206	1.079523195
PGGT1B	1.349383345	1.078537287
ZNF862	1.575539173	1.077523498
MATR3	1.303474906	1.076468582
PAG1	1.236498991	1.075181881
ERO1L	2.249818466	1.071538641
PBRM1	1.416220211	1.071358301
JAG1	1.069589778	1.067033519
CTSC	1.025768569	1.064298507
METTL2A	1.898105627	1.062502764
RFC2	1.421526343	1.05409067

DKC1	1.666041292	1.047930323
USP1	1.018325585	1.045341957
CDV3	1.644914315	1.039617407
CSTF1	1.316345574	1.03723491
ZC3H11A	1.791644439	1.035901815
ZNF326	1.864956156	1.035226732
PRPF3	1.327773993	1.033609437
RPA2	1.003318854	1.031864745
TNPO3	1.278150791	1.02788666
SULT6B1	1.716591067	1.024087011
CLNS1A	1.466906716	1.009842298
SMARCC1	1.322774945	1.008908149
MCM3AP	1.192612513	1.008655458
UBE2I	1.370939224	1.004987207
MYEF2	1.680966286	1.003795741
ECHDC2	-1.296186257	-1.001090731
ROGDI	-1.107985429	-1.013062883
SNTA1	-1.843783592	-1.014938705
AIFM3	-1.398100987	-1.015427986
HLCS	-1.423441959	-1.026973484
ANKRD39	-1.425575027	-1.034801098
DCAF6	-2.213102194	-1.035050897
ATP5S	-1.833190149	-1.050563854
SYNJ2BP	-1.931695181	-1.051549547
PRDX1	1.05533778	-1.051735053
COX17	-1.751697447	-1.053856088
HINT2	-1.569588648	-1.078275286
COX7B	-1.819455822	-1.082756245
GOT1	-2.20425545	-1.112275321
PPP1R14A	-2.037135446	-1.131287547
VDAC1	-2.140958681	-1.133831928
ATP5G2	-1.693341879	-1.138098264
PARK7	-2.279856235	-1.138136014

GJB5	1.111139222	-1.141513261
ATP5I	-1.840790474	-1.147153062
TMSB15A	1.535796427	-1.15018179
GOT2	-1.361735323	-1.168972881
ACAT1	-1.752602147	-1.173036185
CECR1	-1.188084813	-1.186173261
PCGF5	-1.929122719	-1.195874295
MDH2	-2.332714762	-1.205988654
ITGB1BP3	-1.566275694	-1.208668611
ENPP5	-1.785744521	-1.220037704
ACADL	-1.803302639	-1.221774974
FKBP11	-1.394967118	-1.234980211
ACBD7	-1.140081654	-1.248099782
CD74	-1.402358357	-1.258144735
ANXA6	-1.531475071	-1.260928833
HEXB	-1.000828977	-1.280598421
PNO1	-1.80293508	-1.2826575
COX7A2L	-2.015605025	-1.30136179
BNIP3	-1.595705382	-1.328005352
SPA17	-1.020822579	-1.338175559
PKIG	-1.528432567	-1.34829085
RHAG	-1.02531363	-1.357239225
OAT	-2.49899907	-1.361631261
GABARAPL2	-1.23306412	-1.393249041
GYG1	-1.879544138	-1.414170209
GMPR	-2.075239994	-1.438041395
PGK1	-1.581851511	-1.445834828
GSTM4	-1.512452641	-1.451709935
FBLN5	-1.436611202	-1.492974251
PRR5	-2.115305255	-1.49514443
PRKAG2	-2.225927263	-1.509808663
ARHGAP18	-1.391679111	-1.509833552
EPAS1	-1.203717355	-1.510341272

COL4A1	-1.48759009	-1.517665758
SNTB1	-1.443965824	-1.539902939
COL1A1	-1.315496356	-1.551555892
FXYD1	-1.387079467	-1.570029071
IFI44L	-1.337303365	-1.591085899
MAP1LC3A	-1.048442385	-1.608903594
HEBP2	-1.16081149	-1.609816913
PPL	-1.426828953	-1.634860821
SORBS1	-1.469246802	-1.658002896
PEBP1	-1.748231343	-1.66451815
COL4A2	-1.578907558	-1.688522063
GPI	-1.069493774	-1.691381112
SERPINF1	-1.397281963	-1.696157991
CCL5	-1.109553031	-1.772032858
PGM1	-1.759154524	-1.789645729
PLAC9	-1.23178362	-1.792566557
ABAT	-1.372913922	-1.800724993
BIN1	-1.857033315	-1.805251946
PPARG	-1.366697216	-1.829973349
CCNG1	-1.817819725	-1.851649127
UPK3A	-1.480318153	-1.858910264
TPI1	-1.69430135	-1.888377751
CLEC3B	-1.531598746	-1.893222639
GLDC	-1.564249032	-1.912452571
MYH10	-1.575120031	-1.93208765
LRRC20	-2.089373822	-1.933362298
PMP22	-1.226902428	-1.973445497
GAPDH	-1.236287905	-1.97506573
GPD1	-1.821074145	-1.975225236
COL8A1	-1.382043145	-1.984775861
ASPH	-1.840188512	-1.985255629
SLC25A12	-2.19802149	-2.007739273
PABPC4	-1.459162145	-2.011856772

PIP5K1B	-1.131494653	-2.02168383
DPT	-1.308123183	-2.022602555
B2M	-1.105216673	-2.047815602
MR1	-1.140217793	-2.048429498
WFDC2	-1.795908237	-2.084519667
FMO3	-1.456471792	-2.221183265
TPPP3	-1.009791224	-2.223361269
CPT1A	-1.357922073	-2.23155879
GAMT	-1.826047131	-2.231630856
SATB1	-1.227075624	-2.273040443
TNNT3	-1.513997901	-2.339849816
PDGFRL	-1.800141675	-2.371839524
NFKBIE	-1.372821247	-2.402588329
RBP4	-1.103940731	-2.459892494
IL20RB	-1.010991128	-2.561217059
CSPG5	-2.141462953	-2.581255631
OXCT1	-1.869403588	-2.588758755
PSMB8	-1.620828601	-2.592896248
TPM3	-1.474841223	-2.617865293
CSRP2	-1.274203037	-2.620124343
ATP1B2	-1.072050551	-2.634122381
PON2	-1.954705364	-2.645227945
PYGM	-2.102987141	-2.650635686
SLC7A11	-1.868178941	-2.730479253
SLC2A9	-1.354612735	-2.748597191
LAMB2	-1.915486057	-2.857923058
CA2	-1.153542882	-2.917604918
FAM177B	-1.23535219	-2.920998358
MFAP5	-1.544481335	-2.960164026
FHL1	-1.456701548	-3.041851356
KRT6A	-1.037350883	-3.14055249
ACTA2	-1.56258874	-3.241846572
ALDH1A1	-1.427074822	-3.260108361

HSPB8	-1.759665694	-3.32357136
KRT5	1.276836757	-3.348271133
ITLN1	-1.012268432	-3.421464369
UNC45B	-2.001763417	-3.473905388
BHMT	-1.619235379	-3.492767861
RHCG	-1.117440496	-3.497517836
ADH4	-1.879124268	-3.533277119
XDH	-1.00091285	-3.640309512
CHRDL1	-1.350119239	-3.736435992
AGMAT	-1.518843667	-3.73840116
PTPLA	-1.719731661	-3.796454185
ADSSL1	-1.124744305	-3.866619431
GATM	-1.658542074	-3.886763213
TPM1	-1.398433837	-4.007238876
DES	-1.342677011	-4.509259662
MYL4	-1.743138709	-4.523873064
PFKM	-1.687934512	-4.553956394
CRISPLD2	-1.034256986	-4.557077964
KBTBD5	-1.215525597	-4.567147531
SMTNL2	-1.747093833	-4.757551504
INMT	-1.506190488	-4.824161123
PRPH	-1.066754349	-4.904548186
AK1	-1.844438209	-5.176738766
CRYAB	-1.678744326	-5.240546744
CACNG1	-1.30492096	-5.323867555
SMYD1	-1.814332152	-5.73188589
FAAH	-1.608238464	-5.754611085
SLC25A4	-1.24751953	-5.77807223
MYBPC3	-1.589077946	-5.896018351
MYH1	-1.498601798	-6.279124018
MYH4	-1.422995109	-6.515871214
TNNI1	-1.493765717	-6.527468247
MBP	-1.621325411	-6.653087835

Symbol	logFC_Microarray	logFC_RNAseq
MYH7	-1.297431291	-6.678383953
MYH2	-1.534959699	-6.727767502
TNNT1	-1.510615817	-6.875421716
MYH13	-1.244720679	-6.97257457
MYL2	-1.366521528	-7.105320813
KBTBD10	-1.500898816	-7.193339546
TNNI2	-1.369660522	-7.228379118
TNNC2	-1.478950273	-7.534047748
TNNC1	-1.580532451	-7.755150972
MYL3	-1.490827629	-7.786931108
ACTA1	-1.25025588	-7.871633305
MYL1	-1.235456453	-7.899108953
ACTC1	-1.509585867	-7.945791168
ACTN3	-1.894071237	-8.043620356
MYBPC2	-1.549730099	-8.198535133
ADIPOQ	-1.647000481	-8.213830687
CKM	-1.288476705	-8.420752802
MYOZ1	-1.781804064	-8.639080141
MYLPF	-1.226578963	-9.33208102
PVALB	-1.246047342	-9.578303621
Regenerative vs. Wound Healing		
Symbol	**logFC_Microarray**	**logFC_RNAseq**
LAMA1	1.681575881	3.107642499
FBLN1	1.095020252	2.753739025
CCNB1	1.63255645	2.571265222
CCNB3	1.546283843	2.504766175
PCDH18	1.053955619	2.41058588
AURKA	1.566892534	2.404717856
MSI1	1.225454798	2.390891775
TGFBI	1.406601655	2.348763563
MAD2L1	1.632499335	2.231539566
NEK2	1.24166499	2.174606905
KIFC1	1.701683946	2.162698956

CDCA7L	1.018397291	2.157764912
MCM3	1.269945481	2.139733989
PLK1	1.498920574	2.122319124
KIAA0101	1.604164713	2.117462647
SMC2	1.317620085	2.107918358
KIF11	1.488806204	2.102939225
KIF22	1.619286638	2.06396245
ST8SIA2	1.251549538	2.029740373
SAFB	1.605975885	1.999124019
TPX2	1.671174325	1.983177803
FAM54A	1.341149047	1.975071617
STMN1	1.760230349	1.943535247
ZNF367	1.055022489	1.936582169
CDCA5	1.54808286	1.934198947
UHRF1	1.34193544	1.923651937
CRABP2	1.214411766	1.912998733
KIF20A	1.589458139	1.902278368
BRD3	1.11809543	1.892648667
RCC1	1.176652784	1.87015458
CDCA8	1.616120254	1.844058795
CENPF	1.450620796	1.840154909
AURKB	1.751490107	1.833971373
CHEK1	1.110910967	1.822517304
PRC1	1.382568795	1.807828188
CCNA2	1.588922896	1.793986499
MTBP	1.056317552	1.789952822
HAUS1	1.475865613	1.769786394
HIST1H2BJ	1.303769005	1.765956358
FEN1	1.446256135	1.756839918
KIF23	1.527935828	1.719857591
RAD51AP1	1.41138275	1.718392642
MCM2	1.205625785	1.703898956
PBK	1.251373622	1.701420269

MCM6	1.303084192	1.694172193
GINS2	1.510611427	1.687254971
NASP	1.66945096	1.683201303
RRM2	1.721672665	1.662657458
CHAF1A	1.473689647	1.643965336
USP1	1.404084123	1.642606243
RNF168	1.37186688	1.628617206
NUSAP1	1.554603254	1.622824438
PRR11	1.348098887	1.604780366
CSE1L	1.490909407	1.600682611
PDCD11	1.428519593	1.595394439
NCAPH	1.294345584	1.588163322
IQCB1	1.22448104	1.583545017
NCAPD3	1.535563603	1.567952932
CTHRC1	1.498513087	1.556715265
APEX1	1.588553054	1.54079781
TOP2B	1.718954705	1.535247074
B9D1	1.042560637	1.533772027
RBM12B	1.040780775	1.531252867
ZWINT	1.407791174	1.528612024
NDC80	1.588936373	1.526717804
ASF1B	1.101933458	1.524324356
MDN1	1.359188809	1.499898511
PCNA	1.449532342	1.487801304
CDC20	1.588994418	1.485366743
RMI1	1.633736554	1.469359551
ZNF507	1.270105108	1.461192975
EZH2	1.212622337	1.456294924
DYNC1H1	1.794780477	1.45570769
TRIP13	1.575981926	1.452702682
POLA2	1.427674797	1.448620026
EED	1.335952851	1.444943132
CDC25A	1.232485998	1.435353769

HMGB3	1.120089002	1.43263268
TRMT11	1.610579804	1.422105307
COL12A1	1.23276962	1.422002676
PLOD1	1.247398935	1.417171654
CCDC112	1.04988406	1.411357176
LONP1	1.620066611	1.403597261
PRPF40A	1.361970397	1.402580444
SLBP	1.668452238	1.401156031
KIF2C	1.471599364	1.38214715
MCM7	1.426809354	1.376233619
MBD3	1.224976243	1.373415244
SASS6	1.10894975	1.364701689
NUCKS1	1.080829056	1.361647494
BCLAF1	1.470095658	1.357278767
ATAD2	1.479878554	1.356842314
HIST1H2AG	1.259899416	1.324345662
BUB1	1.129499582	1.309715306
PITRM1	1.090096091	1.299297319
TSN	1.203853085	1.291780273
NUP43	1.749672567	1.288698529
BAZ1B	1.462529754	1.287644852
IARS	1.493511565	1.272316047
NEIL3	1.296933523	1.269415689
KPNA2	1.187098237	1.267391697
CBX3	1.416455342	1.252487497
RPA2	1.467321078	1.250810459
ANKRD26	1.152019697	1.25017001
SKP2	1.47290261	1.247808328
POLR3C	1.492365526	1.239026958
CTPS	1.47203687	1.235372152
NCAPG	1.435187808	1.223220035
CDC7	1.659685804	1.220980925
SART3	1.41567608	1.214817793

NUP133	1.106193802	1.214372412
ACP6	1.405503778	1.213841863
PDS5A	1.396402401	1.210468233
DNAJC9	1.404903258	1.209918354
BUB1B	1.231534918	1.207481295
INCENP	1.516049392	1.201788168
PSMD8	1.226514128	1.19363282
TRIM28	1.196686185	1.189473793
SMC4	1.18582971	1.170658111
HELLS	1.269037234	1.156957424
RAD9A	1.46056916	1.147577854
PARP1	1.389916132	1.136469745
HSPA14	1.559926057	1.132243776
CHAF1B	1.395045943	1.12351374
LARP7	1.630962169	1.121571844
SMAD5	1.706437437	1.119467834
RRM1	1.72412682	1.10887192
TMEM138	1.433251602	1.10307947
MCM4	1.454125541	1.102349392
MIPEP	1.178053805	1.100664871
NIPBL	1.431063764	1.099564131
TMPO	1.190672629	1.097330309
SLTM	1.413772491	1.094038608
MTA3	1.5118393	1.089258527
DIS3	1.570052882	1.088546895
PSMD10	1.127284237	1.087950131
APPBP2	1.333530091	1.085959974
NOL9	1.648724454	1.082700549
VRK1	1.345297011	1.079032858
ZBTB8A	1.239900055	1.075126664
ETV4	1.285161818	1.067140835
RFC4	1.520152148	1.047572266
MED4	1.615917662	1.046729455

ANKRD10	1.618808576	1.040224139
RFC2	1.627676725	1.029193094
RAD51	1.368162526	1.028939706
MCM3AP	1.477451611	1.028584852
WDR77	1.488619856	1.021031959
SRRM2	1.132398273	1.019494312
LRPPRC	1.398210814	1.005411721
PCGF5	-1.271493486	-1.001303762
PNO1	-1.001035867	-1.011449177
UBE2E1	1.156582425	-1.016765167
TMUB2	-1.197159952	-1.018581813
RPL14	1.06442255	-1.033652655
COX7A2L	-1.326865172	-1.038946203
OAT	-1.186655574	-1.052620042
PGK1	-1.011204939	-1.065710778
STX5	-1.619340505	-1.077180457
XBP1	-1.115822324	-1.117953851
ITGB1BP3	-1.178040502	-1.119528767
GPD1	-1.040810741	-1.125560294
PELI2	-1.563328446	-1.128725881
PTP4A3	-1.54740307	-1.178902422
ACADL	-1.150827201	-1.193026938
FBP1	-1.359000948	-1.21063746
FAM110B	-1.260664396	-1.211746282
DNAJB5	-1.379458475	-1.21378182
GAMT	-1.272552277	-1.217602864
HSD17B8	-1.098231844	-1.218502721
RND3	-1.056552294	-1.224422548
RNF14	-1.162899882	-1.256237766
CITED2	-1.158451192	-1.259280611
FXYD1	-1.281654431	-1.26051334
BCL2L1	-1.592180197	-1.262573518
RCAN1	-1.233293642	-1.290724068

CD74	-1.07800085	-1.323454506
KEAP1	-1.396304198	-1.33075948
SEMA3F	-1.180584697	-1.359787994
PGM1	-1.343472361	-1.364050493
PRDX6	-1.261915889	-1.379846008
CDKN1B	-1.146621373	-1.387396099
SGMS1	-1.253390758	-1.405462237
EGFR	-1.233600462	-1.422693152
GYG1	-1.329368708	-1.431997309
RIOK3	-1.054898709	-1.43625904
ARHGAP18	-1.331230939	-1.465156247
CCNG1	-1.427373779	-1.495833788
PNRC1	-1.113404133	-1.578437307
SERPINF1	-1.37502794	-1.635488673
SPA17	-1.346828321	-1.668771597
PABPC4	-1.150850513	-1.672948637
GSTM4	-1.297345798	-1.679095506
WSB1	-1.183414766	-1.692795993
DNAJB1	-1.2317327	-1.710719244
MFAP5	-1.24756762	-1.714414565
ZFAND5	-1.242491225	-1.721018779
PLAC9	-1.237803655	-1.72321973
UGDH	-1.047207662	-1.726010915
TPM3	-1.256302409	-1.757641978
PPL	-1.104309198	-1.782759917
USP2	-1.426977025	-1.788861294
OXCT1	-1.225412082	-1.809633415
FCN1	-1.024830218	-1.813528054
LAMB2	-1.323908694	-1.835546153
FHL1	-1.282555714	-1.837307948
PON2	-1.246695713	-1.853805839
RHAG	-1.330402945	-1.903382974
SYT16	-1.528937678	-1.952187312

HBA2	-1.094989424	-2.000657536
SGK1	-1.24077182	-2.045396718
MYC	-1.087659943	-2.059241774
CSRP2	-1.212564077	-2.068316945
G0S2	-1.182025184	-2.07139454
PMP22	-1.238827998	-2.097494008
SOCS1	-1.072763951	-2.143696401
PYGM	-1.411676167	-2.149744439
TNNT3	-1.337531669	-2.231012559
LARP6	-1.580453161	-2.250463532
SCG2	-1.233280839	-2.271756419
MMP19	-1.324476516	-2.352029938
BHMT	-1.30093442	-2.383416653
TPPP3	-1.154838061	-2.389808746
PTPLA	-1.33004948	-2.448568291
HSPB8	-1.071767196	-2.537248098
UCMA	-1.070852439	-2.552982313
SQSTM1	-1.241272581	-2.572967918
ACTA2	-1.338806312	-2.60763373
IRF1	-1.184983287	-2.619729752
GFPT2	-1.01200468	-2.650625357
MYL4	-1.289977575	-2.68116652
PDLIM7	-1.14067578	-2.709895962
CYR61	-1.323059389	-2.728154652
FGL2	-1.462132139	-2.735059744
ARL4D	-1.088345309	-2.755944915
TPM1	-1.251366711	-2.796482174
ALDOA	-1.066482265	-2.848949291
GADD45B	-1.72506605	-2.854287579
SMTNL2	-1.419310004	-2.88689641
AGMAT	-1.170943998	-2.981235596
ARG1	-1.106117494	-3.007478461
FGFBP1	-1.183561384	-3.067809264

TFPI2	-1.138566889	-3.292959877
HBZ	-1.109821725	-3.341589226
AQP4	-1.214599306	-3.380177723
PFKM	-1.417616518	-3.5355142
DES	-1.288766034	-3.579917766
DUSP1	-1.19217523	-3.698381715
MYBPC3	-1.379809348	-3.731048672
AK1	-1.437474793	-3.762280958
EGR1	-1.07853509	-3.763053099
KBTBD5	-1.229927474	-3.777580701
CRYAB	-1.604894043	-3.933910079
HBE1	-1.171460297	-4.006521892
MYH1	-1.248258852	-4.017824114
FAAH	-1.330166301	-4.076964349
TNNI1	-1.154403428	-4.085297192
SLC25A4	-1.093958214	-4.090428108
TNNT1	-1.221512013	-4.108639043
PTGS2	-1.008457828	-4.149433074
MYL2	-1.247295011	-4.183669956
KBTBD10	-1.283872922	-4.415883333
TNNI2	-1.267088126	-4.478292988
MYL1	-1.208658053	-4.543844011
TNNC2	-1.300646577	-4.58311859
MYL3	-1.27998798	-4.590534562
SERPINE1	-1.345779118	-4.62905436
ACTC1	-1.286907341	-4.632952545
ACTA1	-1.26185373	-4.672032915
TNNC1	-1.33456375	-4.68683922
DUSP5	-1.33846471	-4.713807022
ADIPOQ	-1.271351292	-4.795042812
MYH7	-1.231788442	-4.915274638
MMP3	-1.161137698	-5.016746785
CKM	-1.198204618	-5.025329225

MYBPC2	-1.296441783	-5.098959152
MYOZ1	-1.303214295	-5.189963945
ACTN3	-1.418657167	-5.226718197
MBP	-1.531137968	-5.266839799
PVALB	-1.232827434	-5.599308655

Table A.5: List of the top DE genes commonly identified by Microarray and RNA-seq platforms for all three comparisons

A.6 GO Terms Enriched in Wound healing vs. Control

ON TO LO GY	ID	Description	pvalue	p.adjust	geneID	Count
BP	GO: 0010 942	positive regulation of cell death	3.3767E-08	8.1445E-05	ARHGEF2/BCL2L1/BMP2/CYR61/ DDIT4/DUSP1/EGR1/G0S2/GADD4 5B/GADD45G/HMOX1/LGALS9/M MP3/PTGS2/RHOB/SQSTM1/THBS 1/YWHAZ	18
BP	GO: 0019 221	cytokine-mediated signaling pathway	9.0149E-08	0.00010872	ARG1/BCL2L1/CXCR4/EGR1/HM OX1/JUNB/LMNB1/MMP1/MMP2/ MMP3/PELI1/PTGS2/SOCS1/SQST M1/TIMP1/YWHAZ	16
BP	GO: 0032 963	collagen metabolic process	6.2247E-07	0.00050046	ARG1/LARP6/MMP1/MMP13/MMP 19/MMP2/MMP3	7
BP	GO: 0007 162	negative regulation of cell adhesion	9.7048E-07	0.00053711	ARG1/BMP2/DUSP1/LGALS9/PELI 1/SERPINE1/SMAD7/SOCS1/THBS 1/TNC	10
BP	GO: 0008 284	positive regulation of cell proliferation	1.3461E-06	0.00053711	ARG1/BCL2L1/BMP2/CYR61/EGR 1/GLUL/HMOX1/LGALS9/MMP2/ ODC1/PELI1/PTGS2/SCG2/TGM1/ THBS1/TIMP1/TNC	17
BP	GO: 0030 334	regulation of cell migration	1.4271E-06	0.00053711	ARHGEF2/BMP2/CYR61/DUSP1/H MOX1/LGALS9/MMP3/PTGS2/RH OB/RND3/RRAS2/SEMA3F/SERPI NE1/SGK1/SMAD7/THBS1/TIMP1	17
BP	GO: 0001 666	response to hypoxia	1.6679E-06	0.00053711	BMP2/CXCR4/CYBB/DDIT4/EGR1 /HMOX1/MMP2/MMP3/PTGS2/SL C2A1/THBS1	11
BP	GO: 0001 944	vasculature development	3.6943E-06	0.00074256	CHD7/CYBB/CYR61/EGR1/HMOX 1/JUNB/MMP19/MMP2/PTGS2/RH OB/SCG2/SERPINE1/SMAD7/THB S1/ZFAND5	15
BP	GO: 0022 617	extracellular matrix disassembly	4.541E-06	0.00078235	MMP1/MMP13/MMP19/MMP2/MM P3/TIMP1	6
BP	GO: 0001 817	regulation of cytokine production	7.7742E-06	0.00114584	ARG1/ARHGEF2/CYBB/EGR1/HM OX1/LGALS9/PELI1/PTGS2/SERPI NE1/SMAD7/SOCS1/THBS1/UBE2J 1	13
BP	GO: 0035 239	tube morphogenesis	8.076E-06	0.00114584	BMP2/CHD7/CYBB/CYR61/HMOX 1/JUNB/MMP19/MMP2/PTGS2/RH OB/SCG2/SERPINE1/SKI/SMAD7/ THBS1/TNC	16
BP	GO: 0038 066	p38MAPK cascade	1.2566E-05	0.00151544	BMP2/DUSP1/GADD45B/GADD45 G/LGALS9	5
BP	GO: 0001 101	response to acid chemical	1.5653E-05	0.00165388	ARG1/BCL2L1/CYBB/DGAT2/DUS P1/EGR1/MMP2/PTGS2/SOCS1/TN C	10
BP	GO: 0002 704	negative regulation of leukocyte mediated immunity	1.5771E-05	0.00165388	ARG1/HMOX1/LGALS9/SMAD7	4

BP	GO: 0040 017	positive regulation of locomotion	1.7838E-05	0.00179268	ARHGEF2/BMP2/CYR61/HMOX1/ LGALS9/PTGS2/RHOB/RRAS2/SC G2/SEMA3F/SERPINE1/THBS1	12
BP	GO: 0009 636	response to toxic substance	2.2537E-05	0.00217439	ACTB/ARG1/BCL2L1/CYBB/DUSP 1/EGR1/HMOX1/MPO/PTGS2/RHO B/SLC30A1/TNC	12
BP	GO: 0001 816	cytokine production	2.3604E-05	0.00218973	ARG1/ARHGEF2/CYBB/EGR1/HM OX1/LGALS9/PELI1/PTGS2/SERPI NE1/SMAD7/SOCS1/THBS1/UBE2J 1	13
BP	GO: 0007 565	female pregnancy	2.6606E-05	0.00237679	ARG1/JUNB/LGALS9/MMP2/PTGS 2/SLC2A1/TIMP1	7
BP	GO: 0051 707	response to other organism	3.1624E-05	0.00252617	ARG1/BCL2L1/BMP2/CHD7/CHIT 1/CXCR4/DDIT4/JUNB/LGALS9/M PO/ODC1/PELI1/PTGS2/SERPINE1	14
BP	GO: 0043 207	response to external biotic stimulus	3.2467E-05	0.00252617	ARG1/BCL2L1/BMP2/CHD7/CHIT 1/CXCR4/DDIT4/JUNB/LGALS9/M PO/ODC1/PELI1/PTGS2/SERPINE1	14
BP	GO: 2001 237	negative regulation of extrinsic apoptotic signaling pathway	3.6342E-05	0.00265379	ARHGEF2/BCL2L1/HMOX1/SCG2/ SERPINE1/THBS1	6
BP	GO: 0042 035	regulation of cytokine biosynthetic process	3.7408E-05	0.00265379	CYBB/EGR1/HMOX1/THBS1/UBE 2J1	5
BP	GO: 1902 041	regulation of extrinsic apoptotic signaling pathway via death domain receptors	3.7408E-05	0.00265379	ARHGEF2/BCL2L1/HMOX1/SERPI NE1/THBS1	5
BP	GO: 0035 690	cellular response to drug	4.1777E-05	0.00281946	ACTB/ARG1/ARHGEF2/CYBB/DD IT4/EGR1/HMOX1/MMP3/PTGS2/ RHOB	10
BP	GO: 0006 954	inflammatory response	5.0774E-05	0.00310109	BMP2/CXCR4/CYBB/HMOX1/LGA LS9/MMP3/PTGS2/SCG2/SERPINE 1/THBS1/TIMP1/ZYX	12
BP	GO: 0002 695	negative regulation of leukocyte activation	5.9276E-05	0.00340411	ARG1/HMOX1/LGALS9/PELI1/SM AD7/SOCS1	6
BP	GO: 0042 089	cytokine biosynthetic process	6.5955E-05	0.00357144	CYBB/EGR1/HMOX1/THBS1/UBE 2J1	5
BP	GO: 0042 107	cytokine metabolic process	6.5955E-05	0.00357144	CYBB/EGR1/HMOX1/THBS1/UBE 2J1	5
BP	GO: 0050 900	leukocyte migration	6.8112E-05	0.00357144	CXCR4/DUSP1/HMOX1/LGALS9/ MMP1/SCG2/SERPINE1/SLC16A1/ THBS1	9
BP	GO: 0050 868	negative regulation of T cell activation	7.3266E-05	0.00368423	ARG1/LGALS9/PELI1/SMAD7/SO CS1	5
BP	GO: 0050 920	regulation of chemotaxis	7.3318E-05	0.00368423	CXCR4/DUSP1/LGALS9/SCG2/SE MA3F/SERPINE1/THBS1	7

BP	GO:0044706	multi-multicellular organism process	7.7665E-05	0.00382304	ARG1/JUNB/LGALS9/MMP2/PTGS2/SLC2A1/TIMP1	7
BP	GO:0097237	cellular response to toxic substance	8.104E-05	0.00390938	ACTB/ARG1/CYBB/EGR1/HMOX1/MPO/PTGS2/RHOB	8
BP	GO:0071229	cellular response to acid chemical	9.1989E-05	0.00426687	BCL2L1/CYBB/DGAT2/EGR1/MMP2/SOCS1/TNC	7
BP	GO:1901654	response to ketone	9.1989E-05	0.00426687	ARG1/BCL2L1/CYBB/DDIT4/DUSP1/THBS1/TNC	7
BP	GO:0001701	in utero embryonic development	0.00016927	0.00605743	BCL2L1/BMP2/CDKN1C/CHD7/CYR61/JUNB/KEAP1/SLC30A1/ZFAND5	9
BP	GO:1904019	epithelial cell apoptotic process	0.00017077	0.00605743	BCL2L1/HMOX1/SCG2/SERPINE1/THBS1	5
BP	GO:0008285	negative regulation of cell proliferation	0.00035371	0.01079757	ARG1/BMP2/CDKN1C/DUSP1/HMOX1/LGALS9/MXI1/PELI1/PTGS2/SCG2/SKI/THBS1	12
BP	GO:0010035	response to inorganic substance	0.00037527	0.01079757	ARG1/CYBB/DUSP1/HMOX1/JUNB/MMP3/MPO/PTGS2/RHOB/SLC30A1/THBS1	11
BP	GO:0060324	face development	0.00037932	0.01079757	CHD7/MMP2/SKI/ZFAND5	4
BP	GO:0010565	regulation of cellular ketone metabolic process	0.00045674	0.01251887	BMP2/DGAT2/EGR1/ODC1/PTGS2	5
BP	GO:0040013	negative regulation of locomotion	0.00046911	0.01271327	DUSP1/HMOX1/RHOB/SEMA3F/SERPINE1/SMAD7/THBS1/TIMP1	8
BP	GO:0007178	transmembrane receptor protein serine/threonine kinase signaling pathway	0.00048538	0.01281996	BMP2/CDKN1C/CYR61/EGR1/SKI/SMAD7/THBS1/ZYX	8
BP	GO:1904035	regulation of epithelial cell apoptotic process	0.00051378	0.01318339	HMOX1/SCG2/SERPINE1/THBS1	4
BP	GO:0001934	positive regulation of protein phosphorylation	0.00055282	0.01388967	ARHGEF2/BMP2/CXCR4/CYR61/DUSP5/EGR1/GADD45B/GADD45G/LGALS9/PTGS2/SOCS1/SQSTM1/THBS1	13
BP	GO:0033687	osteoblast proliferation	0.00069752	0.01617702	BMP2/CYR61/JUNB	3
BP	GO:0043200	response to amino acid	0.0007133	0.01631468	ARG1/BCL2L1/CYBB/MMP2/SOCS1	5
BP	GO:0043086	negative regulation of catalytic activity	0.00071698	0.01631468	CDKN1C/DUSP1/DUSP5/GADD45B/PPP1R14B/PTGS2/SERPINE1/SMAD7/SOCS1/TFPI2/THBS1/TIMP1	12
BP	GO:0030509	BMP signaling pathway	0.00080324	0.01793897	BMP2/CYR61/EGR1/SKI/SMAD7	5
BP	GO:0071230	cellular response to amino acid stimulus	0.00087901	0.01927431	BCL2L1/CYBB/MMP2/SOCS1	4

BP	GO: 0032 101	regulation of response to external stimulus	0.00089597	0.01929951	ARG1/CXCR4/DUSP1/LGALS9/MMP3/PTGS2/SCG2/SEMA3F/SERPINE1/THBS1/ZYX	11
BP	GO: 0001 935	endothelial cell proliferation	0.00090139	0.01929951	ARG1/BMP2/HMOX1/SCG2/THBS1	5
BP	GO: 0072 593	reactive oxygen species metabolic process	0.00098332	0.02044628	CYBB/CYR61/DDIT4/MMP3/MPO/PTGS2/THBS1	7
BP	GO: 0003 006	developmental process involved in reproduction	0.00099811	0.02057647	BASP1/BCL2L1/CDKN1C/CHD7/CYR61/JUNB/MMP19/PTGS2/TNC/UBE2J1	10
BP	GO: 0031 670	cellular response to nutrient	0.00103331	0.02094401	CYBB/HMOX1/PTGS2/TNC	4
BP	GO: 0071 772	response to BMP	0.00118573	0.02302033	BMP2/CYR61/EGR1/SKI/SMAD7	5
BP	GO: 0071 773	cellular response to BMP stimulus	0.00118573	0.02302033	BMP2/CYR61/EGR1/SKI/SMAD7	5
BP	GO: 0001 649	osteoblast differentiation	0.00125356	0.02308081	BMP2/CYR61/JUNB/RRAS2/SKI/TNC	6
BP	GO: 0002 886	regulation of myeloid leukocyte mediated immunity	0.00158967	0.02700205	ARG1/HMOX1/LGALS9	3
BP	GO: 0034 405	response to fluid shear stress	0.00158967	0.02700205	PTGS2/SMAD7/TFPI2	3
BP	GO: 0031 960	response to corticosteroid	0.00168903	0.0280962	ARG1/CYBB/DDIT4/DUSP1/PTGS2	5
BP	GO: 0009 611	response to wounding	0.00172999	0.02858044	ACTB/ARG1/CYR61/HMOX1/SERPINE1/TFPI2/THBS1/TIMP1/TNC/YWHAZ	10
BP	GO: 0090 049	regulation of cell migration involved in sprouting angiogenesis	0.00178491	0.02908915	HMOX1/PTGS2/THBS1	3
BP	GO: 0031 667	response to nutrient levels	0.00189254	0.03023043	ARG1/CYBB/GLUL/HMOX1/MPO/PTGS2/SLC16A1/SLC2A1/TNC	9
BP	GO: 0071 470	cellular response to osmotic stress	0.00199449	0.03103679	ARHGEF2/PTGS2/SLC2A1	3
BP	GO: 0007 566	embryo implantation	0.00221878	0.03283245	MMP2/PTGS2/TIMP1	3
BP	GO: 0050 777	negative regulation of immune response	0.00237789	0.03455097	ARG1/HMOX1/LGALS9/SMAD7	4
BP	GO: 0000 302	response to reactive oxygen species	0.00271425	0.03873832	ARG1/DUSP1/HMOX1/MMP3/MPO/RHOB	6
BP	GO: 0097 327	response to antineoplastic agent	0.00284352	0.04010858	ARG1/DDIT4/EGR1/HMOX1	4

ONTOLOGY	ID	Description	pvalue	p.adjust	geneID	Count
BP	GO: 1901699	cellular response to nitrogen compound	0.00301581	0.0413303	ACTB/ARG1/ARHGEF2/BCL2L1/CYBB/EGR1/MMP2/MMP3/PTGS2/SOCS1	10
BP	GO: 0046890	regulation of lipid biosynthetic process	0.00314265	0.0426292	BMP2/CYR61/DGAT2/EGR1/PTGS2	5
BP	GO: 0061448	connective tissue development	0.00330319	0.04353719	BMP2/CYR61/DGAT2/EGR1/MMP13/TIMP1	6
BP	GO: 0030217	T cell differentiation	0.00354459	0.0458356	CHD7/EGR1/LGALS9/SMAD7/SOCS1	5
BP	GO: 0002042	cell migration involved in sprouting angiogenesis	0.00357259	0.0458356	HMOX1/PTGS2/THBS1	3
BP	GO: 0030952	establishment or maintenance of cytoskeleton polarity	0.00374679	0.04658374	RHOB/RND3	2
BP	GO: 0032461	positive regulation of protein oligomerization	0.00374679	0.04658374	MMP1/MMP3	2
BP	GO: 0046697	decidualization	0.00374679	0.04658374	JUNB/PTGS2	2
BP	GO: 0072215	regulation of metanephros development	0.00374679	0.04658374	BASP1/EGR1	2
CC	GO: 0031012	extracellular matrix	5.2662E-05	0.01190166	CYR61/MMP1/MMP13/MMP19/MMP2/MMP3/SERPINE1/TFPI2/THBS1/TIMP1/TNC	11
MF	GO: 0004222	metalloendopeptidase activity	0.00013381	0.0373335	MMP1/MMP13/MMP19/MMP2/MMP3	5
GO terms enriched by the top 4 down-regulated genes						
ONTOLOGY	ID	Description	pvalue	p.adjust	geneID	Count
MF	GO: 0015556	C4-dicarboxylate transmembrane transporter activity	0.00462828	0.04516037	SLC25A12	1
MF	GO: 0005326	neurotransmitter transporter activity	0.01016099	0.04516037	SLC25A12	1

Table A.6: Gene ontology terms enriched by the top 91 DE genes in wound healing vs. control comparison, commonly identified by both the analysis of both technologies

A.7 GO Terms Enriched in Regenerative vs. Control

ONTOLOGY	ID	Description	pvalue	p.adjust	geneID	Count
			GO terms enriched by the top 181 up-regulated genes			
BP	GO:0140014	mitotic nuclear division	6.03985E-08	8.77793E-05	AURKA/AURKB/CCNJ/CDC20/CDCA8/FLNA/KIF11/KIF22/KIF23/MAD2L1/MAD2L1BP/MTBP/NEK2/NIPBL/PLK1/PRC1/RCC1/TRIP13	18
BP	GO:0000280	nuclear division	6.51665E-08	8.77793E-05	AURKA/AURKB/CCNJ/CDC20/CDCA8/FLNA/KIF11/KIF22/KIF23/MAD2L1/MAD2L1BP/MTBP/NEK2/NIPBL/PLK1/PRC1/RCC1/RPA2/TOP2B/TRIP13	20
BP	GO:0007059	chromosome segregation	2.27539E-07	0.000149307	AURKB/CDC20/CDCA8/FEN1/KIF22/KIF23/MAD2L1/NEK2/NIPBL/PLK1/PRC1/RCC1/SFPQ/TOP1/TOP2B/TRIP13/UBE2I	17
BP	GO:0000819	sister chromatid segregation	2.90586E-07	0.000149307	AURKB/CDC20/CDCA8/FEN1/KIF22/KIF23/MAD2L1/NEK2/NIPBL/PLK1/PRC1/SFPQ/TOP2B/TRIP13	14
BP	GO:0007052	mitotic spindle organization	3.64094E-07	0.000149307	AURKA/AURKB/CDC20/FLNA/KIF11/KIF23/NEK2/PLK1/PRC1/RCC1/STMN1	11
BP	GO:0008380	RNA splicing	3.87955E-07	0.000149307	CLK3/CLNS1A/CSTF1/DHX15/FUS/HNRNPM/MPHOSPH10/PRPF3/PRPF39/PTBP1/RBMX/RBMXL1/SART3/SFPQ/SNRNP40/SNRPA/SNRPA1/TARDBP/TRA2B/ZNF326/ZRANB2	21
BP	GO:0007088	regulation of mitotic nuclear division	8.17732E-07	0.000275371	AURKA/AURKB/CCNJ/CDC20/KIF11/MAD2L1/MAD2L1BP/MTBP/NEK2/NIPBL/PLK1/RCC1/TRIP13	13
BP	GO:0006325	chromatin organization	2.22437E-06	0.00043043	ANP32E/ASF1B/AURKA/AURKB/BAZ1B/BRD3/CBX3/CHD7/FBL/HCFC1/HELLS/HIST3H2BB/HMGB2/LOXL2/MBD3/NASP/NIPBL/PBRM1/RBM14/SAFB/SART3/SFPQ/SMARCC1/TCF7L1/TOP1	25

BP	GO:001 0564	regulation of cell cycle process	9.52109E-06	0.001508813	APEX1/AURKA/AURK B/CBX3/CCNJ/CDC20/ FEN1/GPNMB/HAUS1/ KIF11/KIF23/MAD2L1/ MAD2L1BP/MTBP/NE K2/NIPBL/PLK1/PRC1/ RBM14/RCC1/RPA2/R RM2/SFPQ/TRIP13	24
BP	GO:003 0198	extracellular matrix organization	1.90826E-05	0.002570432	COL12A1/FN1/HAS2/I TGB1/KAZALD1/LAM A1/LOXL2/MFAP2/M MP13/MMP2/PLOD1/S ULF1/TGFBI/THBS1/T NC	15
BP	GO:005 1983	regulation of chromosome segregation	2.09352E-05	0.002588695	AURKB/CDC20/FEN1/ MAD2L1/NEK2/NIPBL /PLK1/SFPQ/TRIP13	9
BP	GO:190 3311	regulation of mRNA metabolic process	5.08359E-05	0.004891144	APEX1/HNRNPM/MY EF2/PTBP1/RBMX/RB MXL1/SAFB/SART3/S LTM/SNRPA/TARDBP/ TRA2B/VIM	13
BP	GO:004 4772	mitotic cell cycle phase transition	0.000104137	0.008760777	APEX1/AURKA/AURK B/CDC20/GPNMB/HA US1/ITGB1/MAD2L1/ MAD2L1BP/MTBP/NA SP/NEK2/PLK1/RCC1/ RPA2/RPS6KB1/RRM2 /TRIP13	18
BP	GO:000 7094	mitotic spindle assembly checkpoint	0.000228919	0.015417687	AURKB/CDC20/MAD2 L1/PLK1/TRIP13	5
BP	GO:003 1577	spindle checkpoint	0.000228919	0.015417687	AURKB/CDC20/MAD2 L1/PLK1/TRIP13	5
BP	GO:007 1173	spindle assembly checkpoint	0.000228919	0.015417687	AURKB/CDC20/MAD2 L1/PLK1/TRIP13	5
BP	GO:007 1174	mitotic spindle checkpoint	0.000228919	0.015417687	AURKB/CDC20/MAD2 L1/PLK1/TRIP13	5
BP	GO:190 5819	negative regulation of chromosome separation	0.000370043	0.020344809	AURKB/CDC20/MAD2 L1/PLK1/TRIP13	5
BP	GO:003 1145	anaphase-promoting complex-dependent catabolic process	0.000429225	0.023126661	AURKA/AURKB/CDC 20/MAD2L1/PLK1	5
BP	GO:000 1503	ossification	0.000563618	0.027855528	BMP2/CTHRC1/FBL/G PNMB/ID3/JAG1/JUNB /KAZALD1/MMP13/M MP2/NIPBL/RBMX/TN C	13
BP	GO:007 1103	DNA conformation change	0.000675419	0.031922416	ASF1B/HELLS/HIST3H 2BB/HMGB2/NASP/NI PBL/RPA2/SART3/TOP 1/TOP2B	10

BP	GO:007 1824	protein-DNA complex subunit organization	0.00071188	0.032306827	ANP32E/ASF1B/HELL S/HIST3H2BB/HMGB2 /NASP/PBRM1/RPA2/S ART3/SMARCC1	10
BP	GO:004 8514	blood vessel morphogenesi s	0.000875596	0.037442171	CHD7/CYBB/FN1/GPN MB/HAS2/HMOX1/ITG B1/JAG1/JUNB/LAMA 1/LOXL2/MMP2/SMA D7/SULF1/TGFBI/THB S1	16
BP	GO:000 1649	osteoblast differentiation	0.000942854	0.038485583	BMP2/CTHRC1/FBL/G PNMB/ID3/JAG1/JUNB /RBMX/TNC	9
BP	GO:000 7127	meiosis I	0.001064576	0.042240906	AURKA/PLK1/RPA2/T OP2B/TRIP13	5
BP	GO:003 5024	negative regulation of Rho protein signal transduction	0.001110828	0.043272105	ITGB1/STMN1/TNFAI P1	3
BP	GO:003 4502	protein localization to chromosome	0.001124368	0.043272105	AURKB/DKC1/MTBP/ NIPBL/PLK1/RPA2	6
BP	GO:003 5239	tube morphogenesi s	0.001236851	0.046930658	BMP2/CHD7/CTHRC1/ CYBB/FN1/GPNMB/H AS2/HMOX1/ITGB1/JA G1/JUNB/LAMA1/LOX L2/MMP2/NIPBL/SMA D7/SULF1/TGFBI/THB S1/TNC	20
BP	GO:004 5787	positive regulation of cell cycle	0.001322959	0.049500732	APEX1/AURKA/AURK B/CCNJ/FEN1/HCFC1/ KIF23/MAD2L1/MTBP/ NIPBL/PGGT1B/RPS6 KB1/SFPQ	13
CC	GO:000 0785	chromatin	1.22558E-08	4.03217E-06	ANP32E/ASF1B/BAZ1 B/CBX3/HELLS/HIST3 H2BB/HMGB2/JUNB/K IF22/LOXL2/MBD3/M TBP/NASP/NIPBL/PBR M1/PLK1/RBMX/RCC1 /RPA2/SFPQ/SMARCC 1/TARDBP/TMPO/TOP 2B	24
CC	GO:004 4452	nucleolar part	3.64235E-07	3.40189E-05	COIL/DKC1/FBL/IPO1 1/MPHOSPH10/NOL11/ NOLC1/POLR1C/PSPC 1/PWP2/RRP9/SMAD7/ TOP1/UBE2I	14
CC	GO:000 0228	nuclear chromosome	4.00036E-07	3.40189E-05	ANP32E/APEX1/ASF1 B/AURKA/AURKB/BA Z1B/CBX3/FEN1/HMG B2/JUNB/MBD3/NASP/ NEK2/NIPBL/PBRM1/P LK1/RBMX/RCC1/RPA 2/SMARCC1/TARDBP/ TOP1/UBE2I	23

CC	GO:004 4454	nuclear chromosome part	4.13603E-07	3.40189E-05	ANP32E/APEX1/ASF1 B/AURKA/AURKB/BA Z1B/CBX3/FEN1/HMG B2/JUNB/MBD3/NASP/ NIPBL/PBRM1/PLK1/R BMX/RCC1/RPA2/SM ARCC1/TARDBP/TOP1 /UBE2I	22
CC	GO:000 5732	small nucleolar ribonucleopro tein complex	1.05983E-06	6.97368E-05	DKC1/FBL/MPHOSPH 10/NOLC1/RRP9/SNRN P40	6
CC	GO:000 0775	chromosome, centromeric region	2.07646E-06	0.000113859	AURKA/AURKB/BAZ1 B/CBX3/CDCA8/HELL S/KIF22/MAD2L1/MTB P/NEK2/NUP160/NUP8 5/PLK1	13
CC	GO:009 8687	chromosomal region	6.87409E-06	0.000299166	APEX1/AURKA/AURK B/BAZ1B/CBX3/CDCA 8/FEN1/HELLS/KIF22/ MAD2L1/MTBP/NEK2/ NUP160/NUP85/PLK1/ RPA2	16
CC	GO:000 5819	spindle	7.27455E-06	0.000299166	AURKA/AURKB/CBX 3/CDC20/CDCA8/HAU S1/IQCB1/KIF11/KIF22 /KIF23/MAD2L1/MAD 2L1BP/NEK2/NUP85/P LK1/PRC1	16
CC	GO:000 0793	condensed chromosome	8.75241E-06	0.000319949	AURKA/AURKB/BAZ1 B/CBX3/HMGB2/MAD 2L1/NEK2/NUP85/PLK 1/RCC1/RPA2/UBE2I	12
CC	GO:000 0794	condensed nuclear chromosome	3.39329E-05	0.001116391	AURKA/AURKB/NEK 2/PLK1/RCC1/RPA2/U BE2I	7
CC	GO:000 5681	spliceosomal complex	7.59068E-05	0.00202787	DHX15/HNRNPM/MY EF2/PRPF3/PRPF39/RB MX/RBMXL1/SNRNP4 0/SNRPA/SNRPA1/TR A2B	11
CC	GO:000 5635	nuclear envelope	7.60505E-05	0.00202787	BICD2/CBX3/CSE1L/C YBB/IPO11/MAD2L1/ MAD2L1BP/MATR3/M CM3AP/NUP160/NUP8 5/RANBP1/RCC1/RRM 1/TMPO/TRA2B/UBE2I	17
CC	GO:000 1650	fibrillar center	8.01286E-05	0.00202787	COIL/DKC1/FBL/IPO1 1/NOLC1/PSPC1/SMA D7/TOP1/UBE2I	9
CC	GO:001 5030	Cajal body	0.000141662	0.00332905	COIL/DKC1/FBL/NOL C1/PRPF3/SART3	6
CC	GO:000 0922	spindle pole	0.000175451	0.003848233	AURKA/AURKB/CDC 20/HAUS1/KIF11/MAD 2L1/NEK2/PLK1/PRC1	9
CC	GO:012 0114	Sm-like protein family complex	0.000199842	0.004076949	CLNS1A/PRPF3/PRPF3 9/SART3/SNRNP40/SN RPA/SNRPA1	7

CC	GO:006 2023	collagen-containing extracellular matrix	0.000210663	0.004076949	COL12A1/CTHRC1/CT SC/F13A1/FN1/KAZAL D1/LAMA1/LOXL2/MF AP2/MMP2/TGFBI/TH BS1/TNC	13
CC	GO:001 6604	nuclear body	0.000245721	0.004491229	APEX1/BASP1/BAZ1B/ CLK3/COIL/DHX15/D KC1/FBL/HNRNPM/KI F22/NOLC1/PRPF3/PSP C1/RBM14/RPA2/SAR T3/SFPQ/SLTM/SNRN P40/SNRPA1/TARDBP/ UBE2I	22
CC	GO:007 2686	mitotic spindle	0.000267945	0.004639683	AURKA/AURKB/IQCB 1/KIF11/KIF22/KIF23/ MAD2L1	7
CC	GO:000 0790	nuclear chromatin	0.000317633	0.00522507	ANP32E/ASF1B/CBX3/ HMGB2/JUNB/MBD3/ NASP/NIPBL/PBRM1/ RBMX/RCC1/SMARC C1/TARDBP	13
CC	GO:009 7525	spliceosomal snRNP complex	0.000337663	0.005290048	PRPF3/PRPF39/SART3/ SNRNP40/SNRPA/SNR PA1	6
CC	GO:003 1012	extracellular matrix	0.00037665	0.00563263	COL12A1/CTHRC1/CT SC/F13A1/FN1/HNRNP M/KAZALD1/LAMA1/ LOXL2/MFAP2/MMP1 3/MMP2/TGFBI/THBS1 /TNC	15
CC	GO:000 0776	kinetochore	0.000420317	0.006012358	AURKB/KIF22/MAD2L 1/MTBP/NEK2/NUP160 /NUP85/PLK1	8
CC	GO:003 0532	small nuclear ribonucleopro tein complex	0.000575828	0.007893646	PRPF3/PRPF39/SART3/ SNRNP40/SNRPA/SNR PA1	6
CC	GO:000 0779	condensed chromosome, centromeric region	0.000639742	0.008419001	AURKA/AURKB/CBX 3/MAD2L1/NEK2/NUP 85/PLK1	7
CC	GO:000 5876	spindle microtubule	0.000675865	0.008552287	AURKA/AURKB/KIF1 1/PLK1/PRC1	5
CC	GO:000 5643	nuclear pore	0.001425632	0.017371596	BICD2/MAD2L1/MCM 3AP/NUP160/NUP85/R ANBP1	6
CC	GO:005 1233	spindle midzone	0.001928909	0.022664676	AURKA/AURKB/CDC A8/PLK1	4
CC	GO:003 2040	small-subunit processome	0.002204151	0.025005709	FBL/MPHOSPH10/PW P2/RRP9	4
CC	GO:001 6607	nuclear speck	0.002353328	0.02580816	APEX1/BASP1/CLK3/ DHX15/KIF22/PRPF3/P SPC1/RBM14/SART3/S FPQ/SNRNP40/SNRPA 1/TARDBP	13
CC	GO:000 0780	condensed nuclear chromosome, centromeric region	0.002730273	0.02807062	AURKA/AURKB/PLK1	3
CC	GO:000 5721	pericentric heterochromat in	0.002730273	0.02807062	BAZ1B/CBX3/HELLS	3

ONTOLOGY	ID	Description	pvalue	p.adjust	geneID	Count
CC	GO:0005875	microtubule associated complex	0.004174091	0.041614427	AURKA/AURKB/CDCA8/HAUS1/KIF11/KIF22/KIF23	7
CC	GO:0016363	nuclear matrix	0.004434168	0.042907096	HNRNPM/MATR3/PSPC1/SFPQ/VIM/ZNF326	6
CC	GO:0044420	extracellular matrix component	0.004921833	0.046265235	COL12A1/LAMA1/MFAP2/TNC	4
GO terms enriched by the top 166 down-regulated genes						
ONTOLOGY	**ID**	**Description**	**pvalue**	**p.adjust**	**geneID**	**Count**
BP	GO:0030049	muscle filament sliding	6.00774E-29	7.74098E-26	ACTA1/ACTC1/ACTN3/DES/MYBPC2/MYBPC3/MYH2/MYH4/MYH7/MYL1/MYL2/MYL3/MYL4/TNNC1/TNNC2/TNNI1/TNNI2/TNNT1/TNNT3/TPM1/TPM3	21
BP	GO:0033275	actin-myosin filament sliding	6.00774E-29	7.74098E-26	ACTA1/ACTC1/ACTN3/DES/MYBPC2/MYBPC3/MYH2/MYH4/MYH7/MYL1/MYL2/MYL3/MYL4/TNNC1/TNNC2/TNNI1/TNNI2/TNNT1/TNNT3/TPM1/TPM3	21
BP	GO:0006936	muscle contraction	1.14E-25	9.80398E-23	ABAT/ACTA1/ACTA2/ACTC1/ACTN3/ANXA6/ASPH/BIN1/CRYAB/DES/FXYD1/GAMT/MYBPC2/MYBPC3/MYH1/MYH13/MYH2/MYH4/MYH7/MYL1/MYL2/MYL3/MYL4/MYLPF/SNTA1/SNTB1/SORBS1/TNNC1/TNNC2/TNNI1/TNNI2/TNNT1/TNNT3/TPM1/TPM3	35
BP	GO:0006091	generation of precursor metabolites and energy	7.87895E-13	2.55563E-10	ACAT1/ACTN3/ADH4/ADIPOQ/ALDH1A1/ASPH/BNIP3/COX17/COX7A2L/COX7B/GAPDH/GLDC/GPD1/GPI/GYG1/MDH2/OXCT1/PARK7/PFKM/PGK1/PGM1/PRKAG2/PYGM/SLC25A12/SLC25A4/SORBS1/TPI1/XDH	28
BP	GO:0060047	heart contraction	7.93366E-13	2.55563E-10	ACTC1/ASPH/BIN1/DES/EPAS1/FXYD1/MYBPC3/MYH7/MYL1/MYL2/MYL3/MYL4/PEBP1/SNTA1/TNNC1/TNNI2/TNNT1/TNNT3/TPM1	19
BP	GO:0006937	regulation of muscle contraction	2.02141E-11	4.73562E-09	ABAT/ACTN3/ANXA6/BIN1/MYBPC3/MYH7/MYL2/MYL3/TNNC1/TNNC2/TNNI1/TNNI2/TNNT1/TNNT3/TPM1	15

BP	GO:001 6053	organic acid biosynthetic process	2.27305E-10	3.44568E-08	ABAT/ACADL/ACTN3 /ADIPOQ/BHMT/CD74 /CSPG5/GAMT/GAPD H/GATM/GOT1/GOT2/ GPD1/GPI/GSTM4/OA T/PARK7/PFKM/PGK1/ PGM1/PRKAG2/SLC25 A12/TPI1	23
BP	GO:004 6394	carboxylic acid biosynthetic process	2.27305E-10	3.44568E-08	ABAT/ACADL/ACTN3 /ADIPOQ/BHMT/CD74 /CSPG5/GAMT/GAPD H/GATM/GOT1/GOT2/ GPD1/GPI/GSTM4/OA T/PARK7/PFKM/PGK1/ PGM1/PRKAG2/SLC25 A12/TPI1	23
BP	GO:000 6006	glucose metabolic process	3.0181E-10	4.32091E-08	ACTN3/ADIPOQ/CPT1 A/GAPDH/GOT1/GOT2 /GPD1/GPI/MDH2/PFK M/PGK1/PGM1/RBP4/S LC25A12/SORBS1/TPI 1	16
BP	GO:000 6094	gluconeogene sis	5.55427E-10	7.50037E-08	ADIPOQ/GAPDH/GOT 1/GOT2/GPD1/GPI/MD H2/PGK1/PGM1/RBP4/ SLC25A12/TPI1	12
BP	GO:004 4282	small molecule catabolic process	5.82101E-10	7.50037E-08	ABAT/ACADL/ACAT1 /ACTN3/ADH4/ADIPO Q/ALDH1A1/CPT1A/E CHDC2/FAAH/GAPDH /GLDC/GOT1/GOT2/G PI/HEXB/OAT/OXCT1/ PFKM/PGK1/PGM1/SL C25A12/TPI1	23
BP	GO:000 6734	NADH metabolic process	2.46003E-09	2.5358E-07	ACTN3/GAPDH/GPD1/ GPI/MDH2/PFKM/PGK 1/SLC25A12/TPI1	9
BP	GO:004 6031	ADP metabolic process	7.90842E-09	7.54814E-07	ACTN3/AK1/GAPDH/ GPD1/GPI/PFKM/PGK 1/PGM1/PRKAG2/SLC 25A12/TPI1	11
BP	GO:003 0239	myofibril assembly	1.7206E-08	1.47799E-06	ACTA1/ACTC1/MYBP C2/MYBPC3/MYH10/ MYL2/MYOZ1/TNNT1 /TNNT3/TPM1	10
BP	GO:006 1061	muscle structure development	1.97251E-08	1.63973E-06	ACTA1/ACTC1/ACTN 3/BIN1/CRYAB/EPAS1 /FHL1/MYBPC2/MYBP C3/MYH10/MYH7/MY L2/MYL3/MYLPF/MY OZ1/PGK1/RBP4/SMY D1/TNNC1/TNNI1/TN NT1/TNNT3/TPM1/UN C45B	24
BP	GO:001 9320	hexose catabolic process	2.12785E-08	1.71358E-06	ACTN3/ALDH1A1/GA PDH/GPI/PFKM/PGK1/ PGM1/SLC25A12/TPI1	9
BP	GO:001 6052	carbohydrate catabolic process	3.08732E-08	2.41091E-06	ACTN3/ALDH1A1/GA PDH/GPD1/GPI/HEXB/ PFKM/PGK1/PGM1/PR KAG2/PYGM/SLC25A 12/TPI1	13

111

BP	GO:001 0927	cellular component assembly involved in morphogenesis	6.26842E-08	3.75668E-06	ACTA1/ACTC1/MYBP C2/MYBPC3/MYH10/ MYL2/MYOZ1/PMP22/ TNNT1/TNNT3/TPM1	11
BP	GO:004 4283	small molecule biosynthetic process	7.51877E-08	4.40361E-06	ABAT/ACADL/ACAT1 /ACTN3/ADIPOQ/BHM T/CD74/CSPG5/GAMT/ GAPDH/GATM/GOT1/ GOT2/GPD1/GPI/GST M4/MDH2/OAT/PARK 7/PFKM/PGK1/PGM1/P RKAG2/RBP4/SLC25A 12/TPI1/XDH	27
BP	GO:005 5008	cardiac muscle tissue morphogenesi s	9.55064E-08	5.27973E-06	ACTC1/MYBPC2/MYB PC3/MYH7/MYL2/MY L3/TNNC1/TNNI1/TPM 1	9
BP	GO:000 6754	ATP biosynthetic process	2.86592E-07	1.25178E-05	ACTN3/GAPDH/GPD1/ GPI/PFKM/PGK1/PGM 1/PRKAG2/SLC25A12/ TPI1	10
BP	GO:004 3467	regulation of generation of precursor metabolites and energy	1.30628E-06	4.20786E-05	ACTN3/BNIP3/COX17/ COX7A2L/GPD1/PAR K7/PRKAG2/SLC25A1 2/SORBS1	9
BP	GO:007 2521	purine-containing compound metabolic process	1.52082E-06	4.77944E-05	ACAT1/ACTN3/ADSS L1/AK1/COX7A2L/GA MT/GAPDH/GMPR/GP D1/GPI/MYH4/MYH7/ PARK7/PFKM/PGK1/P GM1/PRKAG2/SLC25A 12/SLC2A9/TPI1/XDH	21
BP	GO:005 5001	muscle cell development	2.03135E-06	5.88177E-05	ACTA1/ACTC1/BIN1/ MYBPC2/MYBPC3/M YH10/MYL2/MYOZ1/T NNT1/TNNT3/TPM1	11
BP	GO:005 0879	multicellular organismal movement	2.94258E-06	7.98214E-05	ACTN3/MYH7/TNNC1/ TNNC2/TNNI2/TNNT1/ TNNT3	7
BP	GO:005 0881	musculoskelet al movement	2.94258E-06	7.98214E-05	ACTN3/MYH7/TNNC1/ TNNC2/TNNI2/TNNT1/ TNNT3	7
BP	GO:009 7435	supramolecula r fiber organization	3.21488E-06	8.62995E-05	ACTA1/ACTC1/ARHG AP18/BIN1/COL1A1/C RYAB/DES/DPT/FBLN 5/MFAP5/MYBPC2/M YBPC3/MYH10/MYL2/ MYOZ1/PARK7/SORB S1/TNNT1/TNNT3/TP M1/TPM3/TPPP3	22
BP	GO:001 4706	striated muscle tissue development	3.55829E-06	9.35685E-05	ACTA1/ACTC1/ACTN 3/MYBPC2/MYBPC3/ MYH10/MYH7/MYL2/ MYL3/MYLPF/RBP4/S MYD1/TNNC1/TNNI1/ TPM1	15

BP	GO:004 6434	organophosph ate catabolic process	4.62375E-06	0.000116818	ACAT1/ACTN3/GAPD H/GPD1/GPI/PFKM/PG K1/PGM1/PRKAG2/SL C25A12/TPI1/XDH	12
BP	GO:000 9636	response to toxic substance	5.16253E-06	0.000125298	ABAT/ACTC1/ADIPO Q/BNIP3/CCL5/COL1A 1/CRYAB/FBLN5/GOT 2/INMT/MAP1LC3A/M BP/OXCT1/PARK7/PE BP1/PON2/RBP4/SLC7 A11	18
BP	GO:004 3462	regulation of ATPase activity	6.78748E-06	0.000160471	ATP1B2/GABARAPL2/ MYBPC3/MYL3/MYL4 /TNNC1/TNNT3/TPM1	8
BP	GO:004 6390	ribose phosphate biosynthetic process	7.2546E-06	0.000166921	ACAT1/ACTN3/ADSS L1/AK1/GAPDH/GPD1/ GPI/PFKM/PGK1/PGM 1/PRKAG2/SLC25A12/ TPI1	13
BP	GO:006 2013	positive regulation of small molecule metabolic process	1.61128E-05	0.000346023	ACTN3/ADIPOQ/CPT1 A/GPD1/PARK7/PPAR G/SLC25A12/SORBS1	8
BP	GO:003 1032	actomyosin structure organization	2.32541E-05	0.000483273	ACTA1/ACTC1/MYBP C2/MYBPC3/MYH10/ MYL2/MYOZ1/SORBS 1/TNNT1/TNNT3/TPM 1	11
BP	GO:003 3238	regulation of cellular amine metabolic process	3.21525E-05	0.000622984	ABAT/BHMT/PARK7/ PEBP1/SLC7A11	5
BP	GO:000 5977	glycogen metabolic process	4.57805E-05	0.000854902	GYG1/PFKM/PGM1/PR KAG2/PYGM/SORBS1	6
BP	GO:000 6073	cellular glucan metabolic process	4.57805E-05	0.000854902	GYG1/PFKM/PGM1/PR KAG2/PYGM/SORBS1	6
BP	GO:006 2012	regulation of small molecule metabolic process	5.73655E-05	0.001051239	ACADL/ACTN3/ADIP OQ/BHMT/COX7A2L/ CPT1A/GPD1/PARK7/P PARG/PRKAG2/SLC25 A12/SLC7A11/SORBS1	13
BP	GO:001 5980	energy derivation by oxidation of organic compounds	6.85368E-05	0.001226523	ACTN3/BNIP3/GPD1/G YG1/MDH2/PARK7/PF KM/PGM1/PRKAG2/P YGM/SLC25A12/SORB S1	12
BP	GO:001 4823	response to activity	8.21076E-05	0.001410609	ADIPOQ/ADSSL1/COL 4A2/GOT2/OXCT1/PE BP1	6
BP	GO:003 2781	positive regulation of ATPase activity	0.000107345	0.0017847	ATP1B2/GABARAPL2/ MYBPC3/MYL3/MYL4 /TPM1	6
BP	GO:005 2548	regulation of endopeptidase activity	0.000112971	0.001866194	ASPH/BIN1/CRYAB/G APDH/GPI/MBP/PARK 7/PEBP1/PPARG/PSMB	13

113

					8/SERPINF1/WFDC2/X DH	
BP	GO:001 0038	response to metal ion	0.000176969	0.002797852	ABAT/ACTA1/B2M/B NIP3/CA2/GOT1/GPI/ MAP1LC3A/PARK7/PE BP1/SERPINF1/SLC25 A12/TNNC1	13
BP	GO:004 5471	response to ethanol	0.000211258	0.00331959	ABAT/ACTC1/ADIPO Q/GOT2/OXCT1/PEBP 1/RBP4	7
BP	GO:003 4764	positive regulation of transmembran e transport	0.000249073	0.003820596	ADIPOQ/ATP1B2/CA2/ COX17/FXYD1/ITLN1/ PARK7/SORBS1	8
BP	GO:009 0087	regulation of peptide transport	0.00044907	0.006358535	ABAT/ADIPOQ/CA2/C CL5/CD74/CPT1A/GAP DH/GPI/MBP/MYH10/ OXCT1/PARK7/PFKM/ PKIG/RBP4/SLC25A4/ SLC7A11	17
BP	GO:001 5893	drug transport	0.000462233	0.006509145	ABAT/CA2/NFKBIE/P ARK7/RHAG/SLC25A1 2/SLC25A4/SLC7A11	8
BP	GO:200 0181	negative regulation of blood vessel morphogenesi s	0.000604634	0.008200752	COL4A2/PGK1/PPARG /SERPINF1/SYNJ2BP/ XDH	6
BP	GO:003 8065	collagen-activated signaling pathway	0.000787141	0.010296765	COL1A1/COL4A1/COL 4A2	3
BP	GO:190 1615	organic hydroxy compound metabolic process	0.000851253	0.01107919	ABAT/ACADL/ACTN3 /ADH4/ALDH1A1/EPA S1/GOT1/GPD1/PARK7 /PRKAG2/RBP4/SLC25 A12/SLC7A11/TPI1	14
BP	GO:005 0714	positive regulation of protein secretion	0.000955512	0.012189879	ABAT/GAPDH/GPI/M BP/MYH10/OXCT1/PF KM/RBP4	8
BP	GO:190 4706	negative regulation of vascular smooth muscle cell proliferation	0.00103607	0.013088005	ADIPOQ/PPARG/TPM1	3
BP	GO:001 0951	negative regulation of endopeptidase activity	0.001257369	0.015578074	BIN1/CRYAB/GAPDH/ GPI/PARK7/PEBP1/SE RPINF1/WFDC2	8
BP	GO:003 0073	insulin secretion	0.001325981	0.016011631	ABAT/CCL5/CPT1A/O XCT1/PARK7/PFKM/R BP4/SLC25A4	8
BP	GO:005 5093	response to hyperoxia	0.001329643	0.016011631	BNIP3/COL1A1/PPAR G	3
BP	GO:003 4308	primary alcohol metabolic process	0.001448945	0.017367125	ADH4/ALDH1A1/GPD 1/PARK7/RBP4	5

BP	GO:0035902	response to immobilization stress	0.001670618	0.019480468	GOT1/GPI/PPARG	3
BP	GO:0006820	anion transport	0.001877417	0.021598673	ABAT/CA2/CPT1A/FXYD1/GOT2/NFKBIE/PPARG/RHAG/SLC25A12/SLC25A4/SLC2A9/SLC7A11/VDAC1	13
BP	GO:0048871	multicellular organismal homeostasis	0.001892144	0.021671353	ABAT/ACADL/ACTN3/ADIPOQ/ALDH1A1/B2M/CA2/EPAS1/GATM/IL20RB/RBP4/RHAG	12
BP	GO:0043470	regulation of carbohydrate catabolic process	0.001979379	0.022186624	ACTN3/GPD1/PRKAG2/SLC25A12	4
BP	GO:0033500	carbohydrate homeostasis	0.001988789	0.022186624	ADIPOQ/GPI/OXCT1/PARK7/PFKM/PPARG/RBP4/SERPINF1	8
BP	GO:0042593	glucose homeostasis	0.001988789	0.022186624	ADIPOQ/GPI/OXCT1/PARK7/PFKM/PPARG/RBP4/SERPINF1	8
BP	GO:0000422	autophagy of mitochondrion	0.002079261	0.022898527	BNIP3/GABARAPL2/MAP1LC3A/PARK7/VDAC1	5
BP	GO:0061726	mitochondrion disassembly	0.002079261	0.022898527	BNIP3/GABARAPL2/MAP1LC3A/PARK7/VDAC1	5
BP	GO:0046324	regulation of glucose import	0.002231655	0.024368542	ADIPOQ/ITLN1/PRKAG2/SORBS1	4
BP	GO:0072347	response to anesthetic	0.002231655	0.024368542	ABAT/GOT2/GPI/MAP1LC3A	4
BP	GO:1904659	glucose transmembrane transport	0.002460223	0.026198327	ADIPOQ/ITLN1/PRKAG2/SLC2A9/SORBS1	5
BP	GO:0033032	regulation of myeloid cell apoptotic process	0.002504907	0.026455512	ADIPOQ/CCL5/SLC7A11	3
BP	GO:0009914	hormone transport	0.002527466	0.026476745	ABAT/ADIPOQ/CCL5/CPT1A/OXCT1/PARK7/PFKM/RBP4/SLC25A4	9
BP	GO:0043279	response to alkaloid	0.002668624	0.027817491	ABAT/GOT2/GPI/MAP1LC3A/PPARG	5
BP	GO:0010817	regulation of hormone levels	0.002677042	0.027817491	ABAT/ADH4/ADIPOQ/ALDH1A1/CCL5/CPT1A/OXCT1/PARK7/PEBP1/PFKM/RBP4/SLC25A4	12
BP	GO:0051223	regulation of protein transport	0.002749333	0.028453945	ABAT/ADIPOQ/CCL5/CPT1A/GAPDH/GPI/MBP/MYH10/OXCT1/PARK7/PFKM/PKIG/RBP4/SLC25A4/SLC7A11	15
BP	GO:0150063	visual system development	0.002874592	0.029396123	CHRDL1/COL4A1/COL8A1/CRYAB/LAMB2/MYH10/RBP4/SERPINF1/SLC7A11/UNC45B	10

BP	GO:001 0939	regulation of necrotic cell death	0.003002847	0.029648801	BNIP3/HEBP2/SLC25A 4	3
BP	GO:004 2135	neurotransmitt er catabolic process	0.003002847	0.029648801	ABAT/BHMT/GLDC	3
BP	GO:007 2207	metanephric epithelium development	0.003002847	0.029648801	ACAT1/ADIPOQ/LAM B2	3
BP	GO:007 2243	metanephric nephron epithelium development	0.003002847	0.029648801	ACAT1/ADIPOQ/LAM B2	3
BP	GO:004 8880	sensory system development	0.003196771	0.031087094	CHRDL1/COL4A1/CO L8A1/CRYAB/LAMB2/ MYH10/RBP4/SERPIN F1/SLC7A11/UNC45B	10
BP	GO:003 3028	myeloid cell apoptotic process	0.003557459	0.033580845	ADIPOQ/CCL5/SLC7A 11	3
BP	GO:004 2391	regulation of membrane potential	0.003927447	0.036276094	ABAT/ATP1B2/BIN1/B NIP3/FHL1/FXYD1/GO T1/HEBP2/PARK7/SNT A1	10
BP	GO:001 0907	positive regulation of glucose metabolic process	0.004170648	0.037579578	ACTN3/SLC25A12/SO RBS1	3
BP	GO:004 2572	retinol metabolic process	0.004170648	0.037579578	ADH4/ALDH1A1/RBP4	3
BP	GO:010 6106	cold-induced thermogenesis	0.004383604	0.038953613	ACADL/ACTN3/ADIP OQ/ALDH1A1/EPAS1/ GATM	6
BP	GO:012 0161	regulation of cold-induced thermogenesis	0.004383604	0.038953613	ACADL/ACTN3/ADIP OQ/ALDH1A1/EPAS1/ GATM	6
BP	GO:006 0359	response to ammonium ion	0.004501348	0.03986245	ABAT/GLDC/GOT2/GP I/MAP1LC3A	5
BP	GO:009 7164	ammonium ion metabolic process	0.004623203	0.040557865	ABAT/ACADL/AGMA T/BHMT/CPT1A/PARK 7/PEBP1	7
BP	GO:007 0206	protein trimerization	0.004642829	0.040557865	ADIPOQ/CD74/COL1A 1/ITLN1	4
BP	GO:199 0845	adaptive thermogenesis	0.005448349	0.046801317	ACADL/ACTN3/ADIP OQ/ALDH1A1/EPAS1/ GATM	6
BP	GO:004 2594	response to starvation	0.005543687	0.047304907	ACAT1/ADSSL1/GAB ARAPL2/MAP1LC3A/ MYH13/OXCT1/PPAR G	7
BP	GO:003 2387	negative regulation of intracellular transport	0.00556404	0.047321883	ADIPOQ/CRYAB/PAR K7/PKIG	4
BP	GO:004 4270	cellular nitrogen compound	0.005817869	0.049317924	ACADL/ACAT1/ACTN 3/BHMT/GAPDH/GPD 1/GPI/PABPC4/PFKM/	15

		catabolic process			PGK1/PGM1/PRKAG2/ SLC25A12/TPI1/XDH	
BP	GO:000 6979	response to oxidative stress	0.005916632	0.049990695	ADIPOQ/BNIP3/COL1 A1/CRYAB/EPAS1/FB LN5/MAP1LC3A/PAR K7/PEBP1/PON2/SLC7 A11/TPM1	12
CC	GO:004 4449	contractile fiber part	1.64467E-19	4.73664E-17	ACTA1/ACTA2/ACTC 1/BIN1/CRYAB/DES/M YBPC2/MYBPC3/MYH 1/MYH13/MYH2/MYH 4/MYH7/MYL1/MYL2/ MYL3/MYL4/MYLPF/ MYOZ1/TNNC1/TNNC 2/TNNI1/TNNI2/TNNT 1/TNNT3/TPM1/TPM3	27
CC	GO:004 3292	contractile fiber	9.79609E-19	1.41064E-16	ACTA1/ACTA2/ACTC 1/BIN1/CRYAB/DES/M YBPC2/MYBPC3/MYH 1/MYH13/MYH2/MYH 4/MYH7/MYL1/MYL2/ MYL3/MYL4/MYLPF/ MYOZ1/TNNC1/TNNC 2/TNNI1/TNNI2/TNNT 1/TNNT3/TPM1/TPM3	27
CC	GO:003 0016	myofibril	5.12654E-17	4.51619E-15	ACTA1/ACTC1/BIN1/C RYAB/DES/MYBPC2/ MYBPC3/MYH1/MYH 13/MYH2/MYH4/MYH 7/MYL1/MYL2/MYL3/ MYL4/MYOZ1/TNNC1 /TNNC2/TNNI1/TNNI2/ TNNT1/TNNT3/TPM1/ TPM3	25
CC	GO:003 0017	sarcomere	6.27249E-17	4.51619E-15	ACTA1/ACTC1/BIN1/C RYAB/DES/MYBPC2/ MYBPC3/MYH1/MYH 2/MYH4/MYH7/MYL1/ MYL2/MYL3/MYL4/M YOZ1/TNNC1/TNNC2/ TNNI1/TNNI2/TNNT1/ TNNT3/TPM1/TPM3	24
CC	GO:001 5629	actin cytoskeleton	1.05248E-14	6.06229E-13	ACTA1/ACTA2/ACTC 1/ACTN3/BIN1/CRYA B/MYBPC2/MYBPC3/ MYH1/MYH10/MYH13 /MYH2/MYH4/MYH7/ MYL1/MYL2/MYL3/M YL4/MYLPF/MYOZ1/P GM1/SMTNL2/SORBS 1/TNNC1/TNNC2/TNN I1/TNNI2/TNNT1/TNN T3/TPM1/TPM3	31
CC	GO:000 5865	striated muscle thin filament	1.95955E-13	9.40582E-12	ACTA1/MYBPC2/MYB PC3/TNNC1/TNNC2/T NNI1/TNNI2/TNNT1/T NNT3/TPM1/TPM3	11
CC	GO:001 6460	myosin II complex	3.09294E-13	1.17272E-11	MYBPC3/MYH1/MYH 10/MYH13/MYH2/MY H4/MYH7/MYL1/MYL 3/MYLPF	10

CC	GO:003 6379	myofilament	3.25756E-13	1.17272E-11	ACTA1/MYBPC2/MYB PC3/TNNC1/TNNC2/T NNI1/TNNI2/TNNT1/T NNT3/TPM1/TPM3	11
CC	GO:001 6459	myosin complex	3.7519E-13	1.20061E-11	MYBPC2/MYBPC3/M YH1/MYH10/MYH13/ MYH2/MYH4/MYH7/ MYL1/MYL2/MYL3/M YL4/MYLPF	13
CC	GO:000 5859	muscle myosin complex	1.21857E-12	3.50949E-11	MYBPC3/MYH1/MYH 13/MYH2/MYH4/MYH 7/MYL1/MYL3/MYLPF	9
CC	GO:003 2982	myosin filament	7.53162E-10	1.97191E-08	MYBPC2/MYBPC3/M YH1/MYH10/MYH13/ MYH2/MYH4/MYH7	8
CC	GO:003 1672	A band	7.92628E-07	1.90231E-05	CRYAB/MYBPC2/MY BPC3/MYH1/MYL2/M YL3/MYL4	7
CC	GO:004 4420	extracellular matrix component	2.33869E-06	5.1811E-05	COL1A1/COL4A1/COL 4A2/COL8A1/FBLN5/L AMB2/MFAP5	7
CC	GO:003 2432	actin filament bundle	2.28069E-05	0.00046917	ACTA1/CRYAB/MYH1 0/MYH7/SORBS1/TPM 1/TPM3	7
CC	GO:004 2641	actomyosin	3.36885E-05	0.000646819	ACTA1/ACTC1/MYH1 0/MYH7/SORBS1/TPM 1/TPM3	7
CC	GO:004 3209	myelin sheath	5.78446E-05	0.001041202	CA2/CRYAB/GOT2/GP I/MBP/MDH2/PEBP1/P MP22/SLC25A12/SLC2 5A4	10
CC	GO:003 1674	I band	6.79544E-05	0.001151228	ACTC1/BIN1/CRYAB/ DES/MYBPC2/MYBPC 3/MYH7/MYL3/MYOZ 1	9
CC	GO:009 8644	complex of collagen trimers	7.77269E-05	0.00124363	COL1A1/COL4A1/COL 4A2/COL8A1	4
CC	GO:000 1725	stress fiber	0.000118568	0.001707386	ACTA1/MYH10/MYH7 /SORBS1/TPM1/TPM3	6
CC	GO:009 7517	contractile actin filament bundle	0.000118568	0.001707386	ACTA1/MYH10/MYH7 /SORBS1/TPM1/TPM3	6
CC	GO:006 2023	collagen-containing extracellular matrix	0.000295631	0.004054367	ADIPOQ/ANXA6/CLE C3B/COL1A1/COL4A1/ COL4A2/COL8A1/DPT /FBLN5/LAMB2/MFAP 5/SERPINF1	12
CC	GO:004 2383	sarcolemma	0.0006306	0.008255128	BIN1/CACNG1/DES/F XYD1/GOT2/SNTA1/S NTB1	7
CC	GO:003 0018	Z disc	0.001157694	0.014496348	BIN1/CRYAB/DES/MY BPC2/MYBPC3/MYH7/ MYOZ1	7
CC	GO:003 1307	integral component of mitochondrial outer membrane	0.00130846	0.015143927	BNIP3/CPT1A/SYNJ2B P	3
CC	GO:003 1012	extracellular matrix	0.001314577	0.015143927	ADIPOQ/ANXA6/CLE C3B/COL1A1/COL4A1/	13

					COL4A2/COL8A1/CRISPLD2/DPT/FBLN5/LAMB2/MFAP5/SERPINF1	
CC	GO:0005884	actin filament	0.0015456	0.017120488	ACTA1/ACTC1/ACTN3/SMTNL2/TPM1/TPM3	6
CC	GO:0031306	intrinsic component of mitochondrial outer membrane	0.001644114	0.017507359	BNIP3/CPT1A/SYNJ2BP	3
CC	GO:0005581	collagen trimer	0.001702104	0.017507359	ADIPOQ/COL1A1/COL4A1/COL4A2/COL8A1	5
CC	GO:0030315	T-tubule	0.002455744	0.024388082	BIN1/CACNG1/FXYD1/GOT2	4
CC	GO:0031594	neuromuscular junction	0.002606492	0.025022321	DES/LAMB2/MYH10/SNTA1/SYNJ2BP	5
MF	GO:0003779	actin binding	4.51653E-12	1.74338E-09	ACTN3/ADSSL1/ANXA6/BIN1/MYBPC2/MYBPC3/MYH1/MYH10/MYH13/MYH2/MYH4/MYH7/MYL2/MYL3/MYL4/MYOZ1/SNTA1/SNTB1/SORBS1/TNNC1/TNNC2/TNNI1/TNNI2/TNNT3/TPM1/TPM3	26
MF	GO:0051015	actin filament binding	2.8097E-09	5.42273E-07	ADSSL1/ANXA6/BIN1/MYBPC2/MYBPC3/MYH1/MYH10/MYH13/MYH2/MYH4/MYH7/MYL4/TNNC1/TNNC2/TPM1/TPM3	16
MF	GO:0008307	structural constituent of muscle	8.56116E-09	1.10154E-06	ACTN3/ASPH/MYBPC2/MYBPC3/MYL1/MYL2/MYL3/MYLPF/TPM1	9
MF	GO:0050662	coenzyme binding	9.80247E-08	9.45938E-06	ABAT/ACADL/ACAT1/ACBD7/ADH4/AIFM3/ALDH1A1/FMO3/GAPDH/GLDC/GOT1/GOT2/GPD1/HLCS/OAT/PYGM/XDH	17
MF	GO:0005198	structural molecule activity	1.5661E-07	1.20903E-05	ACTA1/ACTN3/ADIPOQ/ASPH/COL1A1/COL4A1/COL4A2/COL8A1/CRYAB/DES/DPT/FBLN5/KRT6A/LAMB2/MBP/MFAP5/MYBPC2/MYBPC3/MYL1/MYL2/MYL3/MYLPF/PPL/PRPH/SNTA1/SNTB1/TPM1	27
MF	GO:0016769	transferase activity, transferring nitrogenous groups	2.96741E-07	1.90904E-05	ABAT/GAPDH/GATM/GOT1/GOT2/OAT	6
MF	GO:0000146	microfilament motor activity	8.55273E-06	0.000418627	MYH10/MYH13/MYH2/MYH4/MYH7	5

MF	GO:004 8037	cofactor binding	8.67622E-06	0.000418627	ABAT/ACADL/ACAT1 /ACBD7/ADH4/AIFM3/ ALDH1A1/FMO3/GAP DH/GLDC/GOT1/GOT2 /GPD1/GSTM4/HEBP2/ HLCS/OAT/PYGM/XD H	19
MF	GO:000 5516	calmodulin binding	2.54529E-05	0.001002267	MBP/MYH1/MYH10/M YH13/MYH2/MYH4/M YH7/SNTA1/SNTB1/SP A17	10
MF	GO:001 9842	vitamin binding	2.59655E-05	0.001002267	ABAT/ADH4/GLDC/G OT1/GOT2/HLCS/OAT/ PYGM/RBP4	9
MF	GO:003 0170	pyridoxal phosphate binding	4.15816E-05	0.001337543	ABAT/GLDC/GOT1/G OT2/OAT/PYGM	6
MF	GO:007 0279	vitamin B6 binding	4.15816E-05	0.001337543	ABAT/GLDC/GOT1/G OT2/OAT/PYGM	6
MF	GO:001 7022	myosin binding	6.57093E-05	0.001951061	ACTA1/ACTC1/MYBP C3/MYL2/MYL3/MYL 4	6
MF	GO:000 5201	extracellular matrix structural constituent	8.95434E-05	0.002468839	ADIPOQ/COL1A1/COL 4A1/COL4A2/COL8A1/ DPT/FBLN5/LAMB2/M FAP5	9
MF	GO:000 8483	transaminase activity	0.000111398	0.002866646	ABAT/GOT1/GOT2/OA T	4
MF	GO:000 5509	calcium ion binding	0.000228121	0.005503429	ACTN3/ANXA6/ASPH/ CLEC3B/FBLN5/ITLN1 /MYL1/MYL2/MYL3/ MYL4/MYLPF/PVALB /SLC25A12/TNNC1/TN NC2/TNNT1/TNNT3	17
MF	GO:003 0020	extracellular matrix structural constituent conferring tensile strength	0.00089923	0.019283494	COL1A1/COL4A1/COL 4A2/COL8A1	4
MF	GO:004 3531	ADP binding	0.00089923	0.019283494	ACTA1/MYH10/PGK1/ PRKAG2	4
MF	GO:000 3774	motor activity	0.001271875	0.025839145	MYH1/MYH10/MYH13 /MYH2/MYH4/MYH7/ MYL3	7
MF	GO:000 3785	actin monomer binding	0.00212657	0.041042796	MYL2/MYL3/MYL4	3

Table A.7: Gene ontology terms enriched by the top 351 DE genes in regenerative vs. control comparison, commonly identified by the analysis of both technologies

A.8 GO Terms Enriched in Regenerative vs. Wound healing

ONTOLOGY	ID	Description	pvalue	p.adjust	geneID	Count
GO terms enriched by the top 150 up-regulated genes					
BP	GO:0000280	nuclear division	3.1046E-29	5.3026E-26	AURKA/AURKB/BUB1/BUB1B/CCNA2/CCNB1/CCNB3/CDC20/CDCA5/CDCA8/CENPF/CHEK1/INCENP/KIF11/KIF22/KIF23/KIF2C/KIFC1/MAD2L1/MTBP/NCAPD3/NCAPG/NCAPH/NDC80/NEK2/NIPBL/NUSAP1/PDS5A/PLK1/PRC1/RAD51/RCC1/RMI1/RPA2/SMC2/SMC4/TOP2B/TPX2/TRIP13/ZWINT	40
BP	GO:0140014	mitotic nuclear division	5.7191E-28	4.8841E-25	AURKA/AURKB/BUB1/BUB1B/CCNA2/CCNB1/CCNB3/CDC20/CDCA5/CDCA8/CENPF/CHEK1/INCENP/KIF11/KIF22/KIF23/KIF2C/KIFC1/MAD2L1/MTBP/NCAPD3/NCAPG/NCAPH/NDC80/NEK2/NIPBL/NUSAP1/PDS5A/PLK1/PRC1/RCC1/SMC2/SMC4/TPX2/TRIP13/ZWINT	36
BP	GO:0098813	nuclear chromosome segregation	1.381E-26	5.8968E-24	AURKB/BUB1/BUB1B/CCNB1/CDC20/CDCA5/CDCA8/CENPF/DYNC1H1/FEN1/INCENP/KIF22/KIF23/KIF2C/KIFC1/MAD2L1/NCAPD3/NCAPG/NCAPH/NDC80/NEK2/NIPBL/NUSAP1/PDS5A/PLK1/PRC1/RMI1/SMC2/SMC4/TOP2B/TRIP13/ZWINT	32
BP	GO:0000819	sister chromatid segregation	2.3876E-26	8.1561E-24	AURKB/BUB1/BUB1B/CCNB1/CDC20/CDCA5/CDCA8/CENPF/FEN1/INCENP/KIF22/KIF23/KIF2C/KIFC1/MAD2L1/NCAPD3/NCAPG/NCAPH/NDC80/NEK2/NIPBL/NUSAP1/PDS5A/PLK1/PRC1/SMC2/SMC4/TOP2B/TRIP13/ZWINT	30
BP	GO:0010564	regulation of cell cycle process	9.3048E-20	1.4448E-17	APEX1/AURKA/AURKB/BUB1/BUB1B/CBX3/CCNA2/CCNB1/CCNB3/CDC20/CDC25A/CDC7/CDCA5/CENPF/CHEK1/DYNC1H1/EED/EZH2/FEN1/HAUS1/INCENP/KIF11/KIF20A/KIF23/MAD2L1/MTA3/MTBP/NDC80/NEK2/NIPBL/NUSAP1/PCNA/PLK1/PRC1/PRPF40A/RAD51/RCC1/RPA2/RRM2/TPX2/TRIP13	41

BP	GO:00 71103	DNA conformation change	1.1248E-18	1.601E-16	ASF1B/CCNB1/CDCA5/CHAF1A/CHAF1B/GINS2/HELLS/HIST1H2BJ/HMGB3/MCM2/MCM4/MCM6/MCM7/NASP/NCAPD3/NCAPG/NCAPH/NIPBL/NUSAP1/RAD51/RPA2/SART3/SMC2/SMC4/TOP2B	25
BP	GO:00 06260	DNA replication	4.1727E-16	5.0907E-14	CCNA2/CDC7/CHAF1A/CHAF1B/CHEK1/FEN1/GINS2/MCM2/MCM3/MCM4/MCM6/MCM7/NASP/NUCKS1/PCNA/PDS5A/POLA2/RAD51/RFC2/RFC4/RMI1/RPA2/RRM1/RRM2/SLBP	25
BP	GO:00 07088	regulation of mitotic nuclear division	6.5663E-16	7.4768E-14	AURKA/AURKB/BUB1/BUB1B/CCNA2/CCNB1/CCNB3/CDC20/CDCA5/CENPF/CHEK1/KIF11/MAD2L1/MTBP/NDC80/NEK2/NIPBL/NUSAP1/PLK1/RCC1/TRIP13	21
BP	GO:00 51983	regulation of chromosome segregation	1.1471E-13	1.0885E-11	AURKB/BUB1/BUB1B/CCNB1/CDC20/CDCA5/CENPF/DYNC1H1/FEN1/KIF2C/MAD2L1/NDC80/NEK2/NIPBL/PLK1/TRIP13	16
BP	GO:00 07052	mitotic spindle organization	2.3213E-12	1.652E-10	AURKA/AURKB/CCNB1/CDC20/DYNC1H1/KIF11/KIF23/KIFC1/NDC80/NEK2/PLK1/PRC1/RCC1/STMN1/TPX2	15
BP	GO:19 03046	meiotic cell cycle process	3.408E-12	2.2388E-10	AURKA/BUB1/BUB1B/CDC20/CDC25A/NCAPD3/NCAPH/PLK1/RAD51/RMI1/RPA2/SMC2/SMC4/TOP2B/TRIP13	15
BP	GO:00 07094	mitotic spindle assembly checkpoint	1.9122E-11	8.8271E-10	AURKB/BUB1/BUB1B/CCNB1/CDC20/CENPF/MAD2L1/NDC80/PLK1/TRIP13	10
BP	GO:00 71174	mitotic spindle checkpoint	1.9122E-11	8.8271E-10	AURKB/BUB1/BUB1B/CCNB1/CDC20/CENPF/MAD2L1/NDC80/PLK1/TRIP13	10
BP	GO:00 06325	chromatin organization	4.1786E-11	1.6221E-09	ASF1B/ATAD2/AURKA/AURKB/BAZ1B/BRD3/CBX3/CCNA2/CCNB1/CHAF1A/CHAF1B/CHEK1/EED/EZH2/HELLS/HIST1H2AG/HIST1H2BJ/HMGB3/MBD3/MCM2/MTA3/NASP/NIPBL/NUCKS1/RNF168/SAFB/SART3/TRIM28/UHRF1/VRK1	30
BP	GO:19 05819	negative regulation of chromosome separation	5.9007E-11	2.1444E-09	AURKB/BUB1/BUB1B/CCNB1/CDC20/CENPF/MAD2L1/NDC80/PLK1/TRIP13	10
BP	GO:01 40013	meiotic nuclear division	8.0562E-11	2.8667E-09	AURKA/BUB1/BUB1B/CDC20/NCAPH/PLK1/RAD51/RMI1/RPA2/SMC2/SMC4/TOP2B/TRIP13	13
BP	GO:00 33044	regulation of chromosome organization	1.2953E-10	4.3669E-09	ATAD2/AURKB/BUB1/BUB1B/CCNB1/CDC20/CDCA5/CENPF/CHEK1/EED/FEN1/MAD2L1/MCM2/NDC80/NEK2/NIP	21

					BL/PARP1/PLK1/SART3/TRIM28/TRIP13	
BP	GO:1905818	regulation of chromosome separation	8.9136E-09	2.0032E-07	AURKB/BUB1/BUB1B/CCNB1/CDC20/CENPF/MAD2L1/NDC80/PLK1/TRIP13	10
BP	GO:0051310	metaphase plate congression	2.7733E-08	5.996E-07	CCNB1/CDCA5/CDCA8/CENPF/DYNC1H1/KIF22/KIF2C/KIFC1/NDC80	9
BP	GO:0016572	histone phosphorylation	1.596E-07	3.0978E-06	AURKA/AURKB/BAZ1B/CCNA2/CCNB1/CHEK1/VRK1	7
BP	GO:0050000	chromosome localization	1.8909E-07	3.5884E-06	CCNB1/CDCA5/CDCA8/CENPF/DYNC1H1/KIF22/KIF2C/KIFC1/NDC80	9
BP	GO:0061982	meiosis I cell cycle process	5.3739E-07	9.8694E-06	AURKA/CDC25A/PLK1/RAD51/RMI1/RPA2/TOP2B/TRIP13	8
BP	GO:0034502	protein localization to chromosome	5.7109E-07	1.0377E-05	AURKB/BUB1B/CDCA5/EZH2/MTBP/NDC80/NIPBL/PLK1/RPA2	9
BP	GO:0031145	anaphase-promoting complex-dependent catabolic process	9.3982E-07	1.6549E-05	AURKA/AURKB/BUB1B/CCNB1/CDC20/MAD2L1/PLK1	7
BP	GO:0065004	protein-DNA complex assembly	1.0579E-06	1.8438E-05	ASF1B/CENPF/CHAF1A/CHAF1B/HELLS/HIST1H2BJ/MCM2/NASP/PARP1/RAD51/RPA2/SART3	12
BP	GO:2001020	regulation of response to DNA damage stimulus	2.2249E-06	3.7256E-05	BCLAF1/CHEK1/PARP1/PCNA/PSMD10/RAD51/RAD51AP1/RAD9A/RNF168/RPA2/TRIM28/USP1	12
BP	GO:0071478	cellular response to radiation	3.4238E-06	5.5168E-05	AURKB/CDC25A/CHEK1/NIPBL/NUCKS1/PARP1/PBK/PCNA/RAD51/RAD51AP1/RAD9A	11
BP	GO:0071824	protein-DNA complex subunit organization	6.7603E-06	0.00010497	ASF1B/CENPF/CHAF1A/CHAF1B/HELLS/HIST1H2BJ/MCM2/NASP/PARP1/RAD51/RPA2/SART3	12
BP	GO:0042769	DNA damage response, detection of DNA damage	1.506E-05	0.00021874	PARP1/PCNA/RFC2/RFC4/RPA2/USP1	6
BP	GO:0007131	reciprocal meiotic recombination	3.2237E-05	0.00044049	RAD51/RMI1/RPA2/TOP2B/TRIP13	5
BP	GO:0009314	response to radiation	4.6682E-05	0.0006328	AURKB/CDC25A/CHEK1/FEN1/NIPBL/NUCKS1/PARP1/PBK/PCNA/RAD51/RAD51AP1/RAD9A/RNF168/RRM1/USP1	15
BP	GO:0000079	regulation of cyclin-dependent protein serine/threonine kinase activity	0.00035488	0.00401414	CCNA2/CCNB1/CCNB3/CDC25A/PLK1/PSMD10	6
BP	GO:0104004	cellular response to environmental stimulus	0.00046855	0.00501616	AURKB/CDC25A/CHEK1/NIPBL/NUCKS1/PARP1/PBK/PCNA/RAD51/RAD51AP1/RAD9A	11

BP	GO:00 45814	negative regulation of gene expression, epigenetic	0.00056142	0.00588288	ATAD2/EED/EZH2/HELLS/M BD3/TRIM28	6
BP	GO:00 30397	membrane disassembly	0.00068536	0.00705178	CCNB1/PLK1/VRK1	3
BP	GO:00 51081	nuclear envelope disassembly	0.00068536	0.00705178	CCNB1/PLK1/VRK1	3
BP	GO:00 60249	anatomical structure homeostasis	0.000894	0.00867369	APEX1/AURKB/FEN1/IQCB1/ NEK2/PARP1/PCNA/POLA2/R AD51/RFC2/RFC4/RPA2	12
BP	GO:00 01556	oocyte maturation	0.00090265	0.00867369	AURKA/CCNB1/TRIP13	3
BP	GO:00 00077	DNA damage checkpoint	0.00090393	0.00867369	AURKA/CCNB1/CHEK1/PCN A/PLK1/RAD9A/RPA2	7
BP	GO:00 06342	chromatin silencing	0.00117269	0.01088566	ATAD2/EED/HELLS/MBD3/T RIM28	5
BP	GO:00 97711	ciliary basal body-plasma membrane docking	0.00143606	0.01325837	B9D1/DYNC1H1/HAUS1/IQC B1/NEK2/PLK1	6
BP	GO:00 42770	signal transduction in response to DNA damage	0.0021466	0.01919575	AURKA/CCNB1/CHEK1/PCN A/PLK1/PSMD10	6
BP	GO:00 32886	regulation of microtubule-based process	0.00224919	0.01990473	AURKA/CHEK1/DYNC1H1/KI F11/NEK2/PLK1/STMN1/TPX2	8
BP	GO:00 07292	female gamete generation	0.00235104	0.02033725	AURKA/CCNB1/NCAPH/PLK 1/TRIP13	5
BP	GO:00 43388	positive regulation of DNA binding	0.0023576	0.02033725	CDCA5/NIPBL/PARP1/TRIM2 8	4
BP	GO:19 04666	regulation of ubiquitin protein ligase activity	0.00262411	0.02218799	CDC20/MAD2L1/PLK1	3
BP	GO:00 51098	regulation of binding	0.00281448	0.02368047	AURKA/AURKB/CDCA5/CTH RC1/NEK2/NIPBL/NUCKS1/P ARP1/PLK1/STMN1/TRIM28	11
BP	GO:19 05269	positive regulation of chromatin organization	0.00367695	0.02990587	CCNB1/EED/NIPBL/SART3/T RIM28	5
BP	GO:20 00241	regulation of reproductive process	0.00394116	0.03145564	AURKA/CDC20/CDC25A/TRI P13/WDR77	5
BP	GO:00 97421	liver regeneration	0.00559078	0.04206629	AURKA/EZH2/PCNA	3
BP	GO:00 19886	antigen processing and presentation of exogenous peptide antigen via MHC class II	0.00581888	0.04359055	DYNC1H1/KIF11/KIF22/KIF23 /KIF2C	5
BP	GO:00 51606	detection of stimulus	0.00649023	0.04798837	PARP1/PCNA/RFC2/RFC4/RP A2/USP1	6

124

CC	GO:00 00228	nuclear chromosome	8.7177E-31	1.8133E-28	APEX1/ASF1B/AURKA/AUR KB/BAZ1B/BUB1/BUB1B/CB X3/CCNB1/CDCA5/CHAF1A/ CHAF1B/CHEK1/EED/EZH2/F EN1/GINS2/HIST1H2AG/HMG B3/INCENP/LRPPRC/MBD3/M CM2/MCM3/MCM4/MCM6/M CM7/MTA3/NASP/NCAPD3/N CAPH/NDC80/NEK2/NIPBL/N UCKS1/PARP1/PCNA/PLK1/P OLA2/RAD51/RAD51AP1/RA D9A/RCC1/RPA2/SMC2/TRIM 28/UHRF1	47
CC	GO:00 44454	nuclear chromosome part	7.8222E-28	7.2152E-26	APEX1/ASF1B/AURKA/AUR KB/BAZ1B/BUB1/BUB1B/CB X3/CCNB1/CDCA5/CHAF1A/ CHAF1B/EED/EZH2/FEN1/GI NS2/HIST1H2AG/HMGB3/INC ENP/MBD3/MCM2/MCM3/MC M4/MCM6/MCM7/MTA3/NAS P/NCAPD3/NCAPH/NDC80/NI PBL/NUCKS1/PARP1/PCNA/P LK1/POLA2/RAD51/RAD51AP 1/RAD9A/RCC1/RPA2/TRIM2 8/UHRF1	43
CC	GO:00 98687	chromosomal region	1.0407E-27	7.2152E-26	APEX1/AURKA/AURKB/BAZ 1B/BUB1/BUB1B/CBX3/CCN B1/CDCA5/CDCA8/CENPF/C HEK1/FEN1/HELLS/INCENP/ KIF22/KIF2C/MAD2L1/MCM2 /MCM3/MCM4/MCM6/MCM7/ MTBP/NCAPD3/NCAPG/NDC 80/NEK2/NUP133/NUP43/PAR P1/PCNA/PDS5A/PLK1/RAD5 1/RPA2/ZWINT	37
CC	GO:00 00793	condensed chromosome	1.6929E-25	8.8029E-24	AURKA/AURKB/BAZ1B/BUB 1/BUB1B/CBX3/CCNB1/CDC A5/CENPF/CHEK1/INCENP/K IF2C/LRPPRC/MAD2L1/NCAP D3/NCAPG/NCAPH/NDC80/N EK2/NUP133/NUP43/PLK1/RA D51/RAD9A/RCC1/RPA2/SMC 2/SMC4/ZWINT	29
CC	GO:00 00785	chromatin	5.6968E-21	2.3699E-19	ASF1B/BAZ1B/CBX3/CDCA5/ CENPF/CHAF1A/CHAF1B/CH EK1/EED/EZH2/HELLS/HIST1 H2AG/HIST1H2BJ/HMGB3/IN CENP/KIF22/MBD3/MCM2/M CM7/MTA3/MTBP/NASP/NCA PD3/NIPBL/NUCKS1/PCNA/P DS5A/PLK1/RAD51/RAD51AP 1/RCC1/RPA2/TMPO/TOP2B/T RIM28/UHRF1	36
CC	GO:00 00775	chromosome, centromeric region	5.1542E-20	1.7868E-18	AURKA/AURKB/BAZ1B/BUB 1/BUB1B/CBX3/CCNB1/CDC A5/CDCA8/CENPF/HELLS/IN CENP/KIF22/KIF2C/MAD2L1/ MTBP/NCAPD3/NCAPG/NDC 80/NEK2/NUP133/NUP43/PDS 5A/PLK1/ZWINT	25

CC	GO:00 00794	condensed nuclear chromosome	3.4167E-19	1.0152E-17	AURKA/AURKB/BUB1/BUB1 B/CCNB1/CHEK1/INCENP/LR PPRC/NCAPD3/NCAPH/NDC8 0/NEK2/PLK1/RAD51/RAD9A/ RCC1/RPA2	17
CC	GO:00 00779	condensed chromosome, centromeric region	9.9741E-17	2.5933E-15	AURKA/AURKB/BUB1/BUB1 B/CBX3/CCNB1/CENPF/INCE NP/KIF2C/MAD2L1/NCAPD3/ NCAPG/NDC80/NEK2/NUP13 3/NUP43/PLK1/ZWINT	18
CC	GO:00 05819	spindle	1.2305E-13	2.8439E-12	AURKA/AURKB/BUB1B/CBX 3/CCNB1/CDC20/CDC7/CDCA 8/CENPF/HAUS1/INCENP/IQC B1/KIF11/KIF20A/KIF22/KIF2 3/KIFC1/MAD2L1/NEK2/NUS AP1/PLK1/PRC1/TPX2/VRK1	24
CC	GO:00 00776	kinetochore	1.1432E-12	2.3779E-11	AURKB/BUB1/BUB1B/CCNB 1/CENPF/INCENP/KIF22/KIF2 C/MAD2L1/MTBP/NDC80/NE K2/NUP133/NUP43/PLK1/ZWI NT	16
CC	GO:00 00777	condensed chromosome kinetochore	4.9936E-11	9.4425E-10	BUB1/BUB1B/CCNB1/CENPF/ INCENP/KIF2C/MAD2L1/NDC 80/NEK2/NUP133/NUP43/PLK 1/ZWINT	13
CC	GO:00 00790	nuclear chromatin	2.5773E-10	4.4673E-09	ASF1B/CBX3/CDCA5/CHAF1 A/CHAF1B/EED/EZH2/HIST1 H2AG/HMGB3/MBD3/MTA3/ NASP/NCAPD3/NIPBL/NUCK S1/RAD51/RAD51AP1/RCC1/T RIM28/UHRF1	20
CC	GO:00 00784	nuclear chromosome, telomeric region	1.2718E-09	2.0348E-08	APEX1/CBX3/FEN1/MCM2/M CM3/MCM4/MCM6/MCM7/PA RP1/PCNA/RAD51/RPA2	12
CC	GO:00 00780	condensed nuclear chromosome, centromeric region	1.3921E-09	2.0683E-08	AURKA/AURKB/BUB1/BUB1 B/CCNB1/NDC80/PLK1	7
CC	GO:00 00781	chromosome, telomeric region	3.6002E-09	4.9923E-08	APEX1/CBX3/CHEK1/FEN1/M CM2/MCM3/MCM4/MCM6/M CM7/PARP1/PCNA/RAD51/RP A2	13
CC	GO:00 72686	mitotic spindle	6.4038E-09	8.325E-08	AURKA/AURKB/CDC7/IQCB 1/KIF11/KIF22/KIF23/KIFC1/ MAD2L1/NUSAP1/TPX2	11
CC	GO:00 05874	microtubule	1.0844E-08	1.3268E-07	APPBP2/AURKA/AURKB/DY NC1H1/HAUS1/INCENP/KIF1 1/KIF20A/KIF22/KIF23/KIF2C/ KIFC1/LRPPRC/NEK2/NUSAP 1/PLK1/PRC1/STMN1/TPX2	19
CC	GO:00 00792	heterochromat in	2.7176E-08	3.1403E-07	BAZ1B/CBX3/EED/HELLS/IN CENP/MBD3/NCAPD3/TOP2B /TRIM28/UHRF1	10
CC	GO:00 05815	microtubule organizing center	7.174E-08	7.8536E-07	ANKRD26/APEX1/AURKA/A URKB/B9D1/BUB1B/CCNB1/ CCNB3/CDC20/CENPF/CHEK 1/DYNC1H1/HAUS1/IQCB1/K IF23/KIF2C/KIFC1/MCM3/ND C80/NEK2/PCNA/PLK1/RAD5 1/SASS6/TPX2	25

CC	GO:00 00922	spindle pole	9.2206E-08	9.4535E-07	AURKA/AURKB/CCNB1/CDC 20/CENPF/HAUS1/KIF11/MA D2L1/NEK2/PLK1/PRC1/TPX2	12
CC	GO:00 05813	centrosome	9.5444E-08	9.4535E-07	ANKRD26/APEX1/AURKA/A URKB/B9D1/CCNB1/CCNB3/ CDC20/CENPF/CHEK1/DYNC 1H1/HAUS1/IQCB1/KIF23/KIF 2C/MCM3/NDC80/NEK2/PCN A/PLK1/SASS6	21
CC	GO:00 05875	microtubule associated complex	1.0268E-07	9.7083E-07	APPBP2/AURKA/AURKB/CD CA8/DYNC1H1/HAUS1/KIF11 /KIF20A/KIF22/KIF23/KIF2C/ KIFC1	12
CC	GO:00 05657	replication fork	1.3629E-07	1.2325E-06	BAZ1B/GINS2/MCM3/PCNA/P OLA2/RFC2/RFC4/RPA2/UHR F1	9
CC	GO:00 44815	DNA packaging complex	1.6345E-07	1.4165E-06	HIST1H2AG/HIST1H2BJ/NCA PD3/NCAPG/NCAPH/SMC2/S MC4	7
CC	GO:00 00778	condensed nuclear chromosome kinetochore	4.297E-07	3.5751E-06	BUB1/BUB1B/CCNB1/NDC80/ PLK1	5
CC	GO:00 45120	pronucleus	1.7908E-06	1.4326E-05	AURKA/CCNA2/CENPF/EED/ EZH2	5
CC	GO:00 05721	pericentric heterochromat in	2.6515E-06	2.0426E-05	BAZ1B/CBX3/HELLS/INCENP /NCAPD3	5
CC	GO:00 99513	polymeric cytoskeletal fiber	5.8196E-06	4.3231E-05	APPBP2/AURKA/AURKB/DY NC1H1/HAUS1/INCENP/KIF1 1/KIF20A/KIF22/KIF23/KIF2C/ KIFC1/LRPPRC/NEK2/NUSAP 1/PLK1/PRC1/STMN1/TPX2	19
CC	GO:00 05871	kinesin complex	1.2091E-05	8.6722E-05	KIF11/KIF20A/KIF22/KIF23/K IF2C/KIFC1	6
CC	GO:00 43596	nuclear replication fork	1.7257E-05	0.00011965	BAZ1B/GINS2/MCM3/PCNA/P OLA2/RPA2	6
CC	GO:00 45171	intercellular bridge	2.0436E-05	0.00013712	CDC7/CDCA8/IQCB1/KIF20A/ KIF23/TPX2	6
CC	GO:00 05876	spindle microtubule	2.4071E-05	0.00015646	AURKA/AURKB/KIF11/NUSA P1/PLK1/PRC1	6
CC	GO:00 30496	midbody	3.3313E-05	0.00020997	AURKA/AURKB/CDCA8/CEN PF/INCENP/KIF20A/KIF23/NE K2/PLK1/PRC1	10
CC	GO:00 05720	nuclear heterochromat in	5.0356E-05	0.00030806	CBX3/EED/NCAPD3/TRIM28/ UHRF1	5
CC	GO:00 32993	protein-DNA complex	0.00010178	0.00060485	GINS2/HIST1H2AG/HIST1H2 BJ/MCM3/PARP1/PCNA/POL A2/RPA2	8
CC	GO:00 10369	chromocenter	0.00061216	0.00351268	AURKB/CDCA8/INCENP	3
CC	GO:00 30894	replisome	0.00062485	0.00351268	MCM3/PCNA/POLA2/RPA2	4
CC	GO:00 90734	site of DNA damage	0.00089541	0.0049012	CBX3/PARP1/RAD51/RNF168/ RPA2	5
CC	GO:00 51233	spindle midzone	0.00097424	0.00519592	AURKA/AURKB/CDCA8/PLK 1	4
CC	GO:00 05635	nuclear envelope	0.00348734	0.01813417	CBX3/CENPF/CSE1L/LRPPRC /MAD2L1/MCM3AP/NUP133/	12

127

					NUP43/PARP1/RCC1/RRM1/T MPO	
CC	GO:00 00791	euchromatin	0.00438601	0.02225098	CBX3/TRIM28/UHRF1	3
CC	GO:00 43601	nuclear replisome	0.00501931	0.02485753	MCM3/POLA2/RPA2	3
CC	GO:00 16604	nuclear body	0.00643878	0.03114575	APEX1/BAZ1B/BCLAF1/CCN B3/INCENP/KIF22/PCNA/PRP F40A/RAD51/RMI1/RPA2/SAR T3/SLTM/SMC4/SRRM2/ZWI NT	16
CC	GO:00 31080	nuclear pore outer ring	0.010629	0.04912959	NUP133/NUP43	2
CC	GO:00 35098	ESC/E(Z) complex	0.010629	0.04912959	EED/EZH2	2
CC	GO:00 00307	cyclin- dependent protein kinase holoenzyme complex	0.01097332	0.0496185	CCNA2/CCNB1/CCNB3	3
MF	GO:00 03697	single- stranded DNA binding	1.4645E-11	4.13E-09	LONP1/LRPPRC/MCM4/MCM 6/MCM7/NEIL3/NUCKS1/POL R3C/RAD51/RAD51AP1/RPA2 /SMC2/SMC4/TSN	14
MF	GO:00 03682	chromatin binding	7.8791E-10	1.111E-07	APEX1/ATAD2/BRD3/CDCA5 /CENPF/CHAF1A/CHAF1B/EE D/EZH2/MBD3/MTA3/NCAPD 3/NCAPH/NIPBL/NUCKS1/PC NA/RAD51/RCC1/RNF168/SA FB/TOP2B/TRIM28/UHRF1/V RK1	24
MF	GO:00 35173	histone kinase activity	1.5879E-08	1.4926E-06	AURKA/AURKB/BAZ1B/CCN B1/CHEK1/VRK1	6
MF	GO:00 42393	histone binding	1.2862E-07	9.0674E-06	ASF1B/ATAD2/BAZ1B/BRD3/ CHAF1B/MCM2/NASP/NCAP D3/RCC1/RNF168/SART3/UH RF1/VRK1	13
MF	GO:00 16887	ATPase activity	9.3798E-07	5.2902E-05	ATAD2/DYNC1H1/HSPA14/KI F11/KIF20A/KIF22/KIF23/KIF 2C/KIFC1/LONP1/MCM4/MC M6/MCM7/MDN1/RAD51/RFC 2/RFC4/TOP2B	18
MF	GO:01 40097	catalytic activity, acting on DNA	1.1371E-06	5.3443E-05	APEX1/FEN1/GINS2/MCM4/M CM6/MCM7/NEIL3/PCNA/PO LA2/RAD51/RAD9A/TOP2B	12
MF	GO:00 03777	microtubule motor activity	3.3934E-06	0.00013671	APPBP2/DYNC1H1/KIF11/KIF 20A/KIF22/KIF23/KIF2C/KIFC 1	8
MF	GO:00 08094	DNA- dependent ATPase activity	6.1218E-05	0.00215793	MCM4/MCM6/MCM7/RAD51/ RFC2/RFC4/TOP2B	7
MF	GO:00 31491	nucleosome binding	8.9205E-05	0.00279508	EED/MBD3/RCC1/RNF168/UH RF1/VRK1	6
MF	GO:00 03774	motor activity	0.00014528	0.00409697	APPBP2/DYNC1H1/KIF11/KIF 20A/KIF22/KIF23/KIF2C/KIFC 1	8
MF	GO:00 08017	microtubule binding	0.00018488	0.00455043	KIF11/KIF20A/KIF22/KIF23/K IF2C/KIFC1/LRPPRC/NUSAP1 /PLK1/PRC1	10

MF	GO:00 03690	double-stranded DNA binding	0.00019364	0.00455043	APEX1/EED/ETV4/EZH2/FEN 1/HMGB3/KIF2C/MBD3/MCM 2/NEIL3/NUCKS1/PARP1/PCN A/RAD51/RAD51AP1/RPA2/S AFB/SMAD5/UHRF1	19
MF	GO:00 42826	histone deacetylase binding	0.00039949	0.0086658	CDC20/KPNA2/MTA3/NIPBL/ PARP1/RAD9A/TOP2B	7
MF	GO:00 43142	single-stranded DNA-dependent ATPase activity	0.00049107	0.00989158	RAD51/RFC2/RFC4	3
MF	GO:00 16799	hydrolase activity, hydrolyzing N-glycosyl compounds	0.00066705	0.01254047	APEX1/NEIL3/PCNA	3
MF	GO:00 15631	tubulin binding	0.00073865	0.01301878	KIF11/KIF20A/KIF22/KIF23/K IF2C/KIFC1/LRPPRC/NUSAP1 /PLK1/PRC1/STMN1	11
MF	GO:00 16895	exodeoxyribo nuclease activity, producing 5'-phosphomono esters	0.00112841	0.01871836	APEX1/FEN1/RAD9A	3
MF	GO:00 04672	protein kinase activity	0.00127148	0.01905256	AURKA/AURKB/BAZ1B/BUB 1/BUB1B/CCNA2/CCNB1/CC NB3/CDC7/CHEK1/NEK2/PBK /PLK1/TRIM28/VRK1	15
MF	GO:00 03684	damaged DNA binding	0.00135576	0.01905256	APEX1/FEN1/NEIL3/PCNA/RP A2	5
MF	GO:00 08327	methyl-CpG binding	0.00141881	0.01905256	MBD3/UHRF1/WDR77	3
MF	GO:00 70182	DNA polymerase binding	0.00141881	0.01905256	LONP1/PCNA/RAD51	3
MF	GO:00 04529	exodeoxyribo nuclease activity	0.0017521	0.02245871	APEX1/FEN1/RAD9A	3
MF	GO:00 42623	ATPase activity, coupled	0.00183203	0.02246232	DYNC1H1/HSPA14/KIF11/LO NP1/MCM4/MCM6/MCM7/RA D51/RFC2/RFC4/TOP2B	11
MF	GO:00 04386	helicase activity	0.00205114	0.02410094	GINS2/HELLS/MCM2/MCM3/ MCM4/MCM6/MCM7	7
MF	GO:00 03678	DNA helicase activity	0.0025407	0.02865907	GINS2/MCM4/MCM6/MCM7	4
MF	GO:00 16773	phosphotransf erase activity, alcohol group as acceptor	0.00323603	0.03410151	AURKA/AURKB/BAZ1B/BUB 1/BUB1B/CCNA2/CCNB1/CC NB3/CDC7/CHEK1/NEK2/NO L9/PBK/PLK1/TRIM28/VRK1	16
MF	GO:00 19901	protein kinase binding	0.00326504	0.03410151	AURKA/CCNA2/CCNB1/CCN B3/CDC25A/KIF11/KIF20A/PA RP1/PCNA/PLK1/PRC1/RAD9 A/TOP2B/TPX2/VRK1	15
MF	GO:00 08022	protein C-terminus binding	0.00340495	0.03429269	CDC20/CENPF/FBLN1/LAMA 1/MAD2L1/NIPBL/RAD51/TO P2B	8

ONTOLOGY	ID	Description	pvalue	p.adjust	geneID	Count
MF	GO:0019900	kinase binding	0.00392509	0.0381681	AURKA/AURKB/CCNA2/CCNB1/CCNB3/CDC25A/KIF11/KIF20A/PARP1/PCNA/PLK1/PRC1/RAD9A/TOP2B/TPX2/VRK1	16
MF	GO:0016796	exonuclease activity, active with either ribo- or deoxyribonucleic acids and producing 5'-phosphomonoesters	0.00496701	0.04668992	APEX1/DIS3/FEN1/RAD9A	4
GO terms enriched by the top 128 down-regulated genes						
ONTOLOGY	ID	Description	pvalue	p.adjust	geneID	Count
BP	GO:0030049	muscle filament sliding	3.564E-27	4.4122E-24	ACTA1/ACTC1/ACTN3/DES/MYBPC2/MYBPC3/MYH7/MYL1/MYL2/MYL3/MYL4/TNNC1/TNNC2/TNNI1/TNNI2/TNNT1/TNNT3/TPM1/TPM3	19
BP	GO:0033275	actin-myosin filament sliding	3.564E-27	4.4122E-24	ACTA1/ACTC1/ACTN3/DES/MYBPC2/MYBPC3/MYH7/MYL1/MYL2/MYL3/MYL4/TNNC1/TNNC2/TNNI1/TNNI2/TNNT1/TNNT3/TPM1/TPM3	19
BP	GO:0006936	muscle contraction	1.5322E-18	9.4845E-16	ACTA1/ACTA2/ACTC1/ACTN3/ALDOA/CRYAB/DES/FXYD1/GAMT/MYBPC2/MYBPC3/MYH1/MYH7/MYL1/MYL2/MYL3/MYL4/PTGS2/TNNC1/TNNC2/TNNI1/TNNI2/TNNT1/TNNT3/TPM1/TPM3	26
BP	GO:0008015	blood circulation	3.0574E-11	9.4627E-09	ACTA2/ACTC1/ADIPOQ/DES/EGFR/FXYD1/MYBPC3/MYH7/MYL1/MYL2/MYL3/MYL4/PTGS2/PTP4A3/RCAN1/SGK1/TNNC1/TNNI2/TNNT1/TNNT3/TPM1	21
BP	GO:0006937	regulation of muscle contraction	1.4987E-10	3.7107E-08	ACTN3/MYBPC3/MYH7/MYL2/MYL3/PTGS2/TNNC1/TNNC2/TNNI1/TNNI2/TNNT1/TNNT3/TPM1	13
BP	GO:0055008	cardiac muscle tissue morphogenesis	1.191E-08	1.9659E-06	ACTC1/MYBPC2/MYBPC3/MYH7/MYL2/MYL3/TNNC1/TNNI1/TPM1	9
BP	GO:0016053	organic acid biosynthetic process	2.48E-08	3.4114E-06	ACADL/ACTN3/ADIPOQ/ALDOA/BHMT/CD74/FBP1/GAMT/GPD1/GSTM4/HSD17B8/OAT/PFKM/PGK1/PGM1/PTGS2/UGDH/XBP1	18
BP	GO:0046394	carboxylic acid biosynthetic process	2.48E-08	3.4114E-06	ACADL/ACTN3/ADIPOQ/ALDOA/BHMT/CD74/FBP1/GAMT/GPD1/GSTM4/HSD17B8/OAT/PFKM/PGK1/PGM1/PTGS2/UGDH/XBP1	18
BP	GO:0030239	myofibril assembly	3.0348E-08	3.757E-06	ACTA1/ACTC1/MYBPC2/MYBPC3/MYL2/MYOZ1/TNNT1/TNNT3/TPM1	9

BP	GO:00 10927	cellular component assembly involved in morphogenesi s	6.7718E-08	6.9863E-06	ACTA1/ACTC1/MYBPC2/MY BPC3/MYL2/MYOZ1/PMP22/T NNT1/TNNT3/TPM1	10
BP	GO:00 15669	gas transport	3.4002E-07	2.8063E-05	HBA2/HBE1/HBZ/MYC/RHA G	5
BP	GO:00 50879	multicellular organismal movement	5.8978E-07	4.4251E-05	ACTN3/MYH7/TNNC1/TNNC 2/TNNI2/TNNT1/TNNT3	7
BP	GO:00 50881	musculoskelet al movement	5.8978E-07	4.4251E-05	ACTN3/MYH7/TNNC1/TNNC 2/TNNI2/TNNT1/TNNT3	7
BP	GO:00 46031	ADP metabolic process	1.908E-06	0.00012768	ACTN3/AK1/ALDOA/FBP1/G PD1/PFKM/PGK1/PGM1	8
BP	GO:00 06165	nucleoside diphosphate phosphorylati on	2.7516E-06	0.00017564	ACTN3/AK1/ALDOA/FBP1/G PD1/PFKM/PGK1/PGM1	8
BP	GO:00 06091	generation of precursor metabolites and energy	6.4773E-06	0.00036776	ACTN3/ADIPOQ/ALDOA/CO X7A2L/FBP1/GFPT2/GPD1/G YG1/MYC/OXCT1/PFKM/PGK 1/PGM1/PYGM/SLC25A4/UG DH	16
BP	GO:00 55002	striated muscle cell development	9.0079E-06	0.00044217	ACTA1/ACTC1/MYBPC2/MY BPC3/MYL2/MYOZ1/TNNT1/ TNNT3/TPM1	9
BP	GO:00 72525	pyridine-containing compound biosynthetic process	9.9925E-06	0.00045818	ACTN3/ALDOA/FBP1/GPD1/P FKM/PGK1/PGM1/PTGS2	8
BP	GO:00 60537	muscle tissue development	1.0427E-05	0.00046943	ACTA1/ACTC1/ACTN3/EGR1/ MYBPC2/MYBPC3/MYH7/MY L2/MYL3/TNNC1/TNNI1/TPM 1/ZFAND5	13
BP	GO:00 43462	regulation of ATPase activity	1.3552E-05	0.00056874	DNAJB1/MYBPC3/MYL3/MY L4/TNNC1/TNNT3/TPM1	7
BP	GO:00 51259	protein complex oligomerizatio n	1.4577E-05	0.00059167	ACADL/ADIPOQ/ALDOA/AR G1/CD74/CRYAB/FBP1/HBA2 /HBE1/HBZ/HSD17B8/MMP3/ OAT/PFKM/RIOK3/SQSTM1	16
BP	GO:00 09636	response to toxic substance	1.624E-05	0.00063824	ACTC1/ADIPOQ/ARG1/BCL2 L1/CRYAB/DUSP1/EGR1/HB A2/HBE1/HBZ/MBP/OXCT1/P ON2/PRDX6/PTGS2	15
BP	GO:00 44283	small molecule biosynthetic process	3.4872E-05	0.00126975	ACADL/ACTN3/ADIPOQ/AL DOA/BHMT/CD74/EGR1/FBP 1/GAMT/GPD1/GSTM4/HSD1 7B8/OAT/PFKM/PGK1/PGM1/ PTGS2/UGDH/XBP1	19
BP	GO:00 06112	energy reserve metabolic process	3.6658E-05	0.00129744	GFPT2/GYG1/MYC/PFKM/PG M1/PYGM	6
BP	GO:00 06754	ATP biosynthetic process	4.2899E-05	0.00145503	ACTN3/ALDOA/FBP1/GPD1/P FKM/PGK1/PGM1	7
BP	GO:00 97435	supramolecula r fiber organization	5.4691E-05	0.00180553	ACTA1/ACTC1/ALDOA/ARH GAP18/CRYAB/DES/MFAP5/ MYBPC2/MYBPC3/MYL2/MY	17

					OZ1/RND3/TNNT1/TNNT3/TPM1/TPM3/TPPP3	
BP	GO:0016052	carbohydrate catabolic process	9.5995E-05	0.0026706	ACTN3/ALDOA/FBP1/GPD1/PFKM/PGK1/PGM1/PYGM	8
BP	GO:0031032	actomyosin structure organization	9.881E-05	0.00271836	ACTA1/ACTC1/MYBPC2/MYBPC3/MYL2/MYOZ1/TNNT1/TNNT3/TPM1	9
BP	GO:0072524	pyridine-containing compound metabolic process	0.0001171	0.00315149	ACTN3/ALDOA/FBP1/GPD1/PFKM/PGK1/PGM1/PTGS2	8
BP	GO:0006094	gluconeogenesis	0.00020099	0.00507796	ADIPOQ/ALDOA/FBP1/GPD1/PGK1/PGM1	6
BP	GO:0019320	hexose catabolic process	0.00020732	0.00518506	ACTN3/ALDOA/PFKM/PGK1/PGM1	5
BP	GO:0072215	regulation of metanephros development	0.00028791	0.00698885	ADIPOQ/EGR1/MYC	3
BP	GO:0032722	positive regulation of chemokine production	0.00029778	0.00708939	ADIPOQ/CD74/EGR1/MBP	4
BP	GO:0042744	hydrogen peroxide catabolic process	0.00029778	0.00708939	HBA2/HBE1/HBZ/PRDX6	4
BP	GO:0032781	positive regulation of ATPase activity	0.00032743	0.00764828	DNAJB1/MYBPC3/MYL3/MYL4/TPM1	5
BP	GO:1902532	negative regulation of intracellular signal transduction	0.00039095	0.00882081	ACTN3/ADIPOQ/BCL2L1/CD74/DUSP1/DUSP5/FBP1/MYC/PTGS2/RCAN1/RIOK3/SOCS1/XBP1	13
BP	GO:1902106	negative regulation of leukocyte differentiation	0.00040429	0.00892191	ADIPOQ/CD74/IRF1/MYC/SOCS1	5
BP	GO:0001101	response to acid chemical	0.00041439	0.00892191	ADIPOQ/ARG1/BCL2L1/DUSP1/EGFR/EGR1/PTGS2/SERPINF1/SOCS1/XBP1	10
BP	GO:0010226	response to lithium ion	0.00051726	0.01024593	ACTA1/CDKN1B/PTGS2	3
BP	GO:0051195	negative regulation of cofactor metabolic process	0.00051726	0.01024593	ACTN3/FBP1/MMP3	3
BP	GO:1904706	negative regulation of vascular smooth muscle cell proliferation	0.00051726	0.01024593	ADIPOQ/CDKN1B/TPM1	3
BP	GO:0015893	drug transport	0.00056739	0.01097547	ARG1/HBA2/HBE1/HBZ/MYC/RHAG/SLC25A4	7

BP	GO:00 46434	organophosph ate catabolic process	0.00059635	0.01135822	ACTN3/ALDOA/FBP1/GPD1/P FKM/PGK1/PGM1/PRDX6	8
BP	GO:00 05980	glycogen catabolic process	0.00066568	0.01211928	PFKM/PGM1/PYGM	3
BP	GO:00 06525	arginine metabolic process	0.00066568	0.01211928	AGMAT/ARG1/OAT	3
BP	GO:00 46716	muscle cell cellular homeostasis	0.00066568	0.01211928	ALDOA/PFKM/PGK1	3
BP	GO:00 30334	regulation of cell migration	0.0007759	0.0138211	ADIPOQ/CD74/CITED2/CYR6 1/DUSP1/EGFR/FGFBP1/MMP 3/PTGS2/RND3/SEMA3F/SER PINE1/SERPINF1/SGK1/TPM1 /XBP1	16
BP	GO:00 07162	negative regulation of cell adhesion	0.00090684	0.0159243	ADIPOQ/ARG1/CD74/DUSP1/I RF1/MBP/SERPINE1/SOCS1	8
BP	GO:00 51384	response to glucocorticoid	0.0009753	0.016887	ADIPOQ/ARG1/DUSP1/EGFR/ PTGS2/SERPINF1	6
BP	GO:00 40008	regulation of growth	0.0010574	0.01781037	ACTN3/BCL2L1/CDKN1B/CR YAB/CYR61/EGFR/FBP1/FHL 1/GAMT/MYL2/SEMA3F/SGK 1/SOCS1/SQSTM1	14
BP	GO:00 42698	ovulation cycle	0.00116831	0.01915714	EGFR/EGR1/MMP19/SERPINF 1	4
BP	GO:00 09108	coenzyme biosynthetic process	0.00150993	0.02361449	ACTN3/ALDOA/FBP1/GPD1/P FKM/PGK1/PGM1/PTGS2	8
BP	GO:00 44282	small molecule catabolic process	0.00175141	0.02642348	ACADL/ACTN3/ADIPOQ/AL DOA/ARG1/FAAH/OAT/OXC T1/PFKM/PGK1/PGM1	11
BP	GO:00 44042	glucan metabolic process	0.0017822	0.02642348	GYG1/PFKM/PGM1/PYGM	4
BP	GO:00 17001	antibiotic catabolic process	0.00196492	0.02861842	HBA2/HBE1/HBZ/PRDX6	4
BP	GO:00 62012	regulation of small molecule metabolic process	0.00201406	0.02916262	ACADL/ACTN3/ADIPOQ/BH MT/COX7A2L/EGR1/FBP1/GP D1/PTGS2	9
BP	GO:00 02790	peptide secretion	0.00206823	0.02977289	ARL4D/CD74/EGFR/FCN1/MB P/OXCT1/PFKM/SCG2/SLC25 A4/SOCS1/XBP1	11
BP	GO:00 98869	cellular oxidant detoxification	0.00211675	0.03015353	HBA2/HBE1/HBZ/PRDX6/PTG S2	5
BP	GO:00 46390	ribose phosphate biosynthetic process	0.00222503	0.03095037	ACTN3/AK1/ALDOA/FBP1/G PD1/PFKM/PGK1/PGM1	8
BP	GO:00 10332	response to gamma radiation	0.00236849	0.03276196	BCL2L1/CRYAB/EGR1/MYC	4

BP	GO:00 06979	response to oxidative stress	0.00262981	0.03538814	ADIPOQ/ARG1/CRYAB/DUSP 1/EGFR/HBA2/MMP3/PON2/P RDX6/PTGS2/TPM1	11
BP	GO:00 19221	cytokine-mediated signaling pathway	0.00270874	0.03625314	ADIPOQ/ARG1/BCL2L1/CD74 /EGR1/IRF1/MMP3/MYC/PELI 2/PTGS2/SOCS1/SQSTM1	12
BP	GO:00 50679	positive regulation of epithelial cell proliferation	0.00281448	0.03682866	ARG1/EGFR/FGFBP1/MYC/S CG2/XBP1	6
BP	GO:20 00242	negative regulation of reproductive process	0.00285586	0.03682866	CDKN1B/DUSP1/SERPINF1	3
BP	GO:00 30308	negative regulation of cell growth	0.00310167	0.03859161	CDKN1B/CRYAB/FBP1/FHL1/ MYL2/SEMA3F	6
BP	GO:00 51085	chaperone cofactor-dependent protein refolding	0.00327372	0.0395401	CD74/DNAJB1/DNAJB5	3
BP	GO:00 71480	cellular response to gamma radiation	0.00327372	0.0395401	BCL2L1/CRYAB/EGR1	3
BP	GO:00 71549	cellular response to dexamethason e stimulus	0.00327372	0.0395401	ARG1/EGFR/SERPINF1	3
BP	GO:00 09611	response to wounding	0.00358425	0.0423374	ARG1/CYR61/EGFR/HBE1/IR F1/LAMB2/PABPC4/PPL/SER PINE1/TFPI2/TPM1/XBP1	12
BP	GO:00 71230	cellular response to amino acid stimulus	0.00361973	0.04247609	BCL2L1/EGFR/SOCS1/XBP1	4
BP	GO:00 35690	cellular response to drug	0.0036656	0.04281139	ADIPOQ/ARG1/EGFR/EGR1/F BP1/MMP3/MYC/PTGS2/SERP INF1	9
BP	GO:00 10677	negative regulation of cellular carbohydrate metabolic process	0.00372715	0.04332595	ACTN3/ADIPOQ/FBP1	3
BP	GO:00 43200	response to amino acid	0.00392312	0.04476339	ARG1/BCL2L1/EGFR/SOCS1/ XBP1	5
BP	GO:00 35850	epithelial cell differentiation involved in kidney development	0.00421706	0.04709107	ACTA2/ADIPOQ/LAMB2	3
BP	GO:00 71353	cellular response to interleukin-4	0.00421706	0.04709107	ARG1/KEAP1/XBP1	3
BP	GO:00 10942	positive regulation of cell death	0.00440524	0.04847726	ADIPOQ/BCL2L1/CDKN1B/C YR61/DUSP1/EGR1/G0S2/GA DD45B/HBA2/MMP3/MYC/PT GS2/SQSTM1	13

BP	GO:00 00302	response to reactive oxygen species	0.00450203	0.04910586	ARG1/CRYAB/DUSP1/EGFR/ HBA2/MMP3/TPM1	7
BP	GO:00 51271	negative regulation of cellular component movement	0.00458053	0.0493104	ADIPOQ/CDKN1B/CITED2/D USP1/SEMA3F/SERPINE1/SE RPINF1/TPM1	8
BP	GO:00 09746	response to hexose	0.00467243	0.04986611	ADIPOQ/EGR1/OXCT1/PTGS2 /SERPINF1/XBP1	6
BP	GO:00 34405	response to fluid shear stress	0.00474429	0.04998664	CITED2/PTGS2/TFPI2	3
CC	GO:00 44449	contractile fiber part	1.2553E-18	2.95E-16	ACTA1/ACTA2/ACTC1/ALDO A/CRYAB/DES/MYBPC2/MY BPC3/MYH1/MYH7/MYL1/M YL2/MYL3/MYL4/MYOZ1/SQ STM1/TNNC1/TNNC2/TNNI1/ TNNI2/TNNT1/TNNT3/TPM1/ TPM3	24
CC	GO:00 30017	sarcomere	3.6889E-18	4.3344E-16	ACTA1/ACTC1/ALDOA/CRY AB/DES/MYBPC2/MYBPC3/M YH1/MYH7/MYL1/MYL2/MY L3/MYL4/MYOZ1/SQSTM1/T NNC1/TNNC2/TNNI1/TNNI2/ TNNT1/TNNT3/TPM1/TPM3	23
CC	GO:00 43292	contractile fiber	6.1388E-18	4.8087E-16	ACTA1/ACTA2/ACTC1/ALDO A/CRYAB/DES/MYBPC2/MY BPC3/MYH1/MYH7/MYL1/M YL2/MYL3/MYL4/MYOZ1/SQ STM1/TNNC1/TNNC2/TNNI1/ TNNI2/TNNT1/TNNT3/TPM1/ TPM3	24
CC	GO:00 30016	myofibril	3.3189E-17	1.9498E-15	ACTA1/ACTC1/ALDOA/CRY AB/DES/MYBPC2/MYBPC3/M YH1/MYH7/MYL1/MYL2/MY L3/MYL4/MYOZ1/SQSTM1/T NNC1/TNNC2/TNNI1/TNNI2/ TNNT1/TNNT3/TPM1/TPM3	23
CC	GO:00 05865	striated muscle thin filament	1.4689E-14	6.904E-13	ACTA1/MYBPC2/MYBPC3/T NNC1/TNNC2/TNNI1/TNNI2/ TNNT1/TNNT3/TPM1/TPM3	11
CC	GO:00 36379	myofilament	2.4501E-14	9.5964E-13	ACTA1/MYBPC2/MYBPC3/T NNC1/TNNC2/TNNI1/TNNI2/ TNNT1/TNNT3/TPM1/TPM3	11
CC	GO:00 15629	actin cytoskeleton	5.4157E-14	1.8181E-12	ACTA1/ACTA2/ACTC1/ACTN 3/ALDOA/CRYAB/KEAP1/MY BPC2/MYBPC3/MYH1/MYH7/ MYL1/MYL2/MYL3/MYL4/M YOZ1/PDLIM7/PGM1/SMTNL 2/TNNC1/TNNC2/TNNI1/TNN I2/TNNT1/TNNT3/TPM1/TPM 3	27
CC	GO:00 31672	A band	6.4663E-09	1.8995E-07	ALDOA/CRYAB/MYBPC2/M YBPC3/MYH1/MYL2/MYL3/ MYL4	8
CC	GO:00 16459	myosin complex	1.5028E-07	3.924E-06	MYBPC2/MYBPC3/MYH1/MY H7/MYL1/MYL2/MYL3/MYL4	8
CC	GO:00 05859	muscle myosin complex	1.8089E-06	4.2509E-05	MYBPC3/MYH1/MYH7/MYL1 /MYL3	5

CC	GO:00 16460	myosin II complex	6.1417E-06	0.00013121	MYBPC3/MYH1/MYH7/MYL1 /MYL3	5
CC	GO:00 31674	I band	1.0778E-05	0.00021106	ACTC1/ALDOA/CRYAB/DES/ MYBPC2/MYBPC3/MYH7/MY L3/MYOZ1	9
CC	GO:00 05884	actin filament	5.7275E-05	0.00100777	ACTA1/ACTC1/ACTN3/KEAP 1/SMTNL2/TPM1/TPM3	7
CC	GO:00 32432	actin filament bundle	6.0038E-05	0.00100777	ACTA1/CRYAB/MYH7/PDLI M7/TPM1/TPM3	6
CC	GO:00 42641	actomyosin	8.3852E-05	0.00131368	ACTA1/ACTC1/MYH7/PDLIM 7/TPM1/TPM3	6
CC	GO:00 32982	myosin filament	0.00014254	0.00209359	MYBPC2/MYBPC3/MYH1/MY H7	4
CC	GO:00 31430	M band	0.00021065	0.00291194	ALDOA/CRYAB/MYBPC2/M YBPC3	4
CC	GO:00 01725	stress fiber	0.00036707	0.00454006	ACTA1/MYH7/PDLIM7/TPM1 /TPM3	5
CC	GO:00 97517	contractile actin filament bundle	0.00036707	0.00454006	ACTA1/MYH7/PDLIM7/TPM1 /TPM3	5
CC	GO:00 30018	Z disc	0.00177645	0.02048522	CRYAB/DES/MYBPC2/MYBP C3/MYH7/MYOZ1	6
CC	GO:00 31012	extracellular matrix	0.00183059	0.02048522	ADIPOQ/CYR61/FCN1/LAMB 2/MFAP5/MMP19/MMP3/SER PINE1/SERPINF1/TFPI2/UCM A	11
CC	GO:00 97223	sperm part	0.00373016	0.03984492	ALDOA/DNAJB1/PFKM/SPA1 7/SQSTM1	5
MF	GO:00 03779	actin binding	8.4542E-08	2.7053E-05	ACTN3/ALDOA/EGFR/MYBP C2/MYBPC3/MYH1/MYH7/M YL2/MYL3/MYL4/MYOZ1/TN NC1/TNNC2/TNNI1/TNNI2/T NNT3/TPM1/TPM3	18
MF	GO:00 08307	structural constituent of muscle	5.3365E-07	8.5384E-05	ACTN3/MYBPC2/MYBPC3/M YL1/MYL2/MYL3/TPM1	7
MF	GO:00 17022	myosin binding	1.1378E-06	0.00012136	ACTA1/ACTC1/LARP6/MYBP C3/MYL2/MYL3/MYL4	7
MF	GO:00 51015	actin filament binding	2.5028E-05	0.00200224	EGFR/MYBPC2/MYBPC3/MY H1/MYH7/MYL4/TNNC1/TNN C2/TPM1/TPM3	10
MF	GO:00 04601	peroxidase activity	0.00019621	0.01255745	HBA2/HBE1/HBZ/PRDX6/PTG S2	5
MF	GO:00 16684	oxidoreductas e activity, acting on peroxide as acceptor	0.0003137	0.01673062	HBA2/HBE1/HBZ/PRDX6/PTG S2	5
MF	GO:00 03785	actin monomer binding	0.00108201	0.04946311	MYL2/MYL3/MYL4	3

Table A.8: Gene ontology terms enriched by the top 280 DE genes in regenerative vs. wound healing comparison, commonly identified by the analysis of both technologies

Appendix B

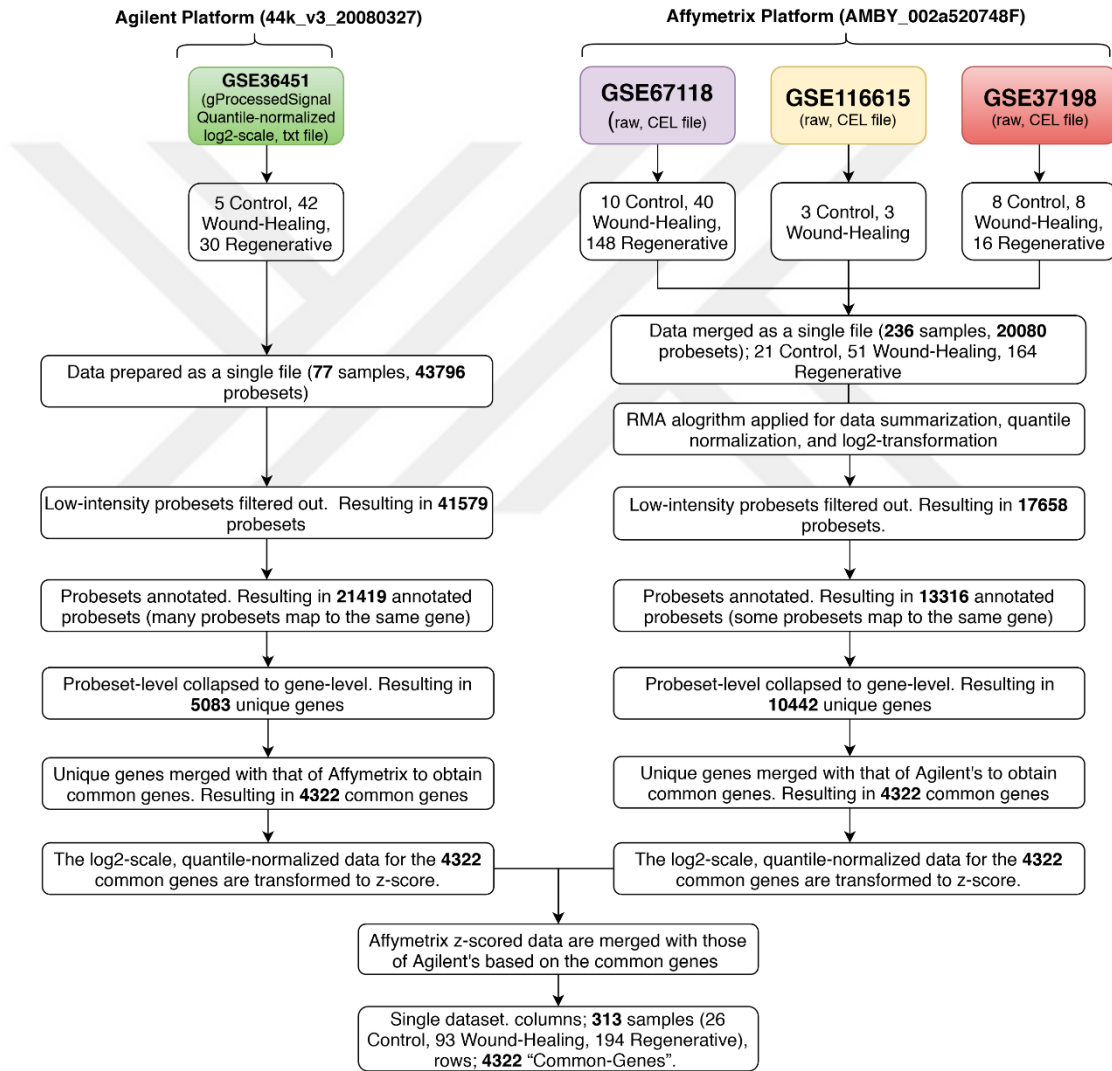## B.1   Microarray Axolotl Data Processing Workflow

Figure B.1: Detailed workflow for Affymetrix and Agilent Microarray axolotl data processing prior to differential expression analysis
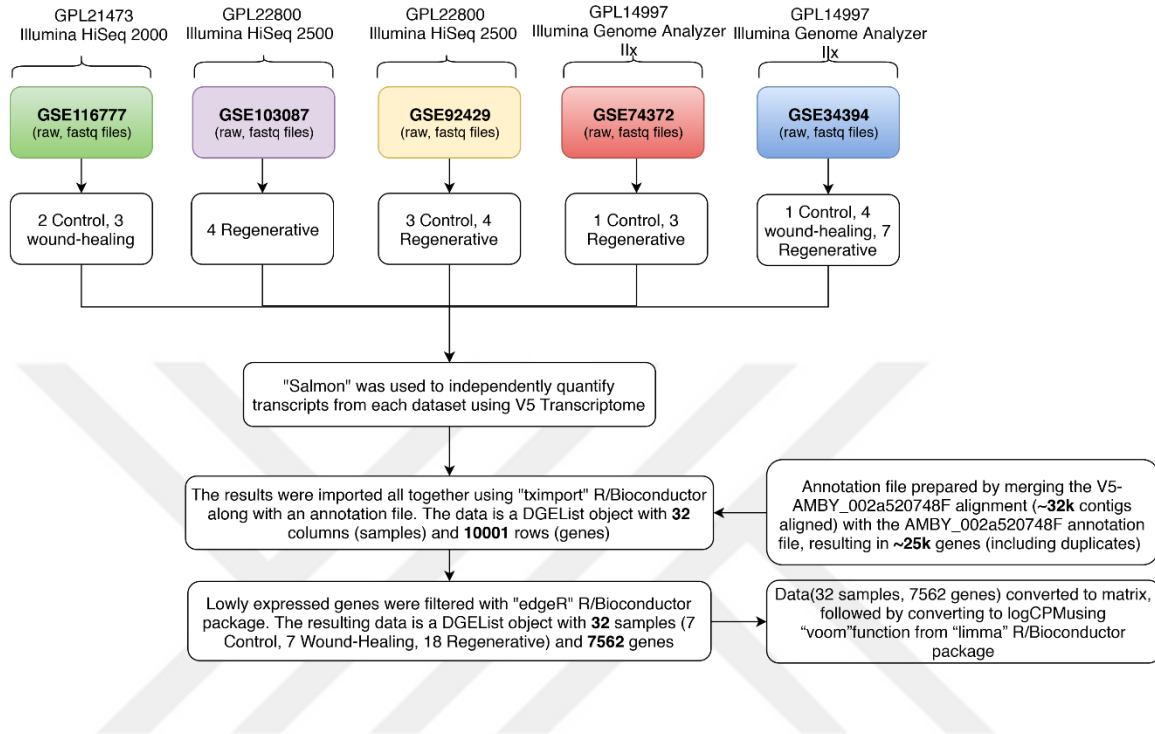
B.2   RNA-Seq Axolotl Data Processing Workflow

Figure B.2: Detailed workflow for Illumina RNA-Seq data processing prior to differential expression analysis

AN INTEGRATIVE GENE-EXPRESSION ANALYSIS OF AXOLOTL LIMB WOUND HEALING AND REGENERATION